Role of differential phosphorylation of c-Jun N-terminal domain in degenerative and inflammatory pathways of the CNS

Die Rolle der unterschiedlichen Phosphorylierung von c-Jun N-terminale Domäne bei degenerativen und entzündlichen Wirkungen im Nervengewebe

Doctoral thesis for a doctoral degree at the
Graduate School of Life Sciences,
Julius-Maximilians-Universität Würzburg,
Section Neuroscience

Submitted by

Chandrakanth Reddy Edamakanti

From

Hyderabad, India

Würzburg 2013

Submitted on: …….…….

Office stamp

Members of the *Promotionskomitee*:

Chairperson: ……Prof. Alexander Buchberger**……..**

Primary Supervisor: ……Prof. Michael Sendtner**…….**

Supervisor (Second): ……Dr. Sibylle Jablonka**…….**

Supervisor (Third): ……Dr. Anna Maria Musti**…….**

Date of Public Defence: …….…….

Date of Receipt of Certificates: ……..

Table of contents

1. Summary **1**

2. Zusammenfassung **3**

3. Introduction **5**

3.1 AP-1 Proteins 5
3.2 Regulation of c-Jun phosphorylation 8
3.3 Modulators of c-Jun activity 11
3.3.1 Negative modulators of c-Jun biological activity 11
3.3.2 Positive modulators of c-Jun biological activity 18
3.4 Role of c-Jun in cellular proliferation 22
3.5 Role of c-Jun in central nervous system 24
3.5.1 Role of c-Jun in neuronal cell death 25
3.5.2 Role of c-Jun in neuronal regeneration 29
3.5.3 Role of c-Jun in neuronal Inflammation 33

4. Materials and Methods **35**

4.1 Devise manufacturers **35**

4.2 Methods **44**

4.2.1 Animals **44**

4.2.2 Cell culture **44**

4.2.2. a Cultures of cerebellar granular neurons 44
4.2.2.b Cultures of cerebellar neuronal/glial cells 45
4.2.2.c Cultures of cerebral microglial cells 45
4.2.2.d PC12 cell cultures 45
4.2.2.e Cell death and survival assay 46
4.2.2.f Immunocytochemistry 46
4.2.2.g Immunohistochemistry 47

4.2.3 Molecular biology techniques **48**

4.2.3.a Molecular cloning 48
4.2.3.b Production of Lentiviral particles 51
4.2.3.c Isolation of Total RNA 53
4.2.3.d Reverse transcriptase polymerase chain reaction 53
4.2.3.e Quantitative realtime PCR 54
4.2.3.f Genotyping of c-Jun Knock out mice 54

4.2.4 Protein biochemistry **58**

4.3.4.a Purification of recombinant proteins 58
4.3.4.b *In Vitro* kinase assay 59
4.3.4.c Immunoprecipitation 60
4.3.4.d Western blot 60
4.3.4.e Luciferase assay 61
4.3.4.f IL-1β immunodetection by ELISA 61
4.3.4.g Mass spectrometry and protein Identification 63

5. Objective of work **65**

5. Results **67**

6.1 Role of c-Jun in neuronal cell death **67**
6.1.1 Phosphorylation of c-Jun N-terminal domain in cerebellar granule neurons 67
6.1.2 Lack of T91/93 phosphorylation impairs cell death but not Neuriteoutgrowth 73
6.1.3 Deregulation of c-Jun phosphorylation at the T91/T93 sites recovers cell death in presence of lithium 83
6.1.4 The T95 site of c-Jun is phosphorylated in vivo 87
6.1.5 JNK-1 phosphorylates T91/93 residues of recombinant c-Jun proteins in vitro 93

6.2 Role of c-Jun in neuronal Inflammation 99

6.2.1 LPS elicits JNK-dependent phosphorylation of c-Jun in Bergemann glia cells 99
6.2.2 Bergmann glia express TLR4 cells 104
6.2.3 c-Jun is required for Il-1β expression in LPS-activated Bergmann glial cells 106
6.2.4 c-Jun is expressed during formation of the Bergmann glial monolayer 110
6.2.5 c-Jun expression in Purkinje cells and granule neurons 112

6. Discussion 117

7.1 Differential phosphorylation of N-terminal c-Jun in neuronal Cells. 117
7.2 In vivo and In vitro phosphorylation of c-Jun at T95-T93-T91 119
7.3 Role of c-Jun in LPS-mediated activation of Bergmann Glial Cells 120
7.5. c-Jun is required for LPS-induced expression of Il-1β 121
7.6. In vivo expression of c-Jun in the postnatal cerebellum 121

8. References 123

9. List of figures and tables 148

10. Abbreviations 150

11. Affidavit 152

12. Curriculum vitae 153

13. Acknowledgements 156

1 Summary

In this study we have investigated the possible role of c-Jun and it's activation by the JNK pathway in neuronal cell death and in the inflammatory response of activated astrocytes. The first part of this thesis focuses on the role of site specific phosphorylation of c-Jun in neuronal cell death. The second part focuses on the function of c-Jun in LPS-mediated activation of Bergmann glia cells.

In the nervous system, activation of c-Jun transcription factor by different isoforms of c-Jun N-terminal kinase (JNK) functions in various cellular programs, including neurite outgrowth, repair and apoptosis. Yet, the regulatory mechanism underlying the functional dichotomy of c-Jun remains to be elucidated. Serine (S) 63/73 and threonine (T) 91/93 of c-Jun are the target phosphorylation sites for JNKs in response to various stimuli. Yet, these two groups of phosphorylation sites are differentially regulated in vivo, as the S63/73 sites are promptly phosphorylated upon JNK activation, whereas T91/93 phosphorylation requires a priming event at the adjacent T95 site. In our study, we used cerebellar granule cell (CGC) apoptosis by trophic/potassium (TK) deprivation as a model system to investigate the regulation and function of site-specific c-Jun phosphorylation at the S63 and T91/T93 JNK-sites in neuronal cell death. In this model system, JNK induces pro-apoptotic genes through the c-Jun/Ap-1 transcription factor. On the other side, a survival pathway initiated by lithium leads to repression of pro-apoptotic c-Jun/Ap-1 target genes without interfering with JNK activity. Yet, the mechanism by which lithium inhibits c-Jun activity remains to be elucidated. We found that TK-deprivation led to c-Jun phosphorylation at all three JNK sites. However, immunofluorescence analysis of c-Jun phosphorylation at single cell level revealed that the S63 site was phosphorylated in all c-Jun-expressing cells, whereas the response of T91/T93 phosphorylation was more sensitive, mirroring the switch-like apoptotic response of cerebellar granular cells (CGCs). Furthermore, we observed that lithium impaired c-Jun phosphorylation at T91/93, without interfering with S63/73 phosphorylation or JNK activation, suggesting that T91/T93 phosphorylation triggers c-Jun pro-apoptotic activity. Notably, expression of a c-Jun mutant lacking the T95-priming site for T91/93 phosphorylation (c-Jun A95) mimicked the effect of lithium on both cell death and c-Jun site-specific phosphorylation, whereas it was fully able to induce

neurite outgrowth in naïve PC12 cells. Vice-versa, a c-Jun mutant bearing aspartate-substitution of T95 overwhelmed lithium-mediate protection of CGCs from TK-deprivation, validating that inhibition of T91/T93/T95 phosphorylation underlies the effect of lithium on cell death. Mass-spectrometry analysis confirmed that c-Jun is phosphorylation at T91/T93/T95 in cells. Moreover, recombinant-JNK phosphorylated c-Jun at T91/T93 in a T95-dependent manner. Based on our results, we propose that T91/T93/T95 phosphorylation of c-Jun functions as a sensitivity amplifier of the JNK cascade, setting the threshold for c-Jun pro-apoptotic activity in neuronal cells.

In the central nervous system (CNS), the c-Jun transcription factor has been mainly studied in neuronal cells and coupled to apoptotic and regenerative pathways following brain injury. Besides, several studies have shown a transcriptional role of c-Jun in activated cortical and spinal astrocytes. In contrast, little is known about c-Jun expression and activation in Bergmann glial (BG) cells, the radial cerebellar astrocytes playing crucial roles in cerebellar development and physiology. In this study, we used neuronal/glial cerebellar cultures from neonatal mice to assess putative functions of c-Jun in BG cells. By performing double immunocytochemical staining of c-Jun and two BG specific markers, S100 and GLAST, we observed that c-Jun was highly expressed in radial glial cells derived from Bergmann glia. Bergmann glia-derived cells expressed toll-like receptor (TLR 4) and treatment with bacterial lipopolysaccharide (Le *et al.*) induced c-Jun phosphorylation at S63, exclusively in BG cells. Moreover, LPS induced IL-1β expression and inhibition of JNK activity abolished both c-Jun phosphorylation and the increase of IL-1β mRNA. Notably, we also observed that LPS failed to induce IL-1β mRNA in neuronal/glial cerebellar cultures generated from conditional knockout mice lacking c-Jun expression in the CNS. These results indicate that c-Jun plays a central role in c-Jun in astroglial-specific induction of IL-1β. Furthermore, we confirmed in vivo that c-Jun is expressed in BG cells, during the formation of the BG monolayer. Altogether, our finding underlines a putative role of c-Jun in astroglia-mediated neuroinflammatory dysfunctions of the cerebellum.

2 Zusammenfassung

In dieser Studie wurde die Rolle des Transkriptionsfaktors c-Jun sowie seine Aktivierung durch den JNK Signalweg beim neuronalen Zelltod und bei der entzündlichen Reaktion von aktivierten Astrozyten untersucht. Der erste Teil dieser Arbeit beschäftigt sich mit der Rolle von mehrfacher c-Jun Phosphorylierung an den Aminosäuren Threonin 91/93/95 beim neuronalen Zelltod. Der zweite Teil konzentriert sich auf die Rolle von c-Jun und seine Transaktivierung in LPS-vermittelter Aktivierung von Bergmann Gliazellen.

Als Modellsystem für den neuronalen Zelltod wurde die Apoptose von cerebellären Granularzellen (CGC) durch trophische Granulazellen Kaliumkonzentration-Erniedrigung (TK) verwendet, da es ein Modell der Um das ist, das Zusammenspiel von pro-apoptotischen und pro-Überleben Signalwegen beim neuronalen Zelltod zu studieren. In diesem Modell induziert die c-Jun N-terminale Kinase (JNK) pro-apoptotische Gene durch den c-Jun/Ap-1 Transkriptionsfaktor. Auf der anderen Seite, führt ein Lithium-induzierter Überleben-Signalweg zur Unterdrückung der pro-apoptotischen c-Jun/Ap-1 Zielgene, ohne Interferenz mit JNK Aktivität. Es blieb jedoch der Mechanismus zu klären, durch den Lithium c-Jun-Aktivität hemmt. In der Arbeit wurde dieses Modellsystem benutzt, um die Regulation und Funktion der c-Jun-Phosphorylierung durch JNK an den Stellen S63 und T91/T93 beim neuronalen Zelltod zu studieren.

Es wurde gefunden, dass TK-Kaliumerniedrigung zu c-Jun phosphorylierung führte und zwar an allen drei durch JNK phosphorylierbaren Ser/Thr (JNK-Stellen). Immunfluoreszenzanalyse von c-Jun Phosphorylierung auf Einzel-Zell-Ebene ergab jedoch, dass die S63-Stelle in allen c-Jun-exprimierenden Zellen phosphoryliert wurde, während T91/T93 Phosphorylierung empfindlicher war, analog zur Schalter-ähnlichen apoptotischen Antwort von CGCs. Umgekehrt verhinderte Lithium T91 und T93 Phosphorylierung und Zelltod ohne Wirkung auf die S63-Seite, was darauf hindeutet, dass T91/T93 Phosphorylierung durch c-Jun eine pro-apoptotische Aktivität auslöst.
Dementsprechend schützte eine c-Jun-Mutation, der die T95 Priming-Stelle für T91/93 Phosphorylierung fehlt (T95A), CGCs vor Apoptose, wohingegen T95A

Neuriten-wachstum in PC12-Zellen induzieren konnte. Umgekehrt führte eine c-Jun Mutante mit Aspartat-Substitution von T95 (T95D) zur Aufhebung der schützenden Wirkung von Lithium auf CGC Apoptose, wodurch bestätigt wurde, dass die Inhibierung der T91/T93/T95 Phosphorylierung der Wirkung von Lithium auf den Zelltod zugrundeliegt. Massenspektrometrie-Analyse bestätigte multiple Phosphorylierung von c-Jun an T91/T93/T95 in den Zellen. Außerdem wurde rekombinantes c-Jun durch JNK an T91/T93 in einer T95-abhängigen Weise phosphoryliert. Basierend auf diesen Ergebnissen wird vorgeschlagen, dass T91/T93/T95 phosphorylierung von c-Jun als Empfindlichkeit-Verstärker der JNK-Kaskade fungiert, der die Schwelle für die pro-apoptotische Aktivität von c-Jun in neuronalen Zellen einstellt.

Im zentralen Nervensystem (ZNS) wurde die Rolle des c-Jun Transkriptionsfaktors hauptsächlich bei neuronalem Zelltod und bei neuronaler Regeneration nach Hirnschädigung untersucht. Außerdem wurde auch eine Rolle für c-Jun bei der Transkription in aktivierten kortikalen und spinalen Astrozyten beschrieben. Im Gegensatz dazu ist wenig bekannt über die Expression von c-Jun und dessen Transaktivierung in Bergmann Gliazellen (BG)-Zellen, die eine entscheidende Rolle bei der Entwicklung des Kleinhirns und dessen Physiologie spielen.

In dieser Arbeit wurde die putative Rolle von c-Jun bei kultivierten neuronalen/BG-Zellen aus dem Maus-Kleinhirn untersucht. Immunfluoreszenzanalyse von c-Jun und zwei für BG-Zellen spezifische Marker, S100 und GLAST, ergab, dass c-Jun in BG-Zellen hoch exprimiert wurde. Außerdem wurde gefunden, dass der Toll-like Rezeptor TLR4 in BG-Zellen exprimiert ist und dass die Behandlung mit bakteriellem Lipopolysaccharid (Le *et al.*) die c-Jun- Phosphorylierung an S63 induziert. Zusätzlich wurde gefunden, dass LPS IL-1b Expression induziert und die Inhibierung von JNK Aktivität verhinderte sowohl c-Jun-Phosphorylierung, als auch die Zunahme von IL-1 b mRNA.

Insbesondere konnte LPS die IL-1b mRNA-Produktion in neuronalen / BG-Kulturen aus konditionellen Knockout Mäusen, denen c-Jun im ZNS fehlte, nicht induzieren, womit gezeigt wurde, dass c-Jun bei der Astroglia-spezifischen Induktion von IL-1 b essentiell ist. Immunohistochemische Analyse von c-Jun-exprimierenden Zellen im postnatalen Kleinhirn bestätigte in-vivo die Expression von c-Jun in BG Zellen und

förderte eine dynamische Expression von c-Jun während der Entwicklung der BG Monolayer zutage. Insgesamt unterstreichen die Befunde dieser Arbeit eine wahrscheinliche Rolle von c-Jun bei Astroglia-vermittelten neuroinflammatorischen Funktionsstörungen des Kleinhirns.

3 Introduction

3.1 AP-1 proteins

The transcription factor activator protein-1 or AP-1 is composed of a variety of dimers which are members of the Jun and Fos families of nuclear factors.

The Fos proteins (c-Fos, FosB, Fra-1, and Fra-2) do not form homodimers but can heterodimerize with members of the Jun family. The Jun proteins (c-Jun, JunB, and JunD) can either homodimerize or heterodimerize with other Jun or Fos members. In addition to Fos proteins, Jun proteins can also heterodimerize efficiently with other transcription factors, such as members of the activator transcription factor (ATF) family (ATF2, ATF3 and B-ATF) as well as members of the MAF family (c-Maf, MafB, MafA MafG/F/K and Nrl) (Angel & Karin, 1991; Gruda MC, 1994; Chinenov Y, 2001). All AP-1 members contain a common domain known as basic leucine zipper that is necessary to form dimeric complexes and interact with the DNA back bone. Initially, AP-1 was found to function in a variety of cellular events involved in normal development and neoplastic transformation. Then, genetically modified mice models have shown that various AP-1 members function in the control of cell proliferation, differentiation and apoptosis. The contribution of cellular functions of AP-1 depends on the composition of AP-1 dimeric subunits, the kind of stimulus and cellular environment. (Jochum *et al.*, 2001; Mechta-Grigoriou *et al.*, 2001; Shaulian & Karin, 2002)

c-Jun, the most studied AP-1 member, can form homodimers and heterodimers with either FOS and ATF proteins, JUN-JUN homodimers and JUN-FOS heterodimers bind preferentially to the DNA responsive element 5′-TGAG/CTCA-3’, that is named 12-*O*-tetradecanoylphorbol-13-acetate (TPA) responsive element (TRE), as it is strongly induced by a tumor promoter 12-*O*-tetradecanoylphorbol-13-acetate (TPA). Instead, JUN-ATF heterodimers bind preferentially to the 5′-TGACGTCA-3′ sequence, known as cyclic AMP responsive element (Chinenov Y, 2001; Ambacher *et al.*). In addition to TPA and c-AMP, c-Jun/AP-1 activity is induced by several other external cues, including serum (Fig 3.1) (Lamph *et al.*, 1988; Ryder & Nathans, 1988) growth factors (Quantin & Breathnach, 1988; Ryder & Nathans, 1988; Wu *et al.*, 1989), cytokines, neurotransmitters, bacterial and viral infections, a variety of

physical and chemical stress (Morton *et al.*, 2003) and oncoproteins, including v-Src or Ha-Ras (Angel & Karin, 1991). The Jun protein was originally identified as an oncoprotein encoded by a cellular insert in the genome of avian sarcoma virus 17.

The c-Jun protein is composed of a N-terminal region containing the JNK binding domain (JBD), the activation domain having several phosphorylation sites (1–190 AA), a hinge region (191– 256AA), a basic, positively charged domain composed of 18 amino acids (257–276AA), the leucine zipper or dimerisation domain (280–308AA) and the C-terminal domain. c-Jun transcriptional activity is mainly dependent on phosphorylation of it's N-terminal domain at serine 63 and 73 (S63&73) and threonine 91 and 93 (T91&93) residues (Smeal *et al.*, 1991; Morton *et al.*, 2003), as well as the dephosphorylation of Thr239 (Papavassiliou *et al.*, 1995; Morton *et al.*, 2003) and acetylation of lysine residues in the basic domain (Vries *et al.*, 2001). To a large extent, c-Jun phosphorylation is under the direct or indirect control of different components of the MAPK family of serine and threonine phosphorylation kinases include the JNK-1, 2 and 3 (Whitmarsh & Davis*, 2000) Phosphorylation of c-Jun at Thr239 and Ser243 by GSK3β function as docking targets for the F-box&WD domain repeated 7 (FBW7) ubiquitin ligase, that allows the subsequent degradation of c-Jun. Recently, it was found that the c-Jun 5'UTR harbours a potent internal ribosomal entry site (Guma *et al.*, 2010) with a virus-like IRES domain that directs cap-independent translation in glioblastoma cells (Blau *et al.*, 2012).

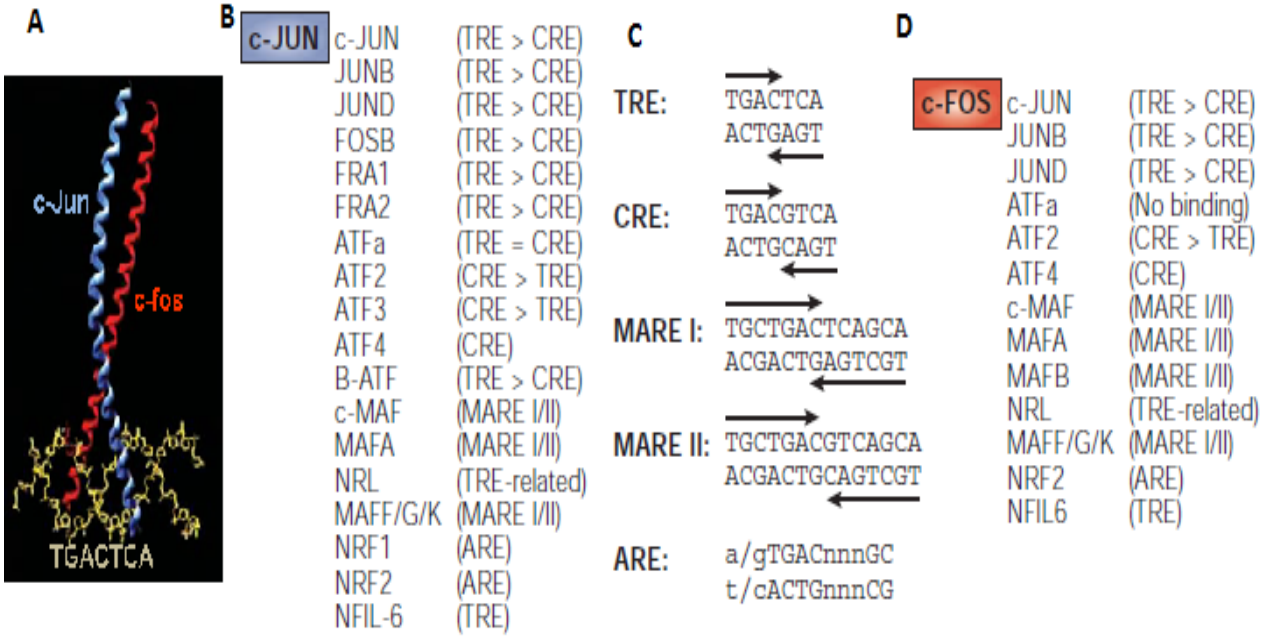

Fig 3.1: The AP-1 transcription factor. AP-1 (activator protein 1) proteins include the JUN, FOS, ATF (activating transcription factor) and MAF (musculoaponeurotic fibrosarcoma) protein families, which can form homodimers and heterodimers through their leucine-zipper domains. The different dimer combinations recognize different sequence elements in the promoters and enhancers of target genes A) The leucine-zipper domain and the adjacent basic domain form an X-shaped α-helical structure in the AP-1 complex, which binds to the DNA backbone B) c-JUN binding partners and the corresponding responsive DNA binding elements C) The main DNA response-element is the TPA-responsive element (TRE), but different dimmers preferentially bind to elements such as the CAMP-RESPONSE ELEMENT (Ambacher *et al.*), the MAF-recognition elements (MAREs) and the antioxidant-response elements (Barnat *et al.*). D) c-FOS binding partners and the corresponding responsive DNA binding elements. NFIL-6, nuclear factor interleukin-6; NRF, nuclear respiratory factor; NRL, neural retina leucine zipper.

From: *Nat Rev Cancer. 2003 Nov;3(11):859-68*

3.2 Regulation of c-Jun phosphorylation

AP-1 activation by JNKs is mainly achieved by phosphorylation of c-Jun N-terminal domain (Davis, 2000). c-Jun N-terminal phosphorylation at serine residues 63, 73 and threonine residues 91, 93 by JNK has shown to induce transcription of several AP-1 target genes, one of which is the c-*Jun* gene itself (Angel *et al.*, 1988). Phosphorylation of c-Jun at both S73 and S63 is important for JNK-induced biological effects. In fact, replacement of these canonical JNK sites of c-Jun with canonical sites for protein kinase A (PKA) phosphorylation abolishes the effect of JNK activation on the induction of c-Jun/AP-1 target genes (Smeal *et al.*, 1991). Similarly, replacement of S63/S73 of c-Jun with alanine residues (JunAA) prevents JNK-mediated (Yang *et al.*, 1997) excitotoxic cell death following exposure to kainate (Behrens *et al.*, 1999).

c-Jun phosphorylation at S63/S73 is induced by a myriad of extracellular signals with either transient or prolonged signalling dynamics (Morton *et al.*, 2003; Vinciguerra *et al.*, 2004) and it functions in diverse physiological pathways, inducing genes involved in cell cycle progression, differentiation and apoptosis (Eferl & Wagner, 2003; Hayakawa *et al.*, 2004; Karin & Gallagher, 2005). Differently T91/T93 phosphorylation by JNK is induced mostly by destructive cues, including genotoxic stress and chemotherapeutic drugs (Morton *et al.*, 2003; Vinciguerra *et al.*, 2008; Madeo *et al.*, 2010). Moreover, T91/T93 phosphorylation requires a priming event at the adjacent T95 (Vinciguerra *et al.*, 2008). Abrogation of this priming site impairs c-Jun activation and lead to selective inhibition of T91/T93 phosphorylation in response to various types of genotoxic stress, including UV radiation and anisomycin (Vinciguerra *et al.*, 2008). Importantly, it has previously shown that in mammal cells the JNK cascade converts damaging stress stimuli in a sensitive switch-like response (Bagowski *et al.*, 2003). Therefore, the differential regulation of the S63/S73 sites versus the T91/T93 may reflect a switch-like response of JNK to genotoxic cues, with small stimuli rising S63/S73 phosphorylation and larger supra-threshold stimuli inducing T91/T93 phosphorylation. Until now, the relevance of c-Jun N-terminal phosphorylation in these processes has been examined only for the S63/S73 sites (Watson *et al.*, 1998; Behrens *et al.*, 1999; Besirli *et al.*, 2005). These studies have shown that S63/S73 phosphorylation is crucial for exitotoxic neuronal

apoptosis. On the other hand, S63/S73 phosphorylation is also involved in neuronal differentiation processes, as neurite outgrowth in PC12 cells (Leppa *et al.*, 1998; Dragunow *et al.*, 2000) and neurotransmitter specification in early neuronal development (Marek *et al.*, 2010). Moreover, S63/S73 phosphorylation is required for c-Jun-dependent induction of inflammatory cytokines in immune-regulatory cells, including spinal astrocytes and Bergman glial cells.

The C-terminal region of c-Jun contains two critical phosphorylation sites, Thr239 and Ser243 which function as docking domain for the F-box&WD domain repeated 7 (FBW7) ubiquitin ligase. This phosphorylation allows the subsequent degradation of c-Jun (Wei *et al.*, 2005). Thr239 residue is phosphorylated by glycogen synthase kinase-3 (GSK3) and this phosphorylation event depends on priming phosphorylation of Ser243 (Morton *et al.*, 2003). In case of viral c-Jun, the phosphorylation of Thr239 is blocked by the substitution of Ser243 with phenylalanine, causing the stabilization of viral Jun protein (v-Jun) (Boyle *et al.*, 1991; Wei *et al.*, 2005). Recently it was been shown that the dual-specificity tyrosine phosphorylation–regulated kinase DYRK2 functions as a priming kinase action on c-Jun (Taira *et al.*, 2012b). Importantly, phosphorylation of c-Jun on both Thr239 and Ser243 is required for the FBW7 ubiquitin ligase engagement at c-terminus domain. On the other side, the phosphatase causing dephopshorylation of Thr239 and thereby giving the stability to c-Jun is yet to be indentified (Fig 3.2).

The stability of c-Jun protein also depends on N-terminal phosphorylation other than C-terminus phosphorylation of c-Jun (Fuchs *et al.*, 1997; Musti *et al.*, 1997). Complete abrogation of N-terminal phosphorylation of c-Jun at all four major phosphorylation sites, i.e. S63&73 and T91&93, will result in a block of FBW7-mediated degradation, independently of the Thr239 and Ser243 phosphorylation. This gives a hint that N-terminal phosphorylation may act as an alternative degradation pathway for preferential removal of the N-terminal activated c-Jun and antagonize the apoptotic JNK signaling (Nateri *et al.*, 2004). It is possible that differently spliced FBW7 isoforms may select the different phosphorylated (S63-T93 or Thr239 & Ser243) substrates (Nateri *et al.*, 2004; Wei *et al.*, 2005).

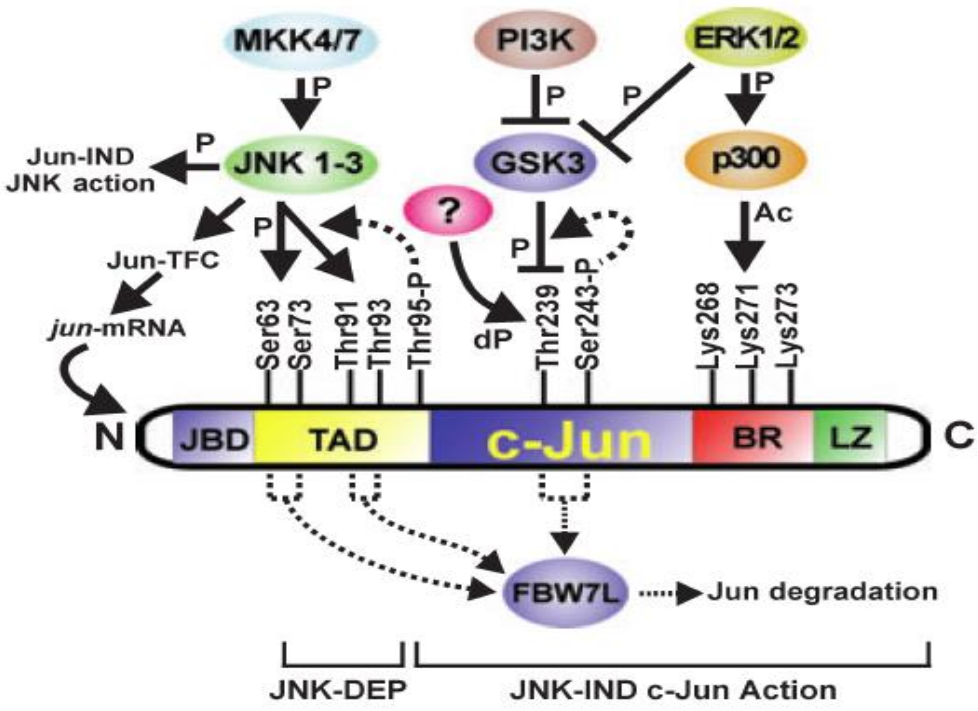

Fig 3.2: Overview of diverging c-Jun activation pathways, via JNK, GSK3 and p300. The scheme shows the c-Jun structural domains, c-Jun phosphorylation sites and kinases that regulate c-Jun phosphorylation. Sharp arrows show activating, and blocked arrows the inhibitory effects, stippled arrows – facilitating effects. The N-terminal and C-terminal ends of c-Jun are marked by N and C, respectively. Ac, acetylating; dP, dephosphorylating; and P, phosphorylating effect; DEP, dependent; IND, independent; JBD, JNK binding domain; TAD, activation domain; BR, basic region; LZ, leucine zipper.

From*: J Neurochem. 2008 Nov;107(4):898-906*

3.3 Modulators of c-Jun activity

c-Jun is an immediate early gene whose expression levels increase within an hour of exposure to a variety of extracellular stimuli. c-Jun is regulated both at the transcriptional and post-translational level (Boyle *et al.*, 1991; Lin *et al.*, 1992), (Pulverer *et al.*, 1991; Smeal *et al.*, 1991). Furthermore, same stimuli may induce both c-Jun expression and N-terminal phosphorylation (Pulverer *et al.*, 1991; Smeal *et al.*, 1991). As previously mentioned, induction of c-Jun transcription by growth factors, tumor promoters or genotoxic stress is mediated by two AP-1/ATF like DNA binding elements present in the c-Jun proximal promoter.

3.3.1 Negative modulators of c-Jun and its cellular functions

1) **Ubiquitination:** Ubiquitination represents a particular case where ubiquitin (Ub), itself a small polypeptide, is linked to lysine residues in a protein to target it for proteasomal degradation (Ciechanover, 1998). It has been demonstrated that c-Jun undergoes degradation by ubiquitination. Three ubiquitin ligases were reported to induce the ubiquitination and degradation of c-Jun. One ligase is the human COP1, which forms a multi-subunit ubiquitin ligase complex, $DCX^{hDET1-hCOP1}$ and promotes c-Jun degradation regardless of c-Jun's phosphorylation status (Wertz *et al.*, 2004; Savio *et al.*, 2007; Migliorini *et al.*, 2011). A second ligase is Itch, whose E3 ligase activity needs to be activated by JNKs through phosphorylation, causing the degradation of c-Jun in a manner independent of c-Jun phosphorylation by JNKs (Gao *et al.*, 2004). The third c-Jun E3 ligase is Fbw7 (also called Fbxw7, CDC4, AGO and SEL10; (Nateri *et al.*, 2004) which forms a ligase complex with SKP1 and CUL1 that is referred to as SCF^{FBW7} (Welcker & Clurman, 2008). C-terminal phosphorylation of c-Jun at T239 by GSK3β (Wei *et al.*, 2005) is required for Fbw7-dependent degradation. In turn, Fbw7 expression and activity impairs neuronal apoptosis allowing c-Jun degradation by the ubiquitin/proteasome system (Fig 3.3)

2) **Sumoylatoin:** Recently, several proteins that share similarity with Ubiquitin (Ub) have been identified. One member of this ubiquitin-like protein family is SUMO-1, a polypeptide of 101 amino acids which can be attached covalently

to proteins in a process that is mechanistically analogous to ubiquitination. It has been shown that c-Jun activation may also be regulated by sumoylation. Sumoylation of c-Jun has been demonstrated to occur at Lys229 (Müller *et al.*, 2000) and at Lys257 (Bossis *et al.*, 2005) Furthermore it has been shown that sumoylation negatively regulates the c-Jun transactivity (Cheng *et al.*, 2005).

3) **DYRK2:** Dual-specificity tyrosine phosphorylation-regulated kinases (DYRKs) constitute an evolutionarily conserved family of protein kinases with key roles in the control of cell proliferation and differentiation. Members of the DYRK family phosphorylate many substrates, including critical regulators of the cell cycle. One characteristic feature of several DYRK kinases is their function as priming kinases, meaning that the phosphorylation of a given residue by a DYRK is prerequisite for the subsequent phosphorylation of a different residue by another protein kinase (GSK3 or PLK). Taira et al. 2012, have shown that DYRK2 expression and activity regulates the levels of c-Jun and c-Myc degradation at the G_1/S boundary. Many tumor cells depend on high levels of c-Jun and c-Myc to enter S phase. Cellular levels of these oncogenic transcription factors are controlled by proteasomal degradation, which is initiated upon phosphorylation by GSK3β. DYRK2 has now been identified as the priming kinase for the phosphorylation of c-Jun and c-Myc by GSK3β. In particular, DYRK2 phosphorylates c-Jun at the T242 priming site for GSK3β phosphorylation at the T239 site, hence allowing Fbw7-dependent degradation of c-Jun (Taira *et al.*, 2012a).

4) **HDACs:** HDACs (Histone deacetylases) are catalytic subunits of multiprotein complexes that deacetylate specific lysines on tail of histones, as well as several other non histone proteins. There is growing evidence for a role of HDACs in neuronal survival. Recent studies provided evidence that HDAC7 and HDAC3-mediated neuroprotection results from inhibition of c-*Jun* expression. HDAC7 inhibits c-Jun transcription by directly associating with c-Jun on the c-*Jun* gene promoter. However, repression of c-Jun transcription by HDAC7 is relieved by c-Jun N-terminal phosphorylation. Furthermore, over-expression of either HDAC3 or HDAC7 impairs cell death of cerebellar

granular neurons upon serum/potassium withdrawal (Weiss *et al.*, 2003; Xia *et al.*, 2007a; Ma & D'Mello, 2011).

5) **Mkp-1:** MAPK phosphatases (Mkp-1) are a family of DUSPs (Dual-specificity phosphotases) that inactivate MAP kinases by dephosphorylation. It has been shown that MKP-1 represses JNK-mediated apoptosis upon γ-radiation in MEFs (Mouse embryonic fibroblasts) (Laderoute *et al.*, 1999). Over expression of Mkp-1 in sympathetic neurons prevents c-Jun N-terminal phosphorylation and c-Jun expression, hence protecting neurons from NGF withdrawal-induced death (Wang *et al.*, 2008; Kristiansen *et al.*, 2010). This study demonstrates that NGF withdrawal leads to JNK-dependent phosphorylation of c-Jun and ATF2., hence inducing the expression of c-Jun/ATF pro-apoptotic target genes, as *dp5*, *bim*, and *puma.* Furthermore, the study shows that ATF binds the *Mkp1 gene* promoter and increases Mkp1 expression, hence acting in a negative feedback manner.

6) **Mbd3/NuRD:** An important mechanism of AP-1 activation is phosphorylation of c-Jun by JNKs. N-terminal phosphorylation of c-Jun activation domain causes the transcriptional activation of several target genes, but the molecular mechanism of target gene activation is not yet clearly understood. Recently, a study by Behrens and collaborators has shown that unphosphorylated c-Jun interacts with Mbd3 and thereby recruits the nucleosome remodelling and deacetylation complex NuRD on its target genes. However, c-Jun N-terminal phosphorylation counteracts Mbd3/c-Jun complex formation, hence resulting in the depression of c-Jun target genes. Subsequently, a co-activator protein binds to c-Jun and further augment the expression of c-Jun target genes. Interestingly, it has been shown the Mbd3/c-Jun complex plays an important role in controlling cellular proliferation in intestinal tumors (Aguilera *et al.*, 2011).

7) **E1A:** Adenoviral induced transformation of cells require E1A interaction with transcriptional regulators, as the transcriptional co-activators p300, also named CREB-binding protein (CBP). E1A and p300/CBP have been shown to affect the transcription levels of common genes (Arany *et al.*, 1995). For example, the c-*Jun* promoter is activated independently by either E1A or p300

(Monique CA Duyndam, 1999). On the other hand, the collagenase promoter is inhibited by E1A, a repression mechanism dependent on the p300/CBP-binding domain of E1A (Dorsman *et al.*, 1995). The binding of E1A to p300/CBP was suggested to be responsible for the effect of E1A on the AP-1 family of transcription factors (Lee *et al.*, 1996; Smits PH, 1996), including c-Jun and c-Fos, which play a central role in proliferation and differentiation. So far, the mechanism of E1A-mediated repression of the collagenase promoter via the c-Jun DBD has been unclear. Similarly, the co-activator CBP/p300 appears to mediate the transcription regulation of c-Jun by E1A, but the mechanism remains unclear. Recently it has been shown that a 12 amino acid motif within the basic region of the c-Jun DBD is required for the repression of c-Jun expression by E1A. Furthermore, the involvement of p300 acetyltransferase activity and c-Jun acetylation at Lys271 seem to be involved in the regulation of collagenease gene expression (Vries *et al.*, 2001).

8) **MEKK1:** c-Jun activity is regulated by mitogen activated protein kinase (MAP) Kinase signaling pathway – MEKK or MKKK – MEK or MKK – MAPK. MEKK1 phosphorylate several substrates and also acts as a ubiquitin (Ub) E3 ligase (Lu *et al.*, 2002). Recent studies have shown that c-Jun is down regulated in response to osmotic stress via ubiquitination-dependent degradation, that seems to mediated by the PHD/RING finger domain of MEKK1, which has E3 ubiquitin ligase activity (Lu *et al.*, 2002; Witowsky & Johnson, 2003). MEKK1 SWIM domain (SWI2/SNF2 and MuDR) represents a novel substrate-binding domain necessary for direct interaction between c-Jun and MEKK1 that promotes MEKK1-dependent c-Jun ubiquitylation (Rieger *et al.*, 2012). Deficiency of MEKK1 has been shown to block posttranslational down regulation of c-Jun in response to osmotic stress (Xia *et al.*, 2007b).

9) **C/EBP alpha:** The transcription factor C/EBP alpha is important for normal myeloid differentiation and inactivation of C/EBP alpha leads to myeloid leukemia. It was shown that c-Jun prevents granulocyte differentiation, as its downregulation is necessary for granulocytic lineage commitment. Down regulation of c-Jun expression was shown to be mediated by C/EBP alpha by

direct interaction with c-Jun, hence abrogating c-Jun binding to its own promoter (Rangatia *et al.*, 2002).

10) **COP1:** constitutive photomorphogenesis protein 1 (COP1), a RING finger ubiquitin ligase targets P53 for ubiquitin degradation, which impairs upon DNA damage and allows the stabilization of P53 (Dornan *et al.*, 2006). It has been also shown that COP1 interacts with c-Jun and modulates its activation (Bianchi *et al.*, 2003). Recent studies using a transgenic mice expressing a COP1 mutant containing a functional E3 ligase RING but lacking the interaction domain WD40, confirmed that the Cop1 negatively regulates cell proliferation in a c-Jun-dependent manner (Migliorini *et al.*, 2011).

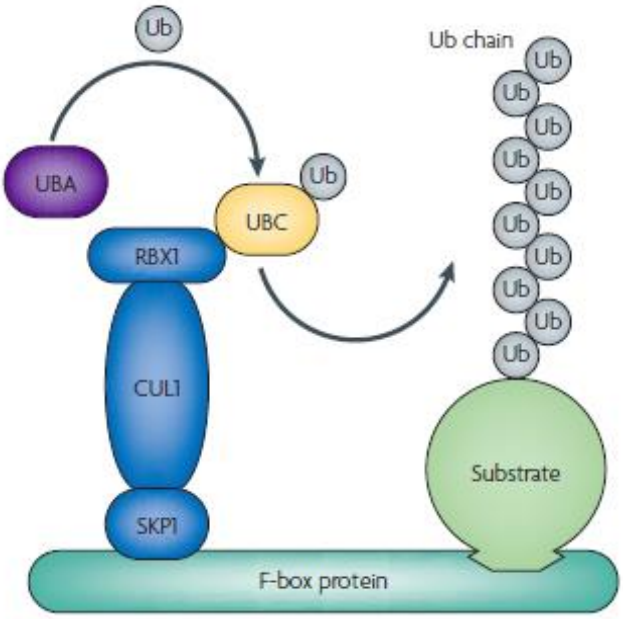

Fig 3.3: Schematic of an E 3 SCF (complex of SKP1, CUL1 and F‑box protein) ubiquitin ligase. The SKP1 (S-phase kinase-associated protein 1)–CUL1 (cullin 1)–RBX1 (RING box 1) core complex recruits substrates (c-Jun) through interchangeable substrate-specific F‑box proteins. RBX1 binds to the E2 ubiquitin-conjugating enzyme (UBC) that was previously charged with ubiquitin (Ub) by an E1 ubiquitin-activating enzyme (UBA). Polyubiquitylated substrates are then targeted for destruction by the proteasome.

From: *Nat Rev Cancer. 2008 Feb;8(2):83-93*

Table:

Modulator	Mechanism	Function
Ubiquitination (Fbw7, COP1, Itch)	Degrades c-Jun protein upon N-terminal phosphorylation dependent and independent manner	Cancer, Neuronal apoptosis
Sumoylation	Sumo-1 conjugation at Lys 242 and 257	---
DYRK	Phosphorylation of c-Jun at Thr242	Breast cancer
HDACs	Inhibition of c-Jun expression	Neuronal cell death
MKP-1	Dephosphorylates JNK and intern reduce the c-Jun activity	Neuronal cell death
MBD3 (NURD)	Unphosphorylated form of c-Jun binds to mbd3 and recruite NuRD repressor complex, which intern releases upon phosphorylation of c-Jun	Intestinal tumors
E1A	Acetylation of Lys271	Proliferation and Differentiation
MEKK1	Ubiquitin degradation	Osmotic stress-Apoptosis
C/EBPalpha	Represses c-Jun binding on DNA promoter	Granulocyte differentiation and apoptosis
Cop1	Reduce the c-Jun activation by ubiquitination	Tumour suppression

Table 3.1: Negative modulators of c-Jun

3.3.2 Positive modulators of c-Jun and its cellular functions

1) **CBP/P300:** Overexpression of p300 leads to efficient stimulation of ATF2 activity, a weak stimulation of the c-Jun activity and no significant activation of either JunD and ATF3. This study also shows that ATF2 is a specific target of p300 and this interaction plays a role in the transactivation of the c-Jun promoter. The CREB binding domain of CBP is sufficient to contact to c-Jun in vitro. Expression of CBP in vivo stimulates c-Jun dependent transcription. Deletion analysis of c-Jun indicates that the CBP binding domain is within the N-terminal domain. Alanine substitutions of S63/73 in c-Jun or the corresponding residues in v-Jun (Ser36/46) leads to reduced binding to CBP in vitro and abolishes augmentation of transcription in vivo. These data are consistent with a mechanism by which CBP acts as a co-activator protein for c-Jun dependent transcription by interacting with the Jun N-terminal activation domain (Arias *et al.*, 1994; Bannister AJ, 1995; Goodman & Smolik, 2000). Furthermore, a phosphorylation independent interaction between CBP and c-*Jun* was also detected (Lee *et al.*, 1996).

2) **RACO-1:** c-Jun is an AP-1 transcription factor known for its role in regulation of cell proliferation, apoptosis and tumorigenesis; however the exact molecular mechanism linking growth factor signaling to c-Jun/AP-1 activation is unclear. Recent studies have shown that RACO-1 (newly identified RING-domain containing protein) is a c-Jun co-activator, linking growth factor signaling to c-Jun/AP-1 activation (Davies *et al.*, 2010; Davies *et al.*, 2013). These studies show that RACO-1 interacts with c-Jun and is both necessary and sufficient for c-Jun/AP-1 activation. Interestingly, coexpression of a constitutively active MEK1 construct, or treatments with the tumour promoter 12-O-tetradecanoyl phorbol 13-acetate (TPA), increased RACO-1 protein levels, hence linking MEK1 activity with c-Jun/AP-1 activation. Moreover, RACO-1 methylation by methyltransferase PRMT1 was shown to induce RACO-1 stability and dimerisation, as well as RACO-1/c-Jun interaction (Davies *et al.*, 2010; Davies *et al.*, 2013).

3) **TCF4:** Nateri *et al.* have shown that the interaction between TCF4 and c-Jun phosphorylated by JNK has an important role in the regulation of intestinal

cancer, thus uncovering a link between JNK and canonical Wnt signaling i.e ß-catenin independent signaling pathway (Veeman *et al.*, 2003). Wnt signaling counteracts ß-catenin degradation, hence allowing ß-catenin to accumulate in the nucleus and to induce gene expression by interacting with members of the LEF/TCF family of transcription factors (Giles *et al.*, 2003). The authors found that N-terminal phosphorylated c-Jun interacts with TCF4 and in turn forms a ternary complex with ß-catenin. The significance of the c-Jun–TCF4 interaction in tumorigenesis was investigated in a mouse model of intestinal cancer that was originated by crossing mice carrying a heterozygous non-sense mutation of the *APC* gene ($Apc^{Min/+}$) with JunAA/+ mice, carrying alanine substitutions of S63/S73 JNK-phosphorylation sites . The authors found that in the $Apc^{Min/+}$; JunAA+/+ mice, lack of c-Jun–TCF4 interaction was associated with an extended lifespan and a reduced number and size of tumors. Furthermore, colon tumor development was prevented in $Apc^{Min/+}$ mice carrying gut-specific knockout of c-Jun. These findings suggest that gut specific inhibition of JNK could result in lack of c-Jun/TCF4 interaction, therefore representing an effective strategy for treatment of intestinal tumors (Nateri *et al.*, 2005).

4) **RACK1:** The c-Jun transcription factor is a highly unstable oncoprotein. As mentioned above several ubiquitin ligases mediate c-Jun degradation. However, c-Jun can be stabilized once it is phosphorylated at the N-terminus by c-Jun N-terminal kinases (JNKs) or other protein kinases (Musti *et al.*, 1997). This phosphorylation decreases c-Jun ubiquitination and degradation. The underlying mechanism for this phenomenon is still unknown. Recently it was shown that the receptor for activated C-kinase 1 (Rack1) can form a complex with c-Jun and ubiquitin ligase Fbw7 (Zhang *et al.*, 2012). However, this study shows that c-Jun is released from the complex upon its N-terminal phosphorylation and cannot be any longer ubiquitinated by Fbw7, suggesting a possible mechanism through which N-terminal phosphorylation of c-Jun augments c-Jun stability. On the other hand, N-terminal phosphorylated c-Jun can still be degraded in shRack1 cells, whereas knockdown of Fbw7 suppresses degradation of JNK-phosphorylated c-Jun. Hao *et al.* (Hao *et al.*, 2007) reported that Fbw7 forms homodimers to efficiently degrade its

substrates. Therefore, the speculation is that Rack1, when over-expressed, might heterodimerise with Fbw7 through the WD40 interaction domain and this might result in more binding to non-phosphorylated c-Jun, but less binding to N-terminal phosphorylated c-Jun. In absence of Rack1, Fbw7 forms homodimers, which bind c-Jun regardless of the phosphorylation status at the N-terminus, thereby targeting N terminal phosphorylated c-Jun for degradation. (Zhang *et al.*, 2012).

5) **Sp1:** Chen et al have demonstrated that c-Jun/Sp1 interaction is essential for growth factor- and phorbol 12-myristate 13-acetate (PMA)-induced genes expression, including human 12(S)-lipoxygenase, keratin 16, cytosolic phospholipase A2, p21(WAF1/CIP1), and neuronal nicotinic acetylcholine receptor beta4. They found that PP2B-dependent dephosphorylation of c-Jun C-terminus (Ser-243) was required for interaction of c-Jun with Sp1 and for the PMA-induced gene regulation (Chen *et al.*, 2007). More recent studies have identified that also calcineurin (Hauwel *et al.*) is involved in the dephosphorylation of c-Jun C-terminus at Ser-243, which in turn increases the interaction between c-Jun and Sp1 and c-Jun-dependent transcription (Huang *et al.*, 2007).

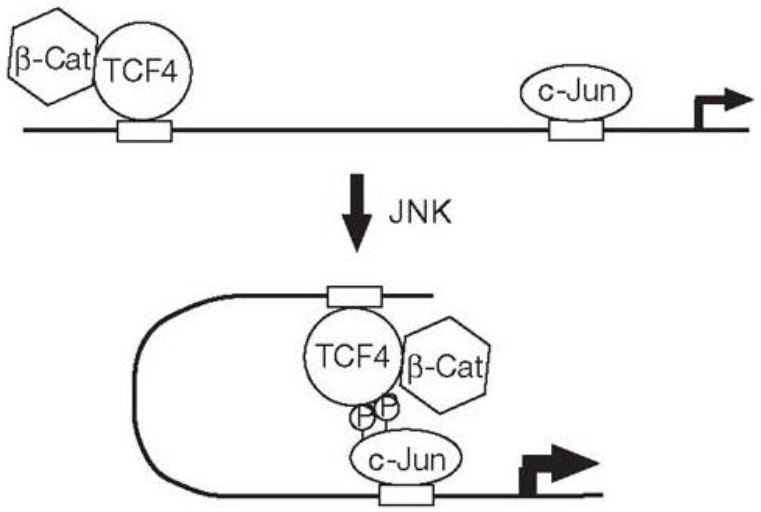

Fig 3.4: Schematic representation of a JNK-dependent interaction between c-Jun and TCF4/ ß -catenin on the c-Jun promoter.

From: *Nature. 2005 Sep 8;437(7056):281-5*

Table 3.2:

Modulator	Mechanism	Function
CBP/P300	p300/CBP enhances c-Jun transcription through two promoter elements, Jun1 and Jun2	Tumours
RACO-1	RACO-1 interact with c-Jun	Intestinal tumour
TCF4	Phosphorylated form of c-Jun binds to TCF4 and forms ternary complex with ß-catenin	Intestinal cancer
RACK-1	Rack1 protects the N-terminal phosphorylated c-Jun from FBW7-mediated degradation	Tumorigenesis
Sp1	dephosphorylation of c-Jun C-terminus (Ser-243) was regulated by PP2B and required for the c-Jun/Sp1 interaction	---

Table 3.2: Positive modulators of c-Jun

3.4 Role of c-Jun in cellular proliferation

A role for AP-1 in the control of cell proliferation has been suggested by the following observations: (i) mitogens stimulate both AP-1 activity, (Donahue *et al.*) ii) expression of various Fos and Jun proteins have distinct expression patterns during cell cycle progression; (iii) cell cycle progression of fibroblasts can be inhibited by intracellular injection of neutralizing antibodies versus various member of AP-1, including c-Jun and c-Fos (Angel & Karin, 1991; Kovary & Bravo, 1991b; Kovary & Bravo, 1991a). Furthermore, the role of c-Fos and c-Jun in cell cycle progression were confirmed by knocking down c-Fos and c-Jun expression in mouse fibroblast and erythroleukaemia (Holt *et al.*, 1986; Nishikura & Murray, 1987; Shaulian & Karin, 2002). In addition, experiments using fibroblasts derived from either c-Fos or c-Jun knockout mice provided genetic support for these conclusions (Brüsselbach S, 1995; Brown *et al.*, 1998) (Johnson *et al.*, 1993; Schreiber *et al.*, 1999). Also, Ha-ras induced transformation of immortalized mouse fibroblasts requires c-Jun and AP-1 expression (Johnson *et al.*, 1996). As regard the role of JNK-mediated phosphorylation of c-Jun in cell proliferation, fibroblasts from c-Jun Ala 63/73 mice have a proliferation defect, indicating that it is important for cell proliferation (Behrens *et al.*, 1999).

c-Jun induction was also shown to be necessary for cell cycle re-entry of fibroblasts after genotoxic stress, as c-Jun -/- fibroblasts undergo prolonged growth arrest and fail to resume proliferation after UV exposure. By contrast cells with constitutive expression of c-Jun fail to arrest and continue to cycle after UV exposure (Shaulian *et al.*, 2000). Presumably, c-Jun negatively regulate p53 transcription by directly binding the p53 promoter, as p53 is upregulated in c-Jun-/- fibroblasts (Schreiber *et al.*, 1999). Furthermore, c-Jun inhibits the expression of the CDK inhibitor $p21^{cip1}$ (Shaulian *et al.*, 2000), a p53 gene target gene that is responsible for antiproliferative activity of p53 (El-Deiry *et al.*, 1993; Xiong *et al.*, 1993). Correspondingly, c-Jun-/- fibroblasts have lower level of G1/CDK activity, due to elevated expression of $p21^{cip1}$ (Schreiber *et al.*, 1999). Hence, it seems that c-Jun regulates cell cycle progression through two different mechanisms: (i) induction of cyclin D1 transcription, (Donahue *et al.*) repression of p21cip1expression. Several AP-1 proteins, including c-Jun, bind to AP-1 regulatory sequences of cyclinD1

(Albanese *et al.*, 1995; Bakiri *et al.*, 2000). In addition, phospho mimicking mutations that replace S63 and 73 of c-Jun with negatively charged residues increases the extent of cyclinD1 induction by mitogens (Bakiri *et al.*, 2000). By contrast, JunB acts as a negative regulator of cell proliferation by repressing cyclinD1 expression and by inducing transcription of the p16Inka gene, a CDK inhibitor blocking Rb phosphorylation by mitogen (Passegue & Wagner, 2000).

As regard tumorigenesis, c-Jun has been shown to be important for the development of both skin and liver tumours. In fact, expression of a dominant-negative c-Jun mutant (TAM67) in basal keratinocytes and a conditional inactivation of c-Jun in the liver, interferes with the development of chemically induced papillomas and liver tumours, respectively (Young *et al.*, 1999; Eferl *et al.*, 2003). Hepatoblasts derived from c-Jun-/- foetuses also display proliferation defect and exhibit extensive apoptosis of hepatoblasts and hematopoietic cells. More importantly, liver regeneration after partial hepatectomy is impaired in absence of c-Jun expression (Behrens *et al.*, 1999).

3.5 Role of c-Jun in central nervous system

Induction of c-Jun expression is a common event in the developing, adult as well as injured nervous system. In the central nervous system (CNS), c-Jun is highly expressed during embryogenesis (Wilkinson *et al.*, 1989; Bennett *et al.*, 1997) and through postnatal day 15 (P15) (Mellström *et al.*, 1991), after then expression decreases to a lower basal level throughout adulthood (Herdegen *et al.*, 1991; Raivich & Behrens, 2006). In the adult brain, c-Jun expression is induced after injury, stress (Herdegen & Waetzig, 2001; Raivich *et al.*, 2004), ischemia and stroke (Jenkins R, 1991; Wessel *et al.*, 1991), as well as in seizures (Morgan & Curran, 1989; Gall *et al.*, 1990; Gass *et al.*, 1993). On the other hand, c-Jun is also induced during learning and memory (Donahue *et al.*, 2002; Konstantin & Steven, 2006), suggesting a functional dichotomy of c-Jun in both injured and unperturbed brain. Functional studies employing in vivo strategies for gene deletion, targeted expression of dominant negative isoforms and pharmacological inhibitors, all appear to confirm a bipotential role of c-Jun in the brain, with a crucial role in neuronal cell death, but also in plasticity and repair (Raivich & Behrens, 2006). However, JNK-dependent phosphorylation of c-Jun is important for neuronal cell death but not for axonal repair, pointing to a complex picture, with only a partial functional overlap between Jun and JNK. Therefore, a better understanding of the non overlapping roles could considerably increase the potential of pharmacological agents to improve neurological outcome during and following brain-damaging conditions; for example by a specific blockade of the unfavourable effects of the cascade during the disease process (Waetzig & Herdegen, 2004).

Neuronal apoptosis contributes to the progression of neuropathological disorders such as stroke and neurodegenerative disease (Mattson, 2000). JNK-dependent activation of c-Jun has been shown to participate to several neuronal death paradigms, including those initiated by beta-amyloid toxicity (Pearson *et al.*, 2006; Thakur *et al.*, 2007; Maria B.Fonseca1, 2012)., trophic factor withdrawal (Eilers *et al.*, 1998; Le-Niculescu *et al.*, 1999), and ischemia (Kuan *et al.*, 2003).

Expression of c-Jun is highly induced in response to neuronal injury (Herdegen & Leah, 1998). Nerve fiber transection results in a characteristic reaction of the injured neuron, the so-called axonal response (also Summary termed cell body response or

chromatolytic response) (Schwaiger *et al.*, 1998; Stoll & Müller, 1999; Goldberg, 2003). On the molecular level, nerve injury results in dramatic changes of the transcriptional program of the injured neuron, some of which are mediated by the induction of immediate-early transcription factors of the AP-1 family (Herdegen & Leah, 1998). How the axonal damage is sensed and converted into a transcriptional nuclear response is unclear. JNKs have been suggested to participate in the initiation of the axonal response, as they are rapidly activated following nerve injury and JNKs can be transported on microtubules along the axon, via their association with motor proteins of the kinesin family (Verhey & Rapoport, 2001). Therefore, it was earlier suggested that the JNK/c-Jun pathway could function as a sensor and trigger the axonal response (Goldstein, 2001).

3.5.1 Role of c-Jun in neuronal cell death

Programmed cell death has been implicated in normal development as well as in the progression of acute and chronic neurodegenerative events, as stroke, spinal cord injury, Alzheimer's disease, Parkinson's disease and Huntington's disease. Several kinases have been involved in regulation of neuronal apoptosis, including GSK3 and JNK protein kinases families.

It has been shown that during embryonic development increase of cell death takes place in coincidence with higher levels of c-Jun expression (Sun *et al.*, 2005). Moreover, it has been found that during brain trauma (Herdegen *et al.*, 1991; Jenkins & Hunt, 1991; Raivich *et al.*, 2004), brain ischemia (Jenkins R, 1991; Wessel *et al.*, 1991) and seizures (Morgan & Curran, 1989; Gall *et al.*, 1990; Gass *et al.*, 1993) c-Jun expression levels are increased. Likewise, c-Jun induction has been observed in human neurodegenerative diseases, such as amylotrophic lateral sclerosis (MIGHELI *et al.*, 1997) and Alzheimer's dementia. In the latter disease, Amyloid-β (Aβ) incubation of neuronal cells results in stress-induced cell death through poorly understood mechanisms (Pearson *et al.*, 2006; Thakur *et al.*, 2007; Fonseca *et al.*, 2012). In a model of Parkinson's disease, where exposure to the neurotoxic chemical MPTP causes degeneration of dopaminergic neurons in the substantia nigra, (Oo *et al.*, 1999; Saporito *et al.*, 1999; Chen *et al.*, 2012), inhibition of JNK/c-Jun pathway reduces MPTP-mediated dopaminergic cell loss (Saporito *et al.*, 1999; Xia *et al.*, 2001; Wang *et al.*, 2004) suggesting that targeting of the JNK/c-

Jun pathway could limit neuronal loss in Parkinson's disease (Silva *et al.*, 2005; Borsello & Forloni, 2007).

As regard studies in primary neuronal cultures, c-Jun has been shown to induce the expression of proapoptoic genes, such as dp5, BIM and PUMA, both in cerebellar granular neurons and sympathetic neurons upon potassium deprivation or trophic factor deprivation, respectively (Whitfield *et al.*, 2001; Besirli *et al.*, 2005; Ma *et al.*, 2007; Towers *et al.*, 2009; Kristiansen *et al.*, 2010). In particular, abrogation of c-Jun expression in postnatal sympathetic neurons has shown that c-Jun is essential for neuronal cell death induced by NGF withdrawal (Palmada *et al.*, 2002). Furthermore, studies in a knock-in mouse model, where the endogenous c-Jun wt gene was replaced by a c-Jun mutant containing alanine substitution of S63-73 (cJunA63-73 mice) (Behrens *et al.*, 1999) have shown that c-Jun phosphorylation at S63/S73 sites is important for cell death by neurotrophic factor deprivation. c-Jun has also been show to be phosphorylated at S63/73 in several other models of neuronal death, including apoptosis of embryonic motoneurons (Sun *et al.*, 2005), cerebellar granule neurons deprived of survival signals(Watson *et al.*, 1998), or in trophic factors-deprived sympathetic neurons (Eilers *et al.*, 2001; Xu *et al.*, 2001). Altogether, these studies suggest that the JNK/c-Jun signaling cascade may be important for developmental neuronal death occurring during the competition of neurons for neurotrophic factors in short supply (Fig 3.5).

Neuronal cell death also increases during inappropriate axonal response to peripheral nerve injury, as failure of axons to reinnervate their target may result in neuronal death, due to lack of trophic support from the peripheral axonal compartment (Sendtner *et al.*, 1996). Interestingly, brain-specific ablation of c-Jun inhibits axon regeneration and muscle reinnervation; however it also prevents axotomy-induced cell death (Raivich *et al.*, 2004). These observations suggest that neurotrophic factors may selectively inhibit the pro-apoptotic function of c-Jun during axonal regeneration. Intriguingly, in a different study, motoneurons from c-JunA63-73 mice were not significantly protected from axotomy-induced cell death (Behrens *et al.*, 1999). This observation raises the question whether signaling pathways regulating c-Jun phosphorylation at T91/T93 are activated in this context. However, so far suitable genetic models to study this aspect of c-Jun activation are missing.

Concerning pathological neuronal cell death, c-Jun phosphorylation at S63-73 is crucial for apoptosis following glutamate neurotoxicity or CNS injury. Primary cortical/hippocampus neurons from cJunA63-73 mice are protected from kainate-induced exitotoxicity (Behrens *et al.*, 1999). Similarly, dopaminergic neurons from c-JunA63-73 mice survive after exposure to radical stress, or transsection of the medial forebrain bundle (Brecht *et al.*, 2005). Conversely, JNK-dependent phosphorylation of c-Jun on S63-73 triggers axotomy-induced apoptosis of dopaminergic neurons (Crocker *et al.*, 2001), or apoptosis of retinal ganglion cells by optic nerve transection (Lingor *et al.*, 2005).

As mentioned above, the functional impact and the regulation of c-Jun phosphorylation at T91-T93 during neuronal death has not been yet elucidated. However, T91/T93 phosphorylation is as important as that of S63-73 for JNK-mediated activation of c-Jun by a variety of stress-signals (Morton *et al.*, 2003; Weiss *et al.*, 2003; Vinciguerra *et al.*, 2008). Moreover, the extent of JNK-dependent phosphorylation of T91-93 and c-Jun activation is tightly dependent on a preceding phosphorylation at the ATM/ATR site T95, suggesting that the integration of different signal-induced pathways is important to activate c-Jun in response to stress (Vinciguerra *et al.*, 2008). In view of these observations, it is important to determine which specific pattern of c-Jun N-terminal phosphorylation is present during different examples of neuronal cell death; as well as to investigate whether and how signaling pathways leading to T91-93 and T95 phosphorylations control c-Jun-mediated neurite outgrowth or c-Jun-mediated cell death, in the context of neuronal injury and regeneration.

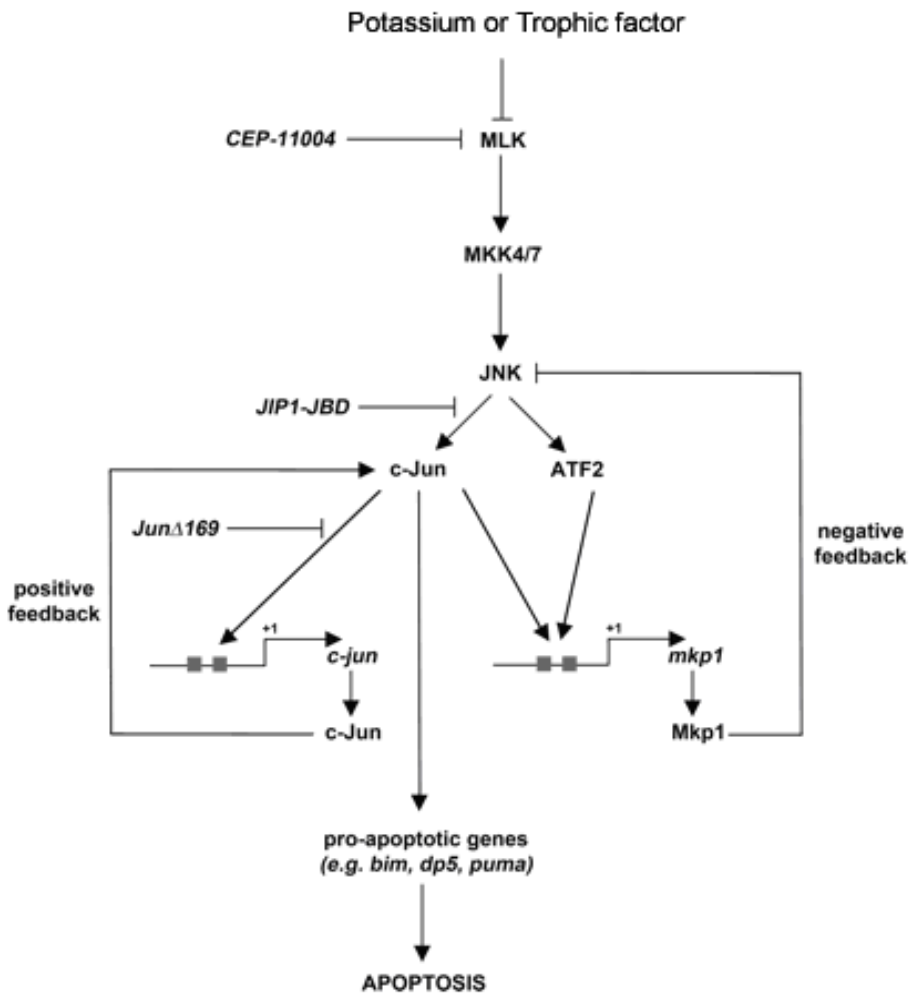

Fig 3.5: Hypothetical model showing the role of the MLK-JNK-c-Jun pathway in trophic factor induced cell death. After NGF or potassium withdrawal, JNK activation leads to phosphorylation of the AP-1 transcription factors c-Jun and ATF2, hence increasing the expression of AP-1 target genes. c-Jun binds to ATF binding sites present in the promoters of *c-Jun* itself (the Jun1 and Jun2 TREs) to enhance its own transcription in a positive feedback manner. c-Jun/Ap-1 also binds to AP-1 sites present in the promoter of pro-apoptotic genes, such as *dp5*, *bim*, and *puma,* as well as to ATF binding sites present in the *mkp1* promoter. This leads to increased expression of Mkp1, which in turn can dephosphorylate JNKs in a negative feedback manner.

From: *The Journal of Neuroscience, August 11, 2010 • 30(32):10820 –10832*

3.5.2 Role of c-Jun in neuronal regeneration

The complexity of polarized neurons needs extremely challenging intracellular signaling pathways to maintain the polarity with defined axonal and dendritic extensions. Following injury, axons of mammalian CNS (Central nervous system) (Tom *et al.*, 2004) do not regenerate, whereas those of PNS do (Peripheral nervous system) (Ertürk *et al.*, 2007). The inability of CNS neurons to regenerate their axons reflects both intrinsic properties of axons and the presence of an inhibitory CNS environment. Upon axonal injury, two phases of regenerative responses takes place: I) rapid and local modifications, as local translation of several proteins involved in the cytoskeleton function (Ex: Importin, vemintin, dynin, actin, GTPases and kinases) (Willis *et al.*, 2005) II) activation of different signaling proteins (Ex: STAT3 and JNK phosphorylation) at injury sites. These events cause cytoskeleton modifications promoting growth cone formation and axonal out growth (Sheu *et al.*, 2000; Charlotta Lindwall, 2012). At later stages, injury signals reach the cell body via retrograde signaling and turn on either regenerative programs or cell death programs (Shin *et al.*, 2012).

Analysis of c-Jun conditional knock out in CNS has shown no phenotypical changes and mice lacking *c-Jun*^{f} in neural cells (*c-Jun*$^{\Delta n}$) were born with Mendelian frequency and were viable and fertile (Raivich *et al.*, 2004). *C-Jun*$^{\Delta n}$ mice lacked neuronal c-Jun immunoreactivity but showed normal brain histology and normal expression of neural markers such as NeuN, MAP-2, neurofilament, synaptophysin, and GFAP. However, by using a well described experimental model of facial nerve transection, Raivich and collaborators have shown that *c-Jun*$^{\Delta n}$ mice had significantly diminished whisker hair motor neurons performance compared to control mice (*c-Jun*^{f}) at both 4 and 15 weeks following facial nerve transection (Raivich *et al.*, 2004). After transection of the facial nerve, the absence of c-Jun caused severe defects in several aspects of the axonal response, including perineuronal sprouting, lymphocyte recruitment, and microglial activation. c-Jun-deficient motorneurons were atrophic, resistant to axotomy-induced cell death, and showed reduced target muscle reinnervation. Furthermore, the axotomized facial motoneurons from *c-Jun*$^{\Delta n}$ mice showed a strong failure in upregulating the expression of galanin, α7β1 integrin and CD44, suggesting that these molecules are crucial for c-Jun-dependent axonal

outgrowth. Importantly, the promoters of both galanin and CD44 genes contain AP-1 sites, which were shown to be functional target site for c-Jun-mediated transactivation (Lee *et al.*, 1993; Anouar *et al.*, 1999).

Activation of both JNK and c-Jun has been also observed in the nuclei of adult rat NG (Nodose ganglia) and DRG (dorsal root ganglia) sensory neurons, following axotomy of the vagus and sciatic nerve, respectively. Using retrograde tracing, it was shown that p-c-Jun and ATF3 were present in regenerative DRG sensory neurons. Furthermore, inhibition of c-Jun activation by two different types of JNK inhibitors prevented axonal outgrowth in NG and DRG sensory neurons. These results indicate that c-Jun activation is associated with axonal outgrowth (Lindwall & Kanje, 2005). Similarly, Trent A. Watkins et al (Watkins *et al.*, 2013) have demonstrated that disruption of either DLK (an upstream regulator of c-Jun) or c-Jun strongly reduces axon re-growth in optic nerve crush, suggesting that the DLK/c-Jun axis is necessary for axonal regrowth upon optic nerve crush.

The striking regenerative capacity of the PNS depends on the surprising plasticity of Schwann cells, capable of switching between differentiation states (Jessen & Mirsky, 2005; Jessen & Mirsky, 2008; Jopling *et al.*, 2011). Schwann cells are principal glia of pheripheral nervous system (PNS). They mainly function to support the conduction of nervous impulses along axons, nerve development and regeneration Glial cells function to support neurons and are involved in important aspects of peripheral nerve biology – the conduction of nervous impulses along axons, nerve development and regeneration, trophic support for neurons and so on. Schwann cell dedifferentiation takes place when cells lose contact with injured axons. This represents a beneficial injury response in the distal stump of cut nerves, as denervated and dedifferentiated cells promote axon regrowth and nerve repair. The instability of myelin differentiation can however also be harmful, as evidenced in demyelinating neuropathies, where metabolic disturbances, immune assault, or genetic abnormalities lead to debilitating dedifferentiation and loss of myelin. Dedifferentiated Schwann cells can readily redifferentiate and myelinate axons if conditions are appropriate. Therefore, these cells can potentially choose between two states throughout life: the myelinated state or the immature/denervated state. Exciting progress has also been made in identifying a group of cell-intrinsic factors in

Schwann cells, including the transcription factors Krox-20 (Egr-2), Sox-10, Oct-6 (SCIP, Tst-1, POU3fl) and NFκB, which act as positive regulators of myelination. Negative transcriptional regulators of myelin differentiation are transcription factors c-Jun, Sox-2, Pax-3, Krox-24 (Egr-1, NGF1A/zif268), and Egr-3. In particular, c-Jun is expressed in immature Schwann cells and is repressed by Krox-20, which is essential for myelination. Also, c-Jun blocks myelination in neuron–Schwann cell co-cultures, it opposes the function of Krox-20 and cAMP-related myelin signals, and drives the dedifferentiation of early myelinating cells back to the immature Schwann cell phenotype (Fig 3.6) (Parkinson *et al.*, 2004).

Recently, Peter J et al (rthur-Farraj *et al.*, 2012) clearly demonstrated that c-Jun activation in Schwann cells is a global regulator of Wallerian degeneration. c-Jun governs major aspects of the injury response, as the expression of trophic factors, adhesion molecules, the formation of regeneration tracks and myelin clearance. A key function of c-Jun is the activation of a repair program aiming to maintain the dediffentiated Schwann cell phenotype. Conversely, c-Jun depletion results in the formation of a dysfunctional repair cell, striking failure of functional recovery and neuronal death (rthur-Farraj *et al.*, 2012).

A different study (Fontana *et al.*, 2012) investigated the molecular mechanism by which c-Jun controls the ability of Schwann cells to support motoneuron survival and axonal regeneration after peripheral nerve injury. This study demonstrates that c-Jun is required for the expression of neurotrophin genes like *Artn*, *BDNF-1*, *GDNF*, *LIF*, and *NGF* purely depends on the expression of c-Jun. Abrogation of c-Jun expression leads to down regulation of these neurtrophin causing a poor functional recovery of neurons (facial nerve) and a poor survival of motoneurons. They also found that cell-specific inactivation of the Ret gene in neurons resulted in regeneration defects, without affecting motoneuron survival. Conversely, administration of recombinant GDNF and Artemin protein substantially ameliorated impaired regeneration caused by c-Jun deficiency.

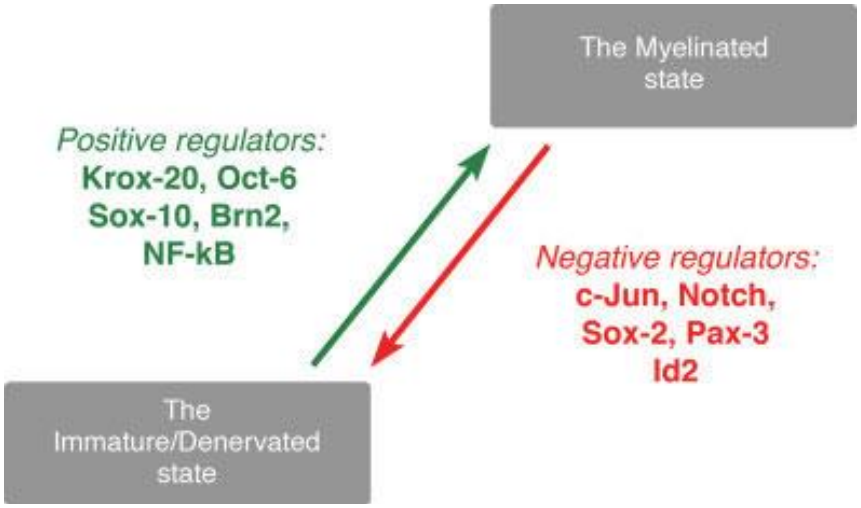

Fig 3.6: A model of the transcriptional regulation of myelination. The myelination status of Schwann cells can be viewed as being determined by the balance between opposing signaling systems. Positive regulators (green) dominate in normal nerves, while the balance shifts to negative regulators (orange) in injured and pathological nerves. During development, negative regulators may also take part in timing the onset and rate of myelination. In vivo evidence for the negative regulators shown only exists for c-Jun and Notch at present, while the molecular identity of the positive regulators is better established.

From: *Glia. 2008 Nov 1;56(14):1552-65*

3.5.2 Role of c-Jun in neuronal Inflammation

Several studies have shown a crucial role of the JNK/c-Jun pathway in the expression of inflammatory cytokines in activated immune-regulatory cells of the cerebrum and spinal astrocytes (Waetzig *et al.*, 2005; Raivich, 2008; Haeusgen *et al.*, 2009). In contrast, little is known about the expression and activation of c-Jun in Bergmann glial (BG) cells, the radial unipolar astrocytes playing important roles in cerebellar development and physiology (Yamada & Watanabe, 2002). BG cells develop from radial glial cells in the ventricular zone and then their somata migrate towards the Purkinje cells layer (PCL) in synchrony with Purkinje cells. In the mouse cerebellum, migration of BG somata starts at embryonic day 14 and ends at postnatal day (P) 7, when they align next to the PCs and establish a monolayer emitting radial fibers to the pial surface (Yamada *et al.*, 2000). During postnatal development of the cerebellum, Bergmann glia provides a scaffold for the migration of newly generated granule cells (GC) (Rakic, 1971; Hatten & Mason, 1990). Moreover, BG cells establish functional interactions with Purkinje cells and have been shown to regulate dendritic arborisation and synaptogenesis of these neurons (Yamada & Watanabe, 2002). Like other astrocytes, Bergmann glial cells respond to neuronal damage with morphological and functional changes, hence becoming reactive or activated glial cells (Furuoka *et al.*; Lafarga *et al.*, 1991; Lafarga *et al.*, 1998).

In vivo, BG gliosis has been associated to loss of Purkinje cells in several examples of cerebellar dysfunctions (Duchala *et al.*, 2004; Liu *et al.*, 2005; Ishida *et al.*, 2007; Weimer *et al.*, 2009). However, molecules and pathways participating to pro-inflammatory functions of BG cells have been poorly elucidated. Neuronal/glial cerebellar cultures from neonatal mice have been widely used to study the response of glial cells to different stimuli (Sass *et al.*, 2001; Ejarque-Ortiz *et al.*, 2007)Previous studies have shown that upon treatments with bacterial LPS, a potent activator of glial cells, these cultures express pro-inflammatory cytokines. However, the exact signaling pathway and glial cell types involved in cytokine induction have not been yet determined. We have used this type of cell cerebellar culture to assess putative functions of c-Jun in activated Bergmann glial cells. We found that c-Jun is highly expressed in the nucleus of radial astrocytes derived from Bergmann glia and its activation by JNK is required for the induction of IL-1β expression in response to bacterial LPS (Albanito *et al.*, 2011).

4 Materials and Methods

4.1 Device manufacturer

SDS polyacrylamide gel electrophoresis Mini Protean Tetra Cell

BioRad, Munich, Germany

Semi-dry western blot chamber Trans-blot SD, Semi-dry transfer cell

BioRad, Munich, Germany

Power supplies Standard Power Pack P25

Powerpac HC 250V 3A 300W

BioRad, Munich, Germany

Centrifuges Centrifuge 5417R

Centrifuge 5804R

Centrifuge 5810R

Eppendorf, Hamburg, Germany

Heat block Thermomixer 5437

Thermomixer comfort

Eppendorf, Hamburg, Germany

Thermocycler personal

Thermocycler gradient

Eppendorf, Hamburg, Germany

Horizontal agarose gel PEQLAB Biotech. GMBH

electrophoresis chamber Erlangen, Germany

Cryostat Modell CM 1950, Leica, Wetzlar, Germany

Confocal microscope FluoView FV1000, Olympus, Hamburg

TCS SP2, Leica, Wetzlar, Germany

X-ray developer X-Omat 2000, Stuttgart, Germany

Tissue homogenizer for RNA POLYTRON PT2100

Photometer BioPhotometer

Eppendorf, Hamburg, Germany

Tissue sonication for protein lysates UP50H - Compact Lab Homogenizer

Nanodrop-Spektrophotometer PEQLAB Biotech. GMBH

4.2 Materials

4.2.1 Laboratory animals

All used mouse lines were housed in the central animal facilities of the University of Wuerzburg. The animal care and ethic committees of our institutions approved all described procedures and experiments. C57Bl/6 mice were used for generation of cerebellar granule cells cultures. Mice carrying a floxed c-Jun allele (c-Jun fl) (Behrens *et al.*, 2002), were kindly provided by Dr. Axel Behrens from Cancer Research UK. c-Jun fl/fl were crossed with mice expressing Cre recombinase beneath the control of Nestin promoter (Tronche *et al.*, 1999) and crossed again to generate c-Jun fl\fl-nestin-Cre+ mice (c-Jun Dn), in which both c-Jun alleles are inactivated in cells derived from embryonic neuroepithelium, resulting in CNS-specific inactivation of c-Jun fl, as previously described (Raivich *et al.*, 2004).

4.2.2 Cell lines

1. HEK293T cells
2. HELA cells
3. PC12
4. NSC34 cells

4.2.3 Chemicals

Unless mentioned all the chemicals used in this study were of analytical grade and purchased from the following companies: Applichem, Amersham, Calbiochem, Chemicon, Fluka, Fermentas, Merck, Invitrogen, Sigma and Roth

4.2.4 Cell culture

- **Components for cerebellar granular neuron**

Bergmann Glia and Microglia	**Source/ Company**
Neurobasal Medium	Invitrogen
Glutamax	GIBCO
Hank's Balanced Salt Solution (HBSS)	PAA
Horse Serum	Linaris
B-27 Supplement	GIBCO

Laminin	Invitrogen
Trypsin (1%)	Worthington
Trypsin Inhibitor (1%)	Sigma
Poly-D-Ornithine	Sigma
1X Phosphate Buffer Saline (PBS)	PAA
0.075M Potassium chloride	Sigma
AraC (Cytosine-1-β-D-arabinofuranoside)	Sigma
DNase I	Sigma
LPS (Lipopoly Sacharide)	

❖ Components for lentivirus production source/company

OptiMEM	Invitrogen
DMEM (high glucose) +HEPES	Invitrogen
MEM	Invitrogen
Fetal Calf Serum	Linaris
Penicillin / Streptomycin	Invitrogen
DMSO	Sigma
Lipofectamine2000	Invitrogen
Glutamax	Life Technologies
Geneticin.(G418)	Invitrogen

❖ Components for 4% paraformaldehyde solution (4% PFA)

1.6g PFA

20ml Distilled water

3 dry pellets of NaOH

Warmed in 60°C water bath till PFA is dissolved.

16.4 ml Na2HPO4 (0.2 M)

3.6 ml NaH2PO4 (0.2M)

pH 7.1 – 7.4

- **Preparation of Mowiol® 4-88 mounting agent. (Polysciences Europe GmbH)**

1. Mix using a magnetic stirrer, 4.8g Mowiol® 4-88 and 12g glycerol (100ml beaker)
2. Add 12ml ddH2O and continue stirring till a clear solution is formed at room temperature.(at least 4 hrs)
3. Add 24ml 0.2 M Tris HCl (ph 8.5). Continue stirring. Heat occasionally to 50°c in a water bath (10 min).
Continue stirring until Mowiol is dissolved.
4. Spin down the solution at 500 x g for 15 minutes to get a clear solution at the top.
5. Preserve the supernatant and store aliquots at -20°c

4.2.5 Buffers and solutions

- **10mM Tris EDTA buffer (TE buffer) (1L)**
  - 10ml 1M Tris-HCl (pH 8.0)
  - 2 ml 500 mM EDTA (pH 8.0)
- **Mouse tail lysis buffer:**
  - 0.1M Tris-HCl (pH 8.5)
  - 5mM EDTA (pH 8.0)
  - 0.2% SDS
  - 200mM NaCl
- **Annealing buffer:**
  - 100mM K-acetate
  - 30mM HEPES-KOH pH 7.4
  - 2mM Mg-acetate
- **Qiagen buffer 1**
  - 50 mM Tris HCl pH 8.0
  - 10 mM EDTA
  - 100 ug/ml RNase A
  - Stored at 2-8C after addition of RNase A
- **Qiagen buffer 2**
  - 200 nM NaOH

  - 1% SDS
- **Qiagen buffer 3**
  - 3 M Potassium acetate, pH 5.5
- **SOC medium**
  - SOB medium
  - 20g tryptone
  - 5g yeast extract
  - 0.58g NaCl
  - 0.19g KCl
  - 4ml 1M NaOH
  - dd H2O to 1 litre and autoclave. Just before use add: 5ml 2M MgCl2 / L
  - For SOC 20 mM of filter sterile glucose is added to SOB
- **RIPA**
  - Tris-HCl: 50 mM, pH 7.4
  - NP-40: 1%
  - Na-deoxycholate: 0.25%
  - NaCl: 150 mM
  - EDTA: 1 mM
- **Lysis buffer I**
  - 20mM tris PH 8.0
  - 20% glycerol
  - 1mM EDTA
  - 5mM MgCl2
  - 0.1M NaCl
  - 5mM DTT
  - protease inhibitor
- **Refolding buffer**
  - 50mM Tris PH 8.0
  - 1.0 M L-Arginin
  - 0.5mM EDTA
  - 5mM glutathione oxidised
  - 2mM glutathione reduced and protease inhibitor

- **Dialysis Buffer**
  - 20mMTris
  - 0.1mM EDTA
  - 10% Glycerol
  - 150mM NaCl

4.2.6 Kits

- 1st strand cDNA synthesis kit for RT-PCR (AMV) Roche
- NucleoSpin_ Plasmid Machery & Nagel
- Big-Dye Terminator Mix Applied Biosystems
- QIAquick® gen Gel Extraction Kit Qiagen
- QIAquick® PCR Purification Kit Qiagen
- Endofree® Plasmid Maxi kit Qiagen
- mouse IL-1β ELISA kit (Pierce/Thermo scientific)
- Pierce GST Spin purification Kit (Thermo scientific)
- In Situ Cell Death Detection Kit- TMR red- Roche
- RNeasy Mini Qiagen Kit (Qiagen)

4.2.7 Plasmids

Clone Name	**Vector backbone**	**Source**
pGEX (GST-cJun wt)	pGEX-4T1	(Vinciguerra et al 2008)- Self cloned
pGEX (GST-cJun A95)	pGEX-4T1	(Vinciguerra et al 2008)- Self cloned
pGEX (GST-cJun A63/73)	pGEX-4T1	(Vinciguerra et al 2008)- Self cloned
FUWG (c-Jun wt-HA)	Fu_eGFP_TrkB	Self cloned in this work
FUWG (c-Jun A95-HA)	Fu_eGFP_TrkB	Self cloned in this work
FUWG (c-Jun D95-HA)	Fu_eGFP_TrkB	Self cloned in this work
FUWG (c-Jun A63/73-HA)	Fu_eGFP_TrkB	Self cloned in this work
FUWG (c-Jun Panala-HA)	Fu_eGFP_TrkB	Self cloned in this work

Table 4.1: List of Plasmids Used

4.2.8 Antibodies for Immunocytochemistry

Primary Antibodies

Antibody	Company	Source	Dilution
Pax2	Abnova	anti mouse	1:50 (IHC)
GLAST	Millipore	anti guinea pig	1:100 (IHC)
anti-GFP	Abcam	anti Chicken	1:1000 (IHC)
c-Jun total	Cellsignalling	Anti rabit	1:1000 (Westernblot) 1:100(IHC)
c-Jun ser63	Cell Signalling	Anti rabit	1:1000 (Westernblot) 1:200 (IHC)
c-Jun Thr91	Cell signalling	Anti rabit	1:1000 (Westernblot) 1:200 (IHC)
S100	Sigma	Anti mouse	1:100 (IHC)
GFAP	Sigma	Anti mouse	1:2000 (IHC)
Calbindin	Sigma-Aldrich	Anit mouse	1:2000 (IHC)
NeuroD1	Abcam	Anti mouse	1:2000 (IHC)
NeuN	Millipore	Anti mouse	1:2000 (IHC)
Pax6			
TLR4/MD2	BioScience	Anti mouse	1:100 (IHC)
CD11b	eBioscience	Anti rat	1:100 (IHC)
HAtag	Biovision	Anti mouse	1:500 (IHC) 1:1000 (Westernblot)
JNK/SAPK	Cell signalling	Anti rabit	1:1000 (Westernblot)
MCM7	Santacruz	Anti mouse	1:1000 (Westernblot)
Tuj1	Neuromics	Anti mouse	1:1000 (IHC)
Tub a	BioScience	Anti mouse	1:500 (IHC)
Neurofilament	Abcam	Anti Rabit	1:1000(IHC)

Table 4.2: List of primary antibodies used

Secondary antibodies

Antibody	Host species	Company	Dilution
Cy5	goatanti- mouse IgG mouse	Jackson	1/800-1/1600 (IHC)
Cy 3	Goat Anti- Rabbit IgG (H+L) Rabbit	Jackson	1/350 (IHC)
DyLight488	goatanti- rabbit IgG Rabbit	Jackson	1/800 (IHC)
Alexa 488	Goat Anti- Rabit IgG Rabbit	Jackson	1/5000

Table 4.3: List of secondary antibodies used

4.2.9 Oligonucleotide sequences

	Forward- 5' to 3'	Reverse- 5' to 3'
Actin	GTGGGCCGCCCTAGGCACCAG	TCTTTAATGTCACGCACGATTTC
ccl2	AGCACCAGCCAACTCTCACT	GGGCGTTAACTGCATCTGGC
IL- 1β	TGAAGGGCTGCTTCCAAACC	AGCTTCTCCACAGCCACAAT
IL-18	ACAACTTTGGCCGACTTCAC	GGGTTCACTGGCACTTTGA
c-Jun loxp	CTCATACCAGTTCGCACAGGCGGC	CCGCTAGCACTCACGTTGGTAGGC
c-Jun Flox	CTCATACCAGTTCGCACAGGCG	CAGGGCGTTGTGTCACTGAGCT
IL-1	CTAGGCCACAGAATTGAAAGATCT	GTAGGTGGAAATTCTAGCATCATCC
GST-c Jun	CGCGGATCCATGACTGCAAAGATG	CCGGAGCTCTGGGTTGAAGTTGCT
FUGW Jun	GGATCCATGACTGCAAGATGG	GCGGCCGCTTATCATCTAGAC

Table 4.4: List of primers used

4.3 Methods

4.3.1 Animals

All used mouse lines were housed in the central animal facilities of the University of Wuerzburg. The animal care and ethic committees of our institutions approved all described procedures and experiments. C57Bl/6 mice were used for generation of cerebellar granule cells cultures. Mice carrying a floxed c-Jun allele (c-Jun fl) (Behrens *et al.*, 1999), were kindly provided by Dr. Axel Behrens from Cancer Research UK. c-Jun fl/fl were crossed with mice expressing Cre-recombinase beneath the control of Nestin promoter (Tronche *et al.*, 1999) and crossed again to generate c-Jun fl\fl-nestin-Cre+ mice (c-Jun Dn), in which both c-Jun alleles are inactivated in cells derived from embryonic neuroepithelium, resulting in CNS-specific inactivation of c-Jun fl, as previously described (Raivich *et al.*, 2004).

4.3.2 Cell culture

4.3.2.a Cultures of cerebellar granular neurons

Cerebellar granule cell cultures were generated from either C57Bl/6 P7 mice as previously described (Albanito *et al.*, 2011). Briefly, mice were deeply anesthetized and injected with saline solution to remove the blood. After the removal of meninges and choroid plexus, cerebella were trypsinized with BME media containing 1% trypsin and DNase I (2mg/ml) for 15 min at 37^0C and then triturated in HBSS containing 10 U/mL DNAse I (Roche Diagnostics). Cells were centrifuged at 2,000 rpm for 7 min and resuspended in BME (Sigma) containing 4 mM glutamine, 10% fetal bovine serum, 100 U/mL Penicillin/streptomycin, and 25 mM KCl (Sigma-Aldrich). After counting, cells were plated on pre-coated Poly-DL-ornithine hydrobromide (PORN- Sigma) glass coverslips (3.5 X 106) or six-well multiwell plates (5 X 106 density). Cultures were maintained at 37oC, 5% CO2, and media were changed every 2 days. After 24 hrs in culture treat the cells with Ara-C for 1 day (Cytosine-1-%-D-arabinofuranoside) to remove proliferating and non neuronal cells. All experiments were performed 6 days after plating (DIV6). For serum potassium withdrawal experiments cells where treated with either 5mM KCl (LK) or with 25mM KCl (HK) for 4hrs to check phosphorylation levels on western blot or treat for 18hrs for apoptotic assays.

4.3.2.b Generation of cerebellar neuronal/glial primary culture

Neuronal/Glial primary cultures were isolated from dissociated cerebellum of 4 day old C57Bl/6 pups. Mice were anesthetized and injected with saline to remove blood and meninges and choroid plexus were removed. Cerebellum was kept in Hank's BSS containing trypsin-DNase and incubated at 37^0C water bath for 10min. Cerebellum was swirled gently every 5 minutes and washed 3 times with HBSS, then triturated the cerebellum in 5ml of BME medium containing DNase and tissue was dissociated by pipetting up and down for ten times from top and ten times by pressing the pipette tip more firmly against bottom of the tube. Now centrifuge the cells at 2000g for 5min at 4^0C. Supernatant was removed and resuspended the granular cells in BME medium containing 10%FCS, 25mM Kcl, 100U/ml penicillin and streptomycin and cells were plated in 10cm petridish for 20min to attach the Bergmann glial cells to bottom, and remaining cells which are floating were decanted. After counting, cells were placed on Poly D,L-ornithin precoated cover slips at 7x10p5 density or six well plate at 8x10p5 density.

4.3.2.c Cultures of cerebral microglial cells

Microglial cultures were made from C57Bl/6 P4 mice as previously described (Polazzi & Contestabile, 2006). Briefly, brain tissue was cleaned from meninges, trypsinized for 15 min and, after mechanical dissociation cell suspension, was washed and plated on poly-L-lysine (Sigma) coated (10 Ag/mL) flasks (75 cm2). Mixed glial cells were cultured in BME (Sigma) supplemented as described above. After 12 days, microglial cells were harvested from the mixed primary glial cultures by mild shaking (200 RPM for 2 h) and collected by centrifugation. After counting, cells were plated as described above.

4.3.2.d PC12 cell culture

PC12 cell line was cultured on poly-D-lysine coated dishes in media containing DMEM (Invitrogen Ltd.) supplemented with 10% horse serum, 5% FCS, 2mM glutamine and penicillin/streptomycin. Cells were grown at 37oC in 5% CO2. For neurite outgrowth, cells were plated at a density of 1X106 cells per 9 cm dish. Once cells were at 60-70% confluent PC12 cells were treated with 50 ng/ml of NGF and maintained for 3 days. PC12 transfections with DNA constructs expressing c-Jun

proteins were performed by using Lipofectamin 2000 reagent (Invitrogen) following manufacture instructions. After transfections, cells were cultured in absence of NGF for 72 hours, then were fixed and processed for immunofluorescensce analysis.

4.3.2.e Cell death and survival assay

Cell death of CGCs was assessed by examining nuclear morphology following DAPI (4′,6′-diamidino-2-phenylindole hydrochloride) staining as previously described (Morrison *et al.*, 2006). Briefly, DAPI stain (0.5µg/ml) was added directly to PBS or to secondary antibody and incubated for 20 minutes at room temperature. Cells were visualized by fluorescence microscopy (SP2 Leica fluorescent microscope). A minimum of 1000 cells were analyzed per treatment. To confirm that condensed nuclei indeed denotes apoptotic cell, we co-stained the DAPI with TUNEL staining (In Situ Cell Death Detection Kit- TMR red- Roche) according to manufacturer's protocol. It is worth noting that in our experimental settings 100% of TUNEL-positive cells were stained as condensed nuclei by DAPI, indicating that this is a valuable assay to measure cell death (see Fig: 6.1).

4.3.2.f Immunocytochemistry

DIV6 cerebellar granule cultures and PC12 cells were permeabilized with a blocking solution containing 0.3% TritonX-100, 10% Goat serum, 0.1% BSA in TBS for 2 hrs at room temperature. Then, cells were incubated over night at 4°C with the following primary antibodies: anti-rabbit c-Jun (Cell Signalling 1:200), anti-rabbit phospho-c-Jun-Ser63 (Cell Signalling 1:200), anti-rabbit phospho-c-Jun-Thr91 (Cell Signalling 1:200), anti-rabbit phospho-c-Jun-Thr93 (Cell Signalling 1:200); or Anti-mouse HA-tag (Biovision), anti anti-mouse NFL (eBioscience). After removing primary antibodies, cells were washed three times (10 min each) with TBS and then incubated in permeabilization solution with Alexa-Fluor-conjugated secondary antibodies for 2 hrs at room temperature. Cells were then treated with DAPI for 10 min to stain the nuclei (Sigma-Aldrich 1:8,000). Finally, cells were washed three times with TBS for 10 min and one time with PBS and mounted by using Mowiol (Sigma-Aldrich). Pictures were taken with the SP2 confocal microscope from Leica. Configurations of c-Jun N-terminal phosphorylation were analysed by

immunocytochemistry 4 hours after treatments by using site-specific c-Jun antibodies recognizing c-Jun when phosphorylated at either S63 or at T91/T93.

4.3.2.g Immunohistochemistry

Perfusion of mice: Clean the mice with 70% ethanol, cut open the abdomen skin to expose abdominal aorta and vena cava. Insert needle in left ventricle and cut immediately the vena cava with forceps. Start perfusion with 4% PFA for 10-15 min to get perfect perfusion. Once perfusion is done remove the cerebellum from brain and leave it in 4% PFA for 2hrs. Wash the tissue with 1XPBS and start hydration by using 10% sucrose leave it for some time. Add drops of 30% sucrose in to tissue containing 10%sucrose and leave for some time until tissue dip in the solution. Change the sucrose solution with fresh 30% sucrose and leave the tissue for overnight in 4^0C. Now place the dehydrated tissue on to tissue base mold. Cover entire tissue block with cryo-embedding media (tissue teck). Slowly place the base mold containing the tissue block into liquid nitrogen till the entire block is submerged into liquid nitrogen to get tissue frozen completely. Store the tissue block in -80^0C until ready for sectioning. Transfer the frozen tissue on to cryotome cryostat (-20^0C) prior to section. Section the frozen tissue into 30µm thickness using cryotome and place the sections on to glass slides. Dry the tissue sections for overnight in room temperature. For immunostaining of the sections mark the tissue with PapPen. Block the slide sections with blocking solution for 1hr. After one hour add the primary antibody (dilute in blocking solution) to the section and leave it for overnight in 4^0C. Next day wash the slide with PBS+0.3% TTX for three times for 5min each. Add the secondary antibody (dilute in blocking solution) to slide, leave for two hours at room temperature. Wash the slide again with PBS+0.3% TTX for three times for 5min each. Mount the slide with cover slip by using aqua poly/mount.

4.3.3 Molecular Biology techniques

4.3.3.a Cloning

1. Restriction enzyme digestion and analysis of DNA fragment

Cloning was done using standard laboratory manual of Sambrook et al. For restriction digestion of plasmids for cloning, 2.0µg DNA was used with 2-5units of restriction enzyme and appropriate buffer depending on the restriction enzyme used. The reaction volume was 50µl. For the cloning of PCR products, the entire volume of the PCR (50µl) was purified using PCR purification kit (Qiagen) and used for the restriction digestion. The reaction was incubated at 37°C for 2-6 hours and analyzed by gel electrophoresis on 0.8% to 2% agarose gel in 1XTAE buffer depending on the size of the expected DNA fragment to be analyzed using UV detector.

2. Polymerase chain reaction (PCR)

DNA vectors expressing HA-tagged human c-Jun proteins were used as templates to amplify c-Jun coding regions that were subsequently cloned into the FUGW vector (Lois *et al.*, 2002) through the BamHI–NotI digestion.(Vinciguerra *et al.*, 2008) The following primers were used for c-Jun sequence amplification: forward 5‘-GGA TCC ATG ACT GCA AGA TGG 3’ and reverse 5‘GCG GCC GCT TAT CAT CTA GAC3. A standard PCR reaction was done as followed: 25ng DNA,1.5µl each of forward and reverse primer (10pmole), 5µl 3prime PCR buffer, 1µl eppendorf triple master mix proof reading DNA polymerase, 1µl 10mM dNTPs and made up the volume to 50µl with H2O

cycle conditions:

Denaturation	5 min 95°C	35x
Melting conditions	30 sec 95°C	
Annealing conditions	30 sec primer specific	
Extension condition	2.5 min 72°C	
	10 min 68°C	
hold	15-22°C	

The amplified product was analysed by gel electrophoresis and nanodrop was used for measuring the concentration of the DNA.

3. Ligation of restriction enzyme digested DNA

The vector backbone and the insert are analysed on agarose gel and the concentration of the DNA is estimated with the help of the marker. Around 25ng of vector was used and 125ng of insert was used for the ligation reaction.

Vector DNA	25ng
Insert DNA	125ng
T4-DNA-ligase	1µl
10x ligase buffer	2µl

Filled up to a total volume of 20µl with water

At the same time a parallel control only containing vector DNA and no insert is performed to test the vector religation. The reactions were incubated overnight at 16°C.

4. Transformation of chemical competent *E.coli*

Thaw the BL21 competent cells or TOP10 chemically competent E.coli cells on ice. Approximately 7µl (50ng) Ligation mixture containing circular DNA was added to competent cells and incubated on ice for 30 minutes. Subsequently the transformation mixture was heat shocked in 42°C water-bath for 90secound. The mixture was kept on ice for two minutes to reduce damage to BL21 cells. Add 1ml L.B (With no antibiotic) medium or SOC medium to transformation mixture. The Tubes were incubated at 37°C for one hour. 10% of transformed cultures were streaked on to LB agar plates with appropriate antibiotic. The agar plates were then incubated at 37°C for overnight. For analysis of positive clones single colonies were picked up from agar plates and inoculated in 5ml of LB medium containing appropriate antibiotic and grown the cells at 37°C for overnight. Next day plasmid DNA was extracted from these cultures by using alkaline lysis method.

5. Isolation of DNA

200ml LB medium containing appropriate antibiotic was inoculated with the positive clone and Endofree maxi kit (Qiagen) was used to isolate DNA suitable for transfection. In general, the bacterial cells were grown overnight at 37oC in a shaker incubator. The bacterial pellet was obtained by centrifuging the bacteria at 6000rpm for 20min. the medium was removed and the pellet was subjected to alkali lysis method of DNA isolation by resuspending in buffer P1 containing RNAse to which, 10ml of lysis buffer P2was added and gently mixed by inverting the tube up and down several times to lyse the bacterial cells. The reaction was neutralized by neutralization buffer P3 to precipitate the protein. The supernatant was passed through cartage to clear the solution. 2.5ml of buffer EB was added to the solution and incubated for 30min of ice to make it endotoxin free. The DNA was column purified and then precipitated with isopropanol. The DNA was pelleted by centrifuging at 15000rpm at 4oC for 30min. The DNA pellet was washed with 70% endofree ethanol, air dried and dissolved in 100µl of endofree TE buffer. The concentration and purity was determined using the nanodrop device by checking the OD at 260 and measuring the OD260/280 ratio respectively.

6. Sequencing of the DNA

DNA sequencing was performed by Sanger sequencing (Sanger et al., 1977) using terminator dye (Applied Biosystems). This causes the four used dideoxynucleotides (ddNTP), lacking the 3´-OH group to get incorporated and labelled with a different fluorescent dye. The fragments of the PCR reaction thus generated are of various lengths depending upon the incorporation of the dideoxynucleotides. These fragments are separated by size by capillary electrophoresis. At the end the sequence is identified by scanning the fluorescent signals of chains separated by size. The sequencing was done by following protocol:

PCR reaction:

DNA	500ng
Termination-mix	2µl
5x sequencing buffer	4µl
Primer	15pmol

Fill up to a total volume of 20µl with HPLC water

Cycle conditions:

10 sec	96°C	25X
4 min	60°C	
5 min	60°C	
hold	22°C	

The PCR product was precipitated by adding 50µl of 100% ethanol and 2µl of 3M sodium acetate. The DNA was pelleted by centrifugation at 14000rpm for 20min at 4°C. the pellet was washes twice with 70% ethanol, air dried and dissolved in 20µl of Hi-Di formamide and used for sequencing capillary loading.

4.3.3.b Production of lentiviral particles

A HIV based lentiviral expression system has been used in this study. The Δ8.9 and VSVG vectors were used as helper plasmid for packaging FuVal expression vector. HEK293T cells were used for packaging. The cells were propagated in DEMEM + 10%FCS in 3, 125 cm flasks up to 90% confluence. On the day of packaging, following reaction was set up in two 50ml reaction tubes:

Protocol for 6 Plates

Day1:

Tube 1		**Tube 2**	
Opti-MEM	9ml	Opti-MEM	9ml
D8.9	45.0µg	Lipofectamin 2000	216µl
VSVG	30.0µg		
Expression plasmid	18.0µg		

Transfection:

The above both reaction mixes were incubated for 5min in Room temperature. Mixed the both reaction and incubated in room temp for 30min

Splitting cells:

The cells were washed with 10ml PBS and the cells were harvested by trypsinization with 0.1% trypsin and incubated the cells for 10 min at 37oC and then centrifuged at

14000 rpm for 5 min and the pelleted cells were resuspended in 30ml optimem with 10%FCS. This was then mixed with the transfection mix making the volume to 48ml. this was then distributed in 6, 10cm petridishes with 8ml each and incubated in the cell culture incubator over night.

Day2: Washing and media change

The cells were washed with PBS and the medium was changed to Neurobasal with 1%glutamax and 2%B27 packaging medium 12 ml in each petridish and were incubated for 48hours. The transfection efficiency was estimated by microscopic examination.

Day 3: check the cells for cell growth and transfection rate by observing fluorescence.

Day 4:

Viral Harvesting

Two SW28 ultracentrifuge tubes and rotor buckets were sterilized with 70% ethanol. Pre-cool the ultracentrifuge to 4^0C. Supernatant from 10cm dishes collected in 50ml falcons and centrifuged at 3,600 rpm for 15min at room temperature in standard cell culture centrifuge. During the run, prepare Millex HV 0.45 filters and 50ml syringes. Few drops of PBS were added to filters to prewet. Supernatant from 50ml falcons were filtered. Filled each SW28 tubes with filtered supernatant, and underlayed the tubes with 4ml of 20% sterile sucrose. Tubes were equilibrated to same level with TBS-5 buffer. Falcons were centrifuged for 2hrs at 25,000 rpm at 4^0C. Supernatants were removed by suction and don't disturb the pellet (appears like an opaque spot) at bottom of tube. Immediately 100µl of ice-cold TBS-5 buffer was added to each pellet, tube were covered with parafilm and kept on Ice and placed the ice box in refrigerator at least for 3hrs or overnight.

Re-suspension of viral pellets

Pellets were dissociated in 100µl TBS-5 buffer by gently pipetting up and down without air bubbles and aliquot the re-suspended viral supernatant in -80^0C.

4.3.3.c Isolation of total RNA

Isolation of total RNA by RNeasy Mini Qiagen protocol:

Cultured cells were Washed in ice cold PBS. Added 200µl of RLT buffer to each well and scraped the cells and collected in 1.5ml eppendorf. Lysate is passed through a

20-gauge needle attached to sterile plastic syringe at least 10times or until a homogeneous lysate is achieved. Equal volume of 70% ethanol has been added to homogenized lysate and mixed well with pipett. Up to 700µl of sample has been added to RNeasy spin column and placed in 2ml collecting eppendorf. Centrifuged the column for 15sec at 10,000rpm and discarded the flow through. 700µl of RW1 buffer added to RNeasy spin column and centrifuged at 10,000rpm for 15sec. Flow through was discarded. Next added 500µl of RPE buffer to column, spin at 10,000 rpm for 2minuts. Discarded the flow through and eluted the RNA by adding 50µl of RNase free H_20 and centrifuge at 10,000 rpm for 1minut.

4.3.3.d Reverse transcriptase polymerase chain reaction

The total RNA isolated by using the qiagen kit was used as the starting material to prepare cDNA by the enzyme reverse transcriptase. This cDNA was used as a template for conducting the PCR reactions by using gene specific primers. For the synthesis of cDNA and the subsequent PCR reactions, the RT-PCR kit from Invitrogen, namely, SuperScript™ III First-Strand Synthesis was used. The procedures involving the preparation of cDNA from the total RNA are summarized in tabular formats presented below.

Denaturation: RNA+Primer (R) + dNTPs (10µl)
65^0C for 15min

Place on ice for at least 1min

↓

Annealing Gene specific primer (10pm) + 10X RT Buffer 1µl + 25mM Mgcl2 4µl + 0.1 M DTT 2 µl + Superscript III RT 1µl

↓

cDNA Synthesis 50 ^{0}C for 50min

↓

Terminate Reaction 85^0C for 5min

↓

Remove RNA Add 1µl RNase H 37^0C for 20min

4.3.3.e Quantitative realtime PCR

Total RNA has been isolated according to RNeasy mini kit protocol (Quiagen). After extraction, RNA was treated with RNAse free DNAse (Promega) for 30 min at 37^0C. The cDNA synthesis was done according to the protocol using the SuperScript Strand cDNA Synthesis kit (Invitrogen). Then, cDNA was diluted five fold in PCR-grade water and amplified with gene-specific oligonucleotide primers by using LightCycler DNA Master SYBR Green I Kit (Roche) on light cycler 1.5 according to manufacturer's instructions. Melting curve analysis was performed to ensure specific PCR product while excluding primer dimers. For each sample, relative levels of target gene transcript were calculated as the ratio of Ct value of target gene to that of GAPDH.

4.3.3.f Genotyping of c-Jun Knock out mice

The head from E14 embryos were put in 300µl lysis buffer and 20µl Proteinase K (20mg/ml).

Incubate head samples at 600C for overnight in a thermomixer. Isolate DNA from the dissolved head.

Add 450µl of 5%SDS and 150µl 3M NaCl and vortex. Add 750µl Chloroform and vortex and centrifuge at 40C for 10min at 14000rpm.

Take the upper phase in a 2ml reaction tube and add 750µl Chloroform and vortex and centrifuge at 40C for 10min at 14000rpm.

Take upper phase in a 1.5ml reaction tube (approximately 600-650µl) add 100% ethanol to a final volume of 1ml.

Mix and centrifuge at 40C for 10min at 14000rpm.

Wash with 500µl 70% ethanol and centrifuge at 40C for 10min at 14000rpm.

Dry the pellet and dissolve in 100µl of TE buffer for over night. Use this as DNA sample for the PCR.

Reaction Conditions: following reaction was set up for the genotyping with the help of PCR amplification. Standard PCR reaction was set up to make 50µl reaction volume with 1 µl DNA, 5 µl 10 x PCR buffer,1 µl dNTP (10 mM), 1 µl each forward and reverse primer (10pmol/µl) with 0.3µl Taq polymerase (5-prime) and make up the volume to 50µl with H2O.

Denaturation	3 min 95°C	35x
Melting conditions	30 sec 95°C	
Annealing conditions	30 sec primer specific	
Extension condition	30 sec 72°C	
	10 min 72°C	
hold	15-22°C	

The product size for the genotyping is 600bp for *c-Jun-/-;* and 300bp & 350bp for *c-Jun+/-*

4.3.3.g Southern blot

Digest 10µg genomic DNA in 100µl total volume with 3 units of BamHI restriction enzyme per µg DNA at 37^0C for 6hrs. Add 6x DNA loading buffer to digested DNA.

Agarose gel electrophoresis:

0.8% of agarose gel was made and submerged gel in 1X TAE buffer with 0.5µg/ml of ethidium bromide. Loaded the samples with HindIII lambda marker. Electrophores at 25 Volts, 35mAmp for overnight (12-16hrs). Photograph with fluorescent ruler

Protein transfer:

Soak the gel in 0.2N HCl until the dye front turns into yellow or keep it for 20min. Now wash the gel with water. Denature the gel by soaking in at least two gel volume of 0.5 N NaOH + 1.5M NaCl solution for 15min twice. Wash the gel again with water. Now soak the gel in 1M tris base + 3M NaCl (PH 7.4) solution for 30min twice. Soak the gel and nylon membrane in 6X SSC for 10min. Now set up transfer in large electrophoresis tray: Fill the transfer buffer (12xSSC) into the two side trays. Place the following items (gel sized, saturated with transfer buffer) on the middle support. All air bubbles should be carefully removed by rolling with glass pippett.

- Wick (3mm paper), this should be same width as gel and long enough to dip into well which contain transfer buffer.
- 3 pieces of Whatmann 3mm paper
- Gel (Upside down)
- Nylon membrane
- 3 pieces of Watmann 3mm paper
- Dry 5cm stack of paper towel (Bunch)

- Glass plate with Weight (1.0K.g)

Surround the gel with plastic wrap or parafilm to prevent the paper towels to come in contact with the wet paper below the gel. Prevent evaporation of transfer solution by sealing with plastic wrap or parafilm on either end of the tray. Let the transfer for overnight.

Next day, take the blotting material and mark the position of the wells with pencil. Dry the membrane at 85^0C for 1hr. Place the dry membrane on paper towel and immobilize the DNA by UV cross linking (100mJ/$cm^{2,}$ push 'optimal cross- linking').

Prehybridisation (2hrs):

Place the membrane in hybridization bottle with 20ml (min. 100µl/cm^2) of prehybridization buffer. Incubate at 63^0C for 2hrs

Prehybridization Buffer (20ml):

Reagent	Final conc.	Volume	mass
Deionized formamide	50%	10ml	
20X SSPE	6x	6ml	
50x Denhardt's reagent	5x	2ml	
20% SDS stick solution	0.5%	500µl	
Salmon Testes DNA (sigma D-9156)		100µg/ml	
10.4mg/ml, boil 5min before use			
dH_20 add to 20ml		1.3ml	

Radioactive labelling of probe:

Amplify your PCR product from DNA (probe) and purify the PCR product with PCR purification kit. Label 50ng PCR probe with ^{32}P using the Prime It® Random primer labelling Kit (Stratagene 300385).

Supplies & Equipment:

- Primer It® random Primer Labelling Kit
- Water bath 37^0C
- Water bath 100^0C
- Microfuge

Reagents:

- Random 9mer primers or specific primers from PCR or sequencing reaction (10ng/µl)

- (A-^{32}P) dCTP
- dNTPs (single tube in powder form)
- Exo Klenow fragment of DNA polymerase I (4u/µl)
- Stop mix

Procedure:

Following things add to bottom of microfuge tube containing dNTPs:

50ng of PCR template (1.5µl)

dH_20 – 40.5µl

Boil the reaction tube in water bath for 5min, centrifuge briefly at room temperature to collect condensed liquid from cap of tube.

Add 5µl isotope dCTP (4u/µl) and 3µl of polymerase mix well and incubate reaction at 37^{0}C for 5-10min. Stop the reaction by adding 2µl of stop solution. Purify the probe with either one of following kits:

- Nuc Trap probe purification push columns (Strategene 400701), for DNA or RNA probe 17bp – 5 kb
- Qiaquick PCR purification Kit (Qiagen 2804) for DNA probes 100bp – 10kb

Now count the radioactivity of probe. Take 1µl probe, dilute with appropriate amount of scintillation fluid, and use same amount of scintillation fluid as negative control count. You should have 1-5x 10^6 cpm per ml hybridization reaction. Denature the probe by boiling for 5min and chill on ice immediately before use.

Hybridization:

Add denatured probe to pre-hybridization solution and incubate overnight at 63^{0}C in hybridization oven.

Washing (at 65^{0}C):

Wash hybridized membrane with 2x SSC+0.1% SDS for 10min. Again was with same buffer for 30min. Then wash membrane with 0.2x SSC+0.1% SDS for 30min and repeat this for two times.

Detection:

Wrap moist blots in plastic wrap prior to autoradiography. Expose to X-ray film with an intensifying screen at room temperature for 48hrs.

4.3.4 Protein biochemistry

4.3.4.a Purification of recombinant protein

1. **Inoculation**

Primary inoculation was done in 5ml L.B medium & grown the culture at 37^0C for overnight. 1ml of primary inoculum was added to 500ml of T.B medium containing ampicillin. Cultures were grown 37^0C until O.D reaches 0.5. Cultures were induced with 0.5mM IPTG for 3hrs at 37^0C. Cultures were centrifuged at 8000rpm for 15min to collect the bacterial pellet.

2. **Cell lyses**

Pellet was suspended in 10ml of lysis Buffer I (20mM tris PH 8.0, 20% glycerol, 1mM EDTA, 5mM MgCl2, 0.1M NaCl, 5mM DTT & protease inhibitor). Pellet was sonicated three times for 30sec each. Lysozyme (50mg/ml) was added to the pellet and incubated for 30min at room temperature and centrifuged at 12000 rpm for 25min. Pellet was resuspended in 10ml lyses buffer I and added 0.5% TTX. Pellet was sonicated twice for 30sec and centrifuged at 12000rpm for 25min. Pellet was resuspended in 10ml of buffer I and sonicate twice for 30sec and centrifuge at 12000rpm.

3. **Solubilisation of Inclusion body**

Dissolve the pellet in 10ml Buffer II (20mM Tris PH 8.0, 0.1mM EDTA, 5mM DTT and 6M guanidium hydrochloride and add protease inhibitor before use). Stir the pellet for 2hrs to overnight in 4^0C till pellet dissolve. Aliquot the dissolved pellet and store at 80^0C for further use

4. **Refolding of protein**

Add 2ml of dissolved inclusion body to 20- 25ml of refolding buffer (50mM Tris PH 8.0, 1.0 M L-Arginin, 0.5mM EDTA, 5mM glutathione oxidised, 2mM glutathione reduced and protease inhibitor). Leave the protein sample at 4^0C for 3 days. Take the protein sample and dialyse against 20mMTris, 0.1mM EDTA, 10% Glycerol and 150mM NaCl for overnight at 4^0C. Aliquot the protein and store at 80^0C for further assays.

5. **Pierce GST spin purification**

Remove bottom tab from the Pierce Glutathione spin column by gently twisting. Place the column into centrifuge and centrifuge at 700g for 2min to remove storage

buffer. Equilibrate the column with two resin bed volumes of Equilibration/Wash buffer. Allow buffer to enter the resin bed and centrifuge at 700xg for 2min to remove buffer. Add 500µl of prepared protein (dissolved and dialysed) to column and for maximal binding incubate the column at 4^0C for 30-60min on an end-over-end rocking platform. Centrifuge the column at 700g for 2min and collect the flow through for analysis. Now wash the resin with two bed volumes of wash buffer for 3times and centrifuge at 700g for 2min. Now elute the GST tagged protein from resin by adding one resin bed volume of elution buffer. Now centrifuge the column at 700g for 2 minutes and collect the eluted protein. Repeat the step for three times.

4.3.4.b In Vitro kinase assay

Kinase assays were performed by using purified GST-c-Jun proteins as substrates (1 µg) and either active recombinant JNK1 (Millipore, 20 ng/20µl reaction) or GSK3 β (Biovision, 5ng/20µl). Assays were performed in a total volume of 20µl, containing 1x kinase buffer (50 mM HEPES [pH 7.4], 1 mM MgCl2, 20 mM beta-glycerophosphate, 1 mM Na3VO4, 0.2 mM dithiothreitol [DTT], 1µM pepstatin A, 1 mM PMSF, Protease inhibitor and 10mM ATP). Reactions were stopped by the addition of SDS sample buffer (100 m*M* Tris [pH 6.8], 2% SDS, 10% glycerol, 5% beta-mercaptoethanol, and 0.25% bromophenol blue). Phosphorylation of GST-c-Jun proteins were analysed by western blot analysis using either pS63 or the pT91/93 phospho-specific c-Jun antibodies described above.

Kinase assays were also performed by using either c-Jun-Ha immunocomplexes or recombinant FL c-Jun protein (200ng, Enzo life sciences) and either active recombinant JNK1 (Millipore, 20 ng/20µl reaction) or GSK3 β (Biovision, 5ng/20µl). Assays were performed in a total volume of 20µl, containing 1x kinase buffer (50 mM HEPES [pH 7.4], 1 mM MgCl2, 20 mM beta-glycerophosphate, 1 mM Na3VO4, 0.2 mM dithiothreitol [DTT], 1µM pepstatin A, 1 mM PMSF, Protease inhibitor and 10mM ATP). Reactions were stopped by the addition of SDS sample buffer (100 m*M* Tris [pH 6.8], 2% SDS, 10% glycerol, 5% beta-mercaptoethanol, and 0.25% bromphenol blue). Phosphorylation of c-Jun proteins were analysed by western blot analysis using either pS63 or the pT91/93 phospho-specific c-Jun antibodies described above.

4.3.4.c Immunoprecipitation

HEK 293T or NSC-34 cells were plated at density of 5million ($5x10^6$) cells per 10cm dish and 18 hours later were transfected by using Lipofectamin 2000 reagent (Invitrogen) with FUGW-c-Jun constructs. 48 hours later total proteins extracted with RIPA buffer as previously described . Primary antibodies, either anti-rabbit c-Jun antibodies (Cell Signalling 9165) or sepharose-conjugated mouse HA antibodies (Covance clone 16B12 monoclonal) were added to total cell extracts and incubated overnight at 4°C. Immuno-precipitated proteins complexes were collected (Vinciguerra *et al.*, 2008)d by using Protein A–agarose beads (Roche) previously washed with PBS and equilibrated with RIPA buffer. After 1 hour incubation, pellets were collected by centrifugation at 1,000 *g*, and beads were washed three times with RIPA buffer. For in vitro phosphorylation assays, immunocomplexes were equilibrated in kinase buffer.

4.3.4.d Western blot

Total lysates were prepared from cerebellar primary cultures by using 1x Laemmli buffer (100mM Tris-HCl, pH6.8, 2% w/v SDS, 20% v/v glycerol, 4% v/v β-mercaptoethanol) and then heating at 100 C for 10 min. The samples were then cooled for 10 min on ice and collected by centrifugation at 14000 rpm for 15 minutes. Proteins were electrophoresed under reducing condition on 10% polyacrilamide gel and transferred onto Hybond C nitrocellulose membrane (Amersham). The membranes were first incubated overnight at 4°C with a rabbit anti c-Jun (Cell Signalling 1:1000), anti rabbit phospho-c-Jun Ser63 (Cell Signaling1:1000) and MCM7 (Santa Cruz 1:2000). Blots were then incubated with peroxidase-linked anti-rabbit (1:6,000, Pierce) or anti-mouse (1:6,000, Chemicon) IgG conjugates for 1 hour at room temperature. Signals were detected with the ECL system (Amersham Biosciences).

4.3.4.e Luciferase assay

For luciferase assays, CGCs were plated into 24-well plates with 500 µl of regular growth medium/well and at DIV5 were transfected using calcium phosphate method as previously described (33). In brief, transfection-solutions contained 87.6 µl of HBS- Hepes-buffer saline and 4.4 µl of 2.5 M calcium chloride with 1.0 µg of either c-Jun-Wt or c-Jun-A95, 250ng of Jun2 Luc and 20ng of Renilla plasmids. 35 µl of

transfection solutions was added to a total of 500 µl of HBSS and added to cells. Precipitation was allowed for 50 min. Then cells were washed with HBSS medium twice and incubated with condition medium. Luciferase activity was then measured using the Dual Luciferase Kit (Promega) according to the manufacturer's recommendations. Firefly luciferase activity was normalized to the internal transfection control provided by the Renilla luciferase activity. The normalized relative light unit values obtained from cells transfected with empty vectors and cultured at 25mM K were set as one-fold induction.

4.3.4.f IL-1beta immunodetection by ELISA

IL-1β release was measured by enzyme-linked immunosorbent assay (ELISA). A mouse IL-1β ELISA kit (Pierce/Thermo scientific) was used to quantify the presence of IL-1β in the supernatant of DIV6 neuronal/glial cerebellar cultures from P4 C57Bl/6 mice, treated with 100 ng/mL LPS for 24 h. Conditioned media were then collected, and the assay was completed following the manufacturer's instructions. Sample absorbance was measured with a spectrophotometric system (1420 Multilabel Counter Victor 2; Wallac) at 450 nm. The actual IL-1β concentration was estimated on the basis of a standard curve at known concentration of recombinant mouse IL-1β (provided by the Kit).

1. **Sample preparation**

100µl per well of Bergmann glia culture supernatant is required. Store the samples to be assayed within 24 hours at 2-8°C. For long-term storage, aliquot and freeze samples at -70°C. Avoid repeated freeze-thaw cycles when storing samples. Test samples and standards must be assayed in duplicate each time the ELISA is performed. Gradually equilibrate samples to room temperature before beginning assay. Reconstitute the standard with ultrapure water. Mix by gently inverting vial. The reconstituted standard will be at 4000pg/mL. Label eight tubes, one for each standard curve point: 2000, 1000, 500, 250, 125, 62.5, 31.25 and 0pg/mL. Prepare 1:2 serial dilutions for the standard curve as follows: Pipette 250µL of Standard diluent into each tube. Pipette 250µL of the reconstituted standard into the first tube (i.e, 2000pg/mL) and mix. Pipette 250µL of this dilution into the second tube (1000pg/mL) and mix. Repeat the serial dilutions (using 250µL) five more times to complete the standard curve points.

2. Assay procedure

Sample Incubation

Add 100µl of Standards or test sample in duplicates to each well. Mix the well by gently tapping the plate several times. Cover the plate with new adhesive cover. Ensure all edges and strips are sealed tightly. Incubate 2hrs at room temperature. Remove cover and wash the plate three times with wash buffer by using squirt bottle to fill wash buffer vigorously to each well.

3. Biotinylated antibody reagent Incubation

Add 100µL of Biotinylated Antibody Reagent to each well containing sample or standard and attach new adhesive cover, ensure all edges and strips are tightly sealed. Incubate the plate for one hour at room temperature, 20-25°C. Carefully remove the adhesive plate cover, discard plate contents and wash three times with wash buffer

4. Streptavidin-HRP solution preparation and Incubation

Prepare Streptavidin-HRP Solution immediately before use. For each strip, mix 2.5µL of Streptavidin-HRP Concentrate with 1mL of Streptavidin-HRP Dilution Buffer. Store Streptavidin-HRP Concentrate reserved for additional strips at 2-8°C.Add 100µL of prepared Streptavidin-HRP Solution to each well. Carefully attach a new adhesive plate cover, ensuring all edges and strips are tightly sealed. Incubate plate for 30 minutes at room temperature, 20-25°C. Carefully remove the adhesive plate cover, discard plate contents and wash three times with wash buffer.

5. Substrate Incubation and stop step

Pipette 100µL of TMB Substrate into each well. Allow colour reaction to develop at room temperature in the dark for 30 minutes. Do not cover plate with aluminium foil or a plate sealer. The substrate reaction yields a blue solution that turns yellow when Stop Solution is added. After 30 minutes, stop the reaction by adding 50µL of Stop Solution to each well.

6. Absorbance measurement

Note: Evaluate the plate within 15 minutes of stopping the reaction. Measure the absorbance on an ELISA plate reader set at 450nm and 550nm. Subtract 550nm values from 450nm values to correct for optical imperfections in the microplate. If an absorbance at 550nm is not available, measure the absorbance at 450nm only. When the 550nm measurement is omitted, absorbance values will be higher.

4.3.4.g Mass spectrometry and protein Identification

1. **Materials**

Solvents (CH3OH, CH3CN, and H2O, HPLC grade), reagent (CH3COONa, KCl, EDTA, pure g99.5%), trifluoroacetic acid (HPLC grade, pure g99.0%), pepsin, and 3,5-dimethoxy-4-hydroxycinnamic acid (pure g99.0%), R-cyano-4-hydroxy-trans-cynnamic acid (R-CHCA, pure g99.0%) were purchased from Sigma Aldrich Fluka (Milano, Italy). HAP (BIO-GEL HTP) was purchased from Biorad (Milan, Italy).

2. **In-gel digestion**

For MS analysis, the spots of interest were excised from 1-DE gels and analyzed by matrix-assisted laser desorption ionization/time-of-flight (MALDI-TOF/TOF). After SDS PAGE, discrete band was excised from the blue-coomassie-stained gel. The in-gel digestion with proteinase K was carried out as previously described (Napoli *et al.*, 2010). To obtain extensively cleaved protein the digestion was performed at 37 °C for 18 hrs twice. Peptides were subsequently extracted twice with 100 µL of 50% ACN/2% trifluoroacetic acid (TFA); the extracted solutions were then combined and dried with the Speed Vac concentrator. The peptide pellets were then resuspended in 100 µL of 40% ACN/0.1%. For MS MS/MS experiments, the peptic peptide mixture (10µL) was desalted and concentrated in ZipTipC18 devices (Millipore).

3. **Optimized enrichment procedure for phosphopeptides**

Hydroxyapatite affinity chromatography (HAP) was performed in order to obtain an enriched fraction of phosphopeptides. HAP spin down column was manufactured in our laboratory using BIO-GEL HTTP/ sample ratio 2:1(mg/µL). 10mL of the reconstituted peptides mixture was dried in a vacuum centrifuge and resuspended in 100µl of loading buffer (TRIS 10mM, EDTA, 1mM pH 7). The peptides solution was loaded onto 20mg of HAP that was previously packed with loading buffer. The HAP-bound peptides were incubated at room temperature for 15 min twice. After, the column was washed with loading buffer to remove un-retained peptides. The phosphopeptides were eluted with 100 µl of elution buffer (KCl 100 mM, TRIS 20mM, EDTA 2 mM, pH 8). All fraction, were dried in a vacuum centrifuge, resuspended in 100 µL of 40% ACN/0.1%, desalted in reverse-phase Zip Tips.

4. **Protein Identification by MALDI MS and MS/MS analysis**

10 µl of the all fractions was desalted using ZipTipC18 prior MS analysis. Peptides was elute directly into 5 µl of matrix solution (5 mg/µL R-cyano-4-hydroxycinnamic

acid (CHCA) in 50% ACN, 0.1% v/v TFA) in order to maximize concentration of peptides in sample spot. Mass spectrometry analyses were performed using a 5800 MALDI TOF-TOF Analyzer (AB SCIEX) equipped with a neodymium: yttrium-aluminum-garnet laser (laser wavelength was 349 nm), in reflection positive-ion mode with a mass accuracy of 5 ppm. At least 4000 laser shots were typically accumulated with a laser pulse rate of 400 Hz in the MS mode, whereas in the MS/MS mode spectra up to 5000 laser shots were acquired and averaged with a pulse rate of 1000 Hz. MS/MS experiments were performed at a collision energy of 1kV, ambient air was used as collision gas with medium pressure of 10-6 Torr. After acquisition, spectra were handled using Data Explorer version 4.0. For peptide mass fingerprinting, MASCOT (http://www.matrixscience.com) search engines were used. c-Jun was identified based on the assumptions that peptides were monoisotopic. The search was performed using the human protein database of the swiss prot. A mass tolerance of 50 ppm was used and up to 4 missed pepsin cleavage was allowed.

5 Objective of the work

In the central nervous system, activation of the c-Jun transcription factor by the c-Jun-N-terminal kinase (JNK) plays an important role in various cellular programs, including neuronal differentiation, repair and apoptosis. JNK induces c-Jun activity by phosphorylating its N-terminal domain at both serine (S) 63/73 and threonine (T) 91/93 residues. However, these two groups of phosphorylation are differentially regulated, as the S63/73 sites are promptly phosphorylated upon JNK activation, but can also be phosphorylated by other proline-directed kinases, while phosphorylation at T91/93 is strictly dependent on JNK activity and requires a priming phosphorylation event at the adjacent T95Q96 site. A wide number of studies have shown that c-Jun phosphorylation at the S63/73 sites acts in both degenerative and regenerative pathways of the CNS, suggesting that additional phosphorylation at the T91/93 sites may be crucial for c-Jun degenerative activity.

Our aim was to investigate the role and regulation of c-Jun phosphorylation at T91/93/95 in neuronal cell death. As paradigm of neuronal cell death, we have chosen the potassium/trophic deprivation of cerebellar granule cell (GCs), which triggers apoptosis in a way that is dependent on JNK-dependent activation of c-Jun. On the other side, it is known that lithium counteracts GC apoptosis by inhibiting GSK3 activity, without interfering with JNK activation. Therefore, how GSK3 activity is linked to c-Jun-dependent apoptosis of GCs remain to be elucidated. We have investigated the regulation and function of site-specific regulation of c-Jun phosphorylation at the S63 and T91/T93 JNK sites in cerebellar granule cells CGC apoptosis by trophic/potassium (TK) deprivation. We found that lithium protects CGCs from TK deprivation by inhibiting multisite phosphorylation of c-Jun at T91/T93/T95, which triggers the onset of c-Jun pro-apoptotic activity. Furthermore, we show that abrogation of T91/T93/T95 phosphorylation has no consequence on the capacity of c-Jun to induce neurite outgrowth in PC12 cells, suggesting that site-specific regulation of c-Jun phosphorylation is one possible mechanism underlying the functional dichotomy of the JNK/c-Jun pathway in the brain.

On the other hand, the JNK/c-Jun pathway is involved in the up-regulation of inflammatory cytokines in activated immune-regulatory cells of the cerebrum and spinal astrocytes (Waetzig *et al.*, 2005; Raivich, 2008; Haeusgen *et al.*, 2009). In

contrast, little is known about the expression and activation of c-Jun in Bergmann glial (BG) cells. We have used neuronal/glial cultures of mouse neonatal cerebellar cells to assess putative roles of c-Jun in activated Bergmann glial cells. We provide evidence that the induction of IL-1β gene expression in response to LPS, the major structural component of the outer wall of gram-negative bacteria and a potent activator of astrocytes and microglia, is dependent on c-Jun. Furthermore, c-Jun expression in BG cells was confirmed in vivo by characterizing the cell-type and layer-distribution of c-Jun-expressing cells in the early postnatal cerebellum. In the present study, we have used neuronal/glial cultures of mouse neonatal cerebellar cells to assess putative roles of c-Jun in activated Bergmann glial cells. We provide evidence that the induction of IL-1β gene expression in response to LPS, the major structural component of the outer wall of gram-negative bacteria and a potent activator of astrocytes and microglia, is dependent on c-Jun. Furthermore, c-Jun expression in BG cells was confirmed in vivo by characterizing the cell-type and layer-distribution of c-Jun-expressing cells in the early postnatal cerebellum.

6 Results

6.1 Role of c-Jun in neuronal cell death

6.1.1 Phosphorylation of c-Jun N-terminal domain in cerebellar granule neurons

To investigate the possible regulative role of c-Jun phosphorylation at T91/T93 in neuronal death, we set up a previously described experimental system consisting in primary cultures of mouse CGCs undergoing c-Jun-dependent programmed cell death in response to trophic/potassium (TK) deprivation (Watson *et al.*, 1998). P7 mouse cerebella were used to generate CGCs, which were cultured for 7 days (DV7) in presence of serum and high potassium concentration (25mM); CGC culture were then switched to low potassium concentration (5mM) for further 18 hours. Cell death of CGCs was assessed at single cell level by examining nuclear morphology of DAPI-stained nuclei using immunofluorescence microscopy. It is worth noting that in our experimental settings (Fig 6.1 AI - A III) 100% of DAPI-stained condensed nuclei resulted TUNEL-positive, confirming that morphological analysis of DAPI-stained nuclei is a valuable assay to detect cell death. In line with previous studies (Hongisto *et al.*, 2003; Ambacher *et al.*, 2012) fig 6.1 IV shows that approximately 55% of cells presented condensed nuclei in TK-deprived CGC cultures, whereas the JNK-specific inhibitor SP100125 (SP) and lithium reduced the frequency of condensed nuclei to 8% and 18%, respectively.

Once established that cell death was dependent on JNK activity and sensitive to lithium, we then investigated the regulation of site-specific c-Jun N-terminal phosphorylation by TK deprivation, using site-specific c-Jun antibodies recognizing c-Jun when phosphorylated at S63 (c-Jun-p63) or at T91/T93 (c-Jun-p91/93), or for total-c-Jun. Site-specific c-Jun phosphorylation was analysed by western-blot analysis at 4 hrs after TK deprivation, as maximal c-Jun N-terminal phosphorylation by TK was reported to arise at this time period (Coffey *et al.*, 2002). As shown in fig.1B, we found that TK deprivation induced c-Jun protein levels and c-Jun phosphorylation at both S63 and T91/T93 in a SP-sensitive manner (Fig 6.1B-C). This finding is in agreement with several previous studies demonstrating that both c-Jun expression and N-terminal phosphorylation are dependent on JNK activity

(Morton *et al.*, 2003; Hess *et al.*, 2004; Karin & Gallagher, 2005). In contrast, lithium significantly impaired T91/T93 phosphorylation, whereas had no effects on S63 phosphorylation or JNK activation. These results are in line with recent studies by Ambacher and co-workers, reporting that inhibition of the lithium-sensitive kinase GSK3 β in CGCs protects from TK deprivation-induced apoptosis, but has no effect on either JNK activation or c-Jun phosphorylation on S63 (Ambacher *et al.*, 2012). Similarly, an earlier study by Hongisto and co-workers has shown that the protective effect of lithium on CGCs is coupled to inhibition of c-Jun target genes, without affecting JNK activation (Hongisto *et al.*, 2003). However, neither study investigated the levels of T91/T93 phosphorylation, therefore missing the site-specific effect of either lithium or GSK3 β inhibitors on c-Jun phosphorylation.

Next, we confirmed the pattern of S63 and T91/93 phosphorylation at single cell level. To this aim, we used site-specific c-Jun phospho-antibodies or total-c-Jun antibodies to perform immunofluorescence analysis of c-Jun phosphorylation after 4 hrs of TK-deprivation (Fig 6.1D-F). In addition, parallel CGC cultures were TK-deprived for 18 hrs and analysed for condensed nuclei by DAPI staining (Fig 6.1G). As shown in fig 6.1D-H, the percentage of TK-deprived cells resulting positive for either total-c-Jun or c-Jun-p63 antibodies were very comparable, indicating that c-Jun was phosphorylated at S63 in the vast majority of c-Jun-expressing cells (70% of total cells). On the other hand, the percentage of cells positive for c-Jun-p91/93 was circa 55% of total TK-deprived cells, indicating that extensive N-terminal phosphorylation at both S63 and T91/T93 is present only in a subpopulation of c-Jun-expressing cells. This finding suggests that TK-deprivation differentially regulates S63 and T91/T93 phosphorylation of c-Jun, with the T91/T93 sites responding in a sensitive fashion and mirroring the switch-like apoptotic response of TK-treated CGCs (compare the percentage of apoptotic cells with that of T91/T93 positive cells).

A

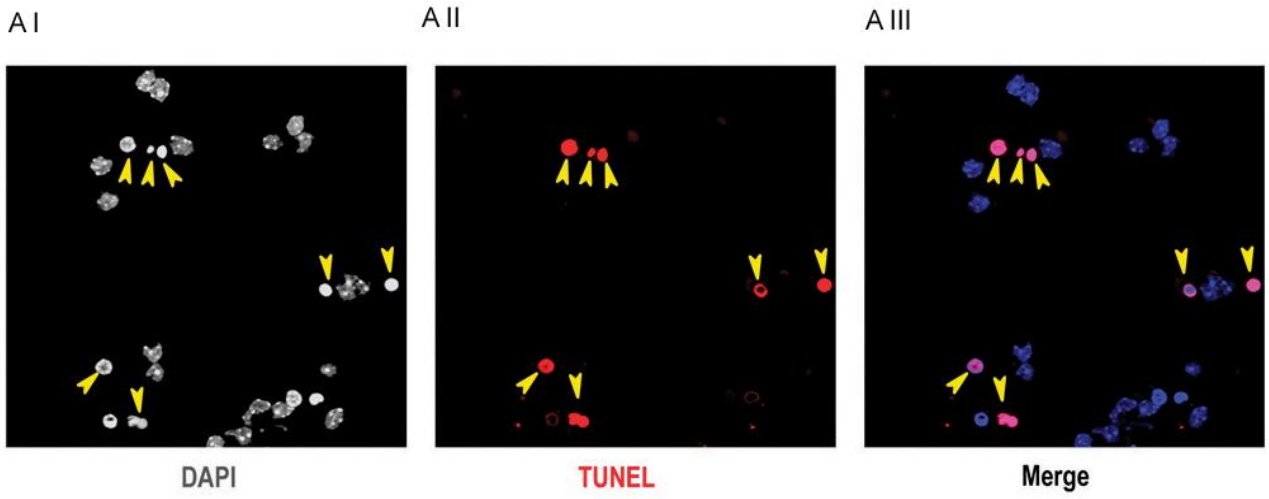
A I
A II
A III
DAPI
TUNEL
Merge

A IV

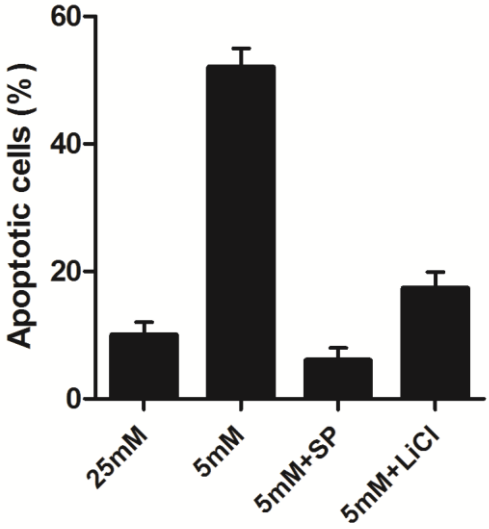
Apoptotic cells (%)
60
40
20
0
25mM
5mM
5mM+SP
5mM+LiCl

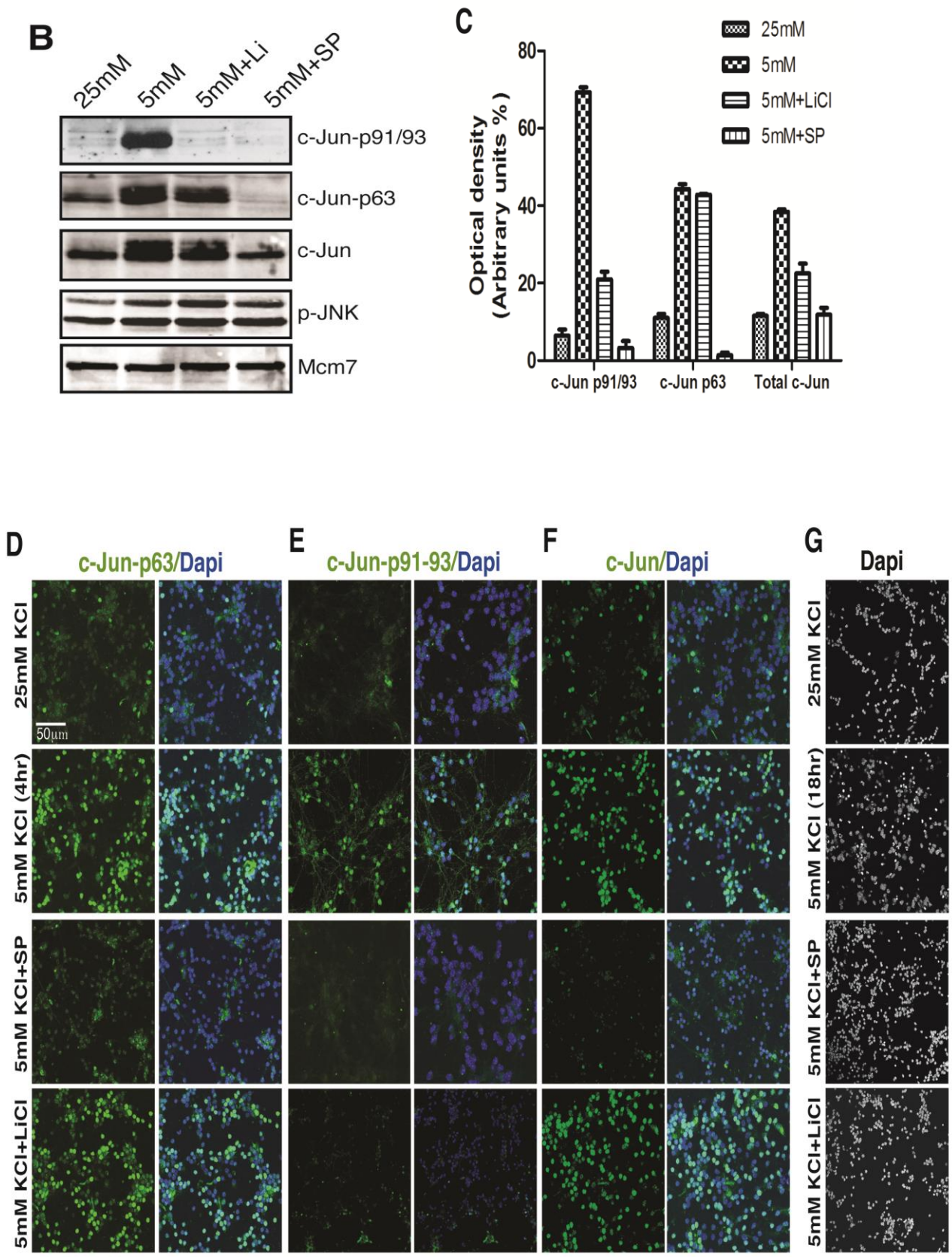
B
25mM
5mM
5mM+Li
5mM+SP
c-Jun-p91/93
c-Jun-p63
c-Jun
p-JNK
Mcm7
C
25mM
5mM
5mM+LiCl
5mM+SP
Optical density
(Arbitrary units %)
80
60
40
20
0
c-Jun p91/93
c-Jun p63
Total c-Jun
D
c-Jun-p63/Dapi
E
c-Jun-p91-93/Dapi
F
c-Jun/Dapi
G
Dapi
25mM KCl
5mM KCl (4hr)
5mM KCl+SP
5mM KCl+LiCl
50µm
5mM KCl (18hr)

H

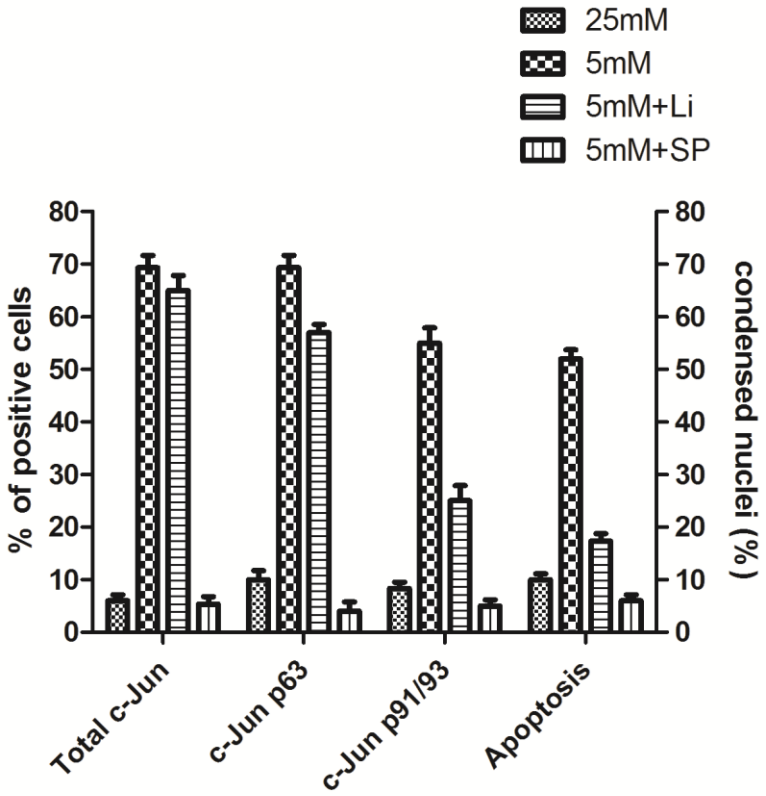

Fig 6.1: c-Jun N-terminal phosphorylation in cerebellar granule neurons. A TUNEL assay of CGCs**.** Confocal analysis of CGCs cultured in 25mM K and then switched to 5mM K medium for 18 hrs. Cells were then fixed and nuclei were either stained with DAPI (Gaudilli+¿re *et al.*) or by TUNEL (**A II**) or Merge (**A III**) staining as described in methods. **A IV** Cerebellar granule cells (CGCs) were cultured in 25mM K and then switched to 5mM K medium for 18 hrs, either in absence or in presence 10 □M SP600125 (SP) or 10mM LiCl, as indicated. Cells were then fixed and nuclei were stained with DAPI. Condensed nuclei were counted by fluorescence microscopy. Columns indicate the average percentage number of condensed nuclei present in 10 different fields, with bars indicating SD. **B** Western blot analysis of CGCs cultured either in 25mM K or 5mM K medium for 4 hrs and treated with either SP600125 (10mM) or LiCl (10mM) as indicated. c-Jun N-terminal phosphorylation or phosphorylated JNK (p-JNK), were determined by using the indicated antibodies. c-Jun expression levels were measured by using a total c-Jun antibody, as indicated.

Protein levels were normalized by using the Mcm7 antibody. **C** Densitometric analysis of western blot analysis shown in panel C. Values are presented as optical density (OD; expressed in arbitrary units) relative to the control (Mcm7). Bars represent SD from three different densitometric quantification of analogous experiments shown in panel C. **D-F** Immunofluorescence analysis of CGCs cultured in 25mM K or 5mM K medium for 4 hrs and treated with either SP600125 (10mM) or LiCl (10mM) as indicated. Cells were then fixed and nuclei were stained with DAPI; c-Jun N-terminal phosphorylation and expression was detected by immunocytochemical staining using c-Jun-p63 Ab (D), or c-Jun-pT91/T93 (E), or c-Jun total Ab (F). **G** Immunofluorescence analysis of CGC cultures TK-deprived for 18 hrs and analysed for condensed nuclei by DAPI staining. **H** Quantification of results shown in D-G. Columns indicate the average percentage number of immunoreactive cells (D-F) or condensed nuclei (G) present in 10 different fields, with bars indicating SD.

6.1.2 Lack of T91/93 phosphorylation impairs cell death but not neurite outgrowth

As c-Jun phosphorylation at T91-93 is dependent on the T95 priming site (Vinciguerra M et al 2008), we then validated the role of the T91/T93 sites in neuronal cell death by analysing a c-Jun mutant bearing alanine substitution of T95 (c-JunA95). This c-Jun mutant has been previously described to lack T91/T93 phosphorylation in response to anisomycin, UV radiation and etoposide (Vinciguerra *et al.*, 2008).

To this aim, we used a lentiviral approach to reintroduce the expression of either influenza-hemagglutinin (HA)-tagged c-Jun-wt or c-JunA95 proteins in primary CGCs cultures generated from conditional KO mice lacking c-Jun expression in the CNS Fig (6.2A-6.2C) (c-Jun DN mice) (Vinciguerra *et al.*, 2004). Since the percentage of lentiviral-infected cells was circa 70% of total cells, we used the non-infected cells as internal control. As expected from previous studies, Fig 6.3C shows that the rate of TK-induced apoptosis resulted reduced in CGCs generated from JunDN mice (19% versus 60% of c-Jun-expressing CGCs). In contrast, TK-deprivation efficiently induced cell death in CGCs expressing c-Jun-wt proteins. In contrast, cell death was impaired in CGCs expressing the c-JunA95 mutant. These results indicate that reintroduction of c-Jun-wt expression, but not that of the c-JunA95 mutant, restores the standard rate of CGC apoptosis by TK-deprivation in c-JunDN mice. Notably, c-Jun-wt was fully phosphorylated at both S63 and T91/T93 in response to TK deprivation, whereas N-terminal phosphorylation of c-JunA95 was restricted to S63 (Fig 6.3D), confirming the crucial role of the T95 site in priming T91/T93 phosphorylation by TK-deprivation.

As c-Jun functions as a transcriptional factor, we next evaluated whether the inability of the c-JunA95-HA mutant to rescue TK-induced apoptosis was coupled to the lack of c-Jun activity. To this end, we carried out reporter gene assays using a Jun2-luciferase (Jun2-luc) reporter, previously shown to be induced by TK-deprivation in murine CGCs and containing 2 copies of the c-Jun/AP-1 target site “TTACCTCA” (Yuan *et al.*, 2009). The Jun2-luc reporter was transfected by calcium phosphate method in CGCs generated from c-JunDN mice, either alone or together with expression vectors expressing either c-Jun-wt-HA or c-JunA95-HA proteins. As

shown in figure 6.3E, the c-Jun-luc reporter was not induced by TK-deprivation, in agreement with the lack of endogenous c-Jun expression in CGCs from c-JunDN mice. Conversely, re-introduction of c-Jun-wt-HA caused approximately a 3-fold increase of luciferase activity in response to TK-deprivation, whereas c-JunA95-HA had a very limited effect. Notably, the western analysis shown in figure 6.3D indicates that c-Jun-wt-HA and c-JunA95-HA proteins have equal steady-state expression levels in CGCs. Taken together, these results suggest that lack of c-Jun phosphorylation at the T91/T93/T95 sites impairs the induction of c-Jun activity by TK-deprivation and in turn protects from cell death.

Next, we investigated the capability of the c-JunA95 mutant to induce neurite outgrowth in PC12 cells cultured in absence of NGF, a well described process that is induced by ectopic expression of c-Jun and depend on S63/S73 phosphorylation (Leppa *et al.*, 1998; Dragunow *et al.*, 2000). As shown in figure 6.4, c-Jun-wt and c-JunA95 were equally able to induce neurite outgrowth in naïve PC12 cells. These results exclude that the effect of the c-JunA95 mutant on cell death was secondary to a defect altering c-Jun activity independently of T91/T93 phosphorylation. Also, they establish that c-Jun phosphorylation on T91/T93/T95 is required for neuronal cell death of CGCs, whereas it has no roles in Jun-dependent neurite outgrowth in naïve PC12 cells.

A

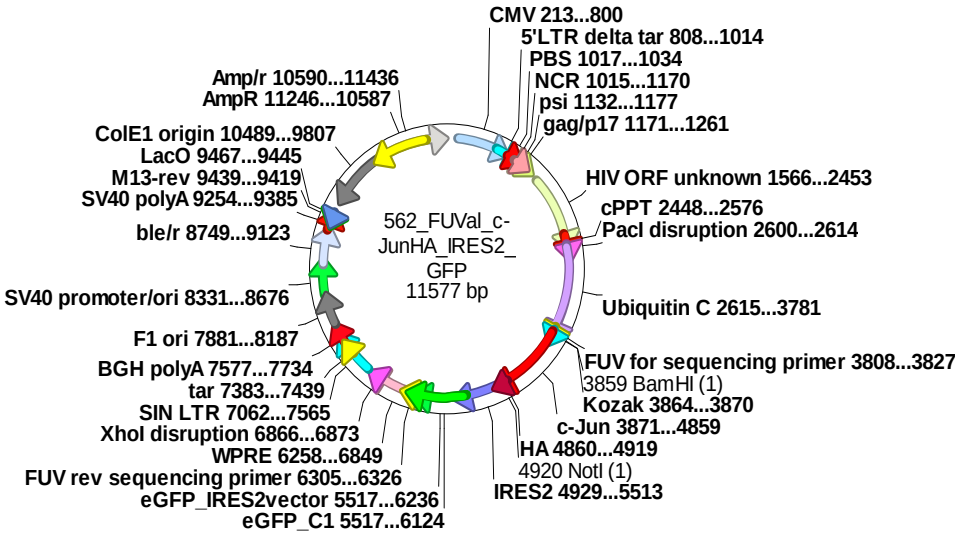
CMV 213...800
5'LTR delta tar 808...1014
PBS 1017...1034
NCR 1015...1170
psi 1132...1177
gag/p17 1171...1261
HIV ORF unknown 1566...2453
cPPT 2448...2576
PacI disruption 2600...2614
Ubiquitin C 2615...3781
FUV for sequencing primer 3808...3827
3859 BamHI (1)
Kozak 3864...3870
c-Jun 3871...4859
HA 4860...4919
4920 NotI (1)
IRES2 4929...5513
562_FUVal_c-JunHA_IRES2_GFP
11577 bp
Amp/r 10590...11436
AmpR 11246...10587
ColE1 origin 10489...9807
LacO 9467...9445
M13-rev 9439...9419
SV40 polyA 9254...9385
ble/r 8749...9123
SV40 promoter/ori 8331...8676
F1 ori 7881...8187
BGH polyA 7577...7734
tar 7383...7439
SIN LTR 7062...7565
XhoI disruption 6866...6873
WPRE 6258...6849
FUV rev sequencing primer 6305...6326
eGFP_IRES2vector 5517...6236
eGFP_C1 5517...6124

B

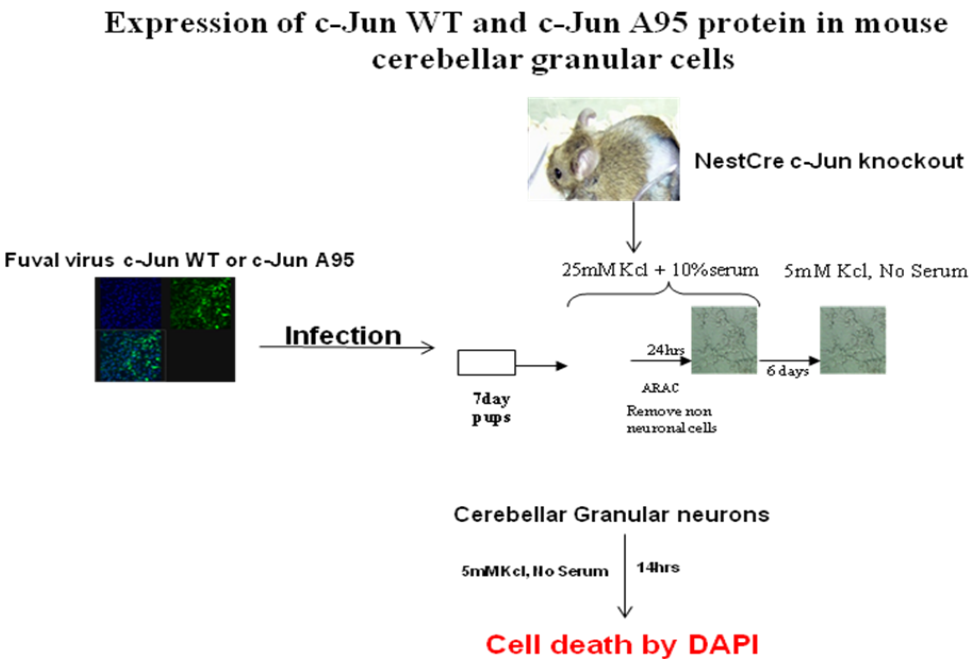
Expression of c-Jun WT and c-Jun A95 protein in mouse cerebellar granular cells
NestCre c-Jun knockout
Fuval virus c-Jun WT or c-Jun A95
Infection
7day pups
25mM Kcl + 10%serum
24hrs
ARAC
Remove non neuronal cells
5mM Kcl, No Serum
6 days
Cerebellar Granular neurons
5mMKcl, No Serum
14hrs
Cell death by DAPI

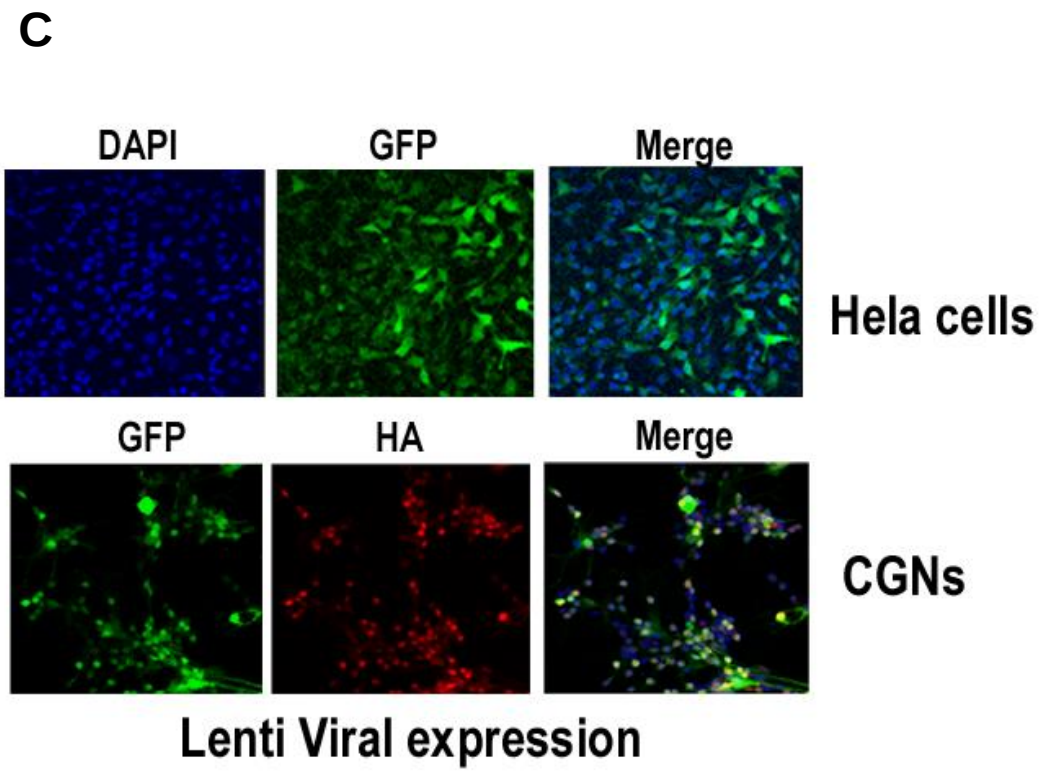

Fig 6.2: Generation of lentivirus constructs: A) Vector back bone used for lenti viral constructs- influenza-hemagglutinin (HA)-tagged c-Jun-wt or c-JunA95 proteins. **B)** Schematic representation of lentiviral expression of c-Jun in primary CGCs of CNS specific c-Jun conditional knockout mice. **C)** The efficiency of lenti viral transduction in HELA and CGCs.

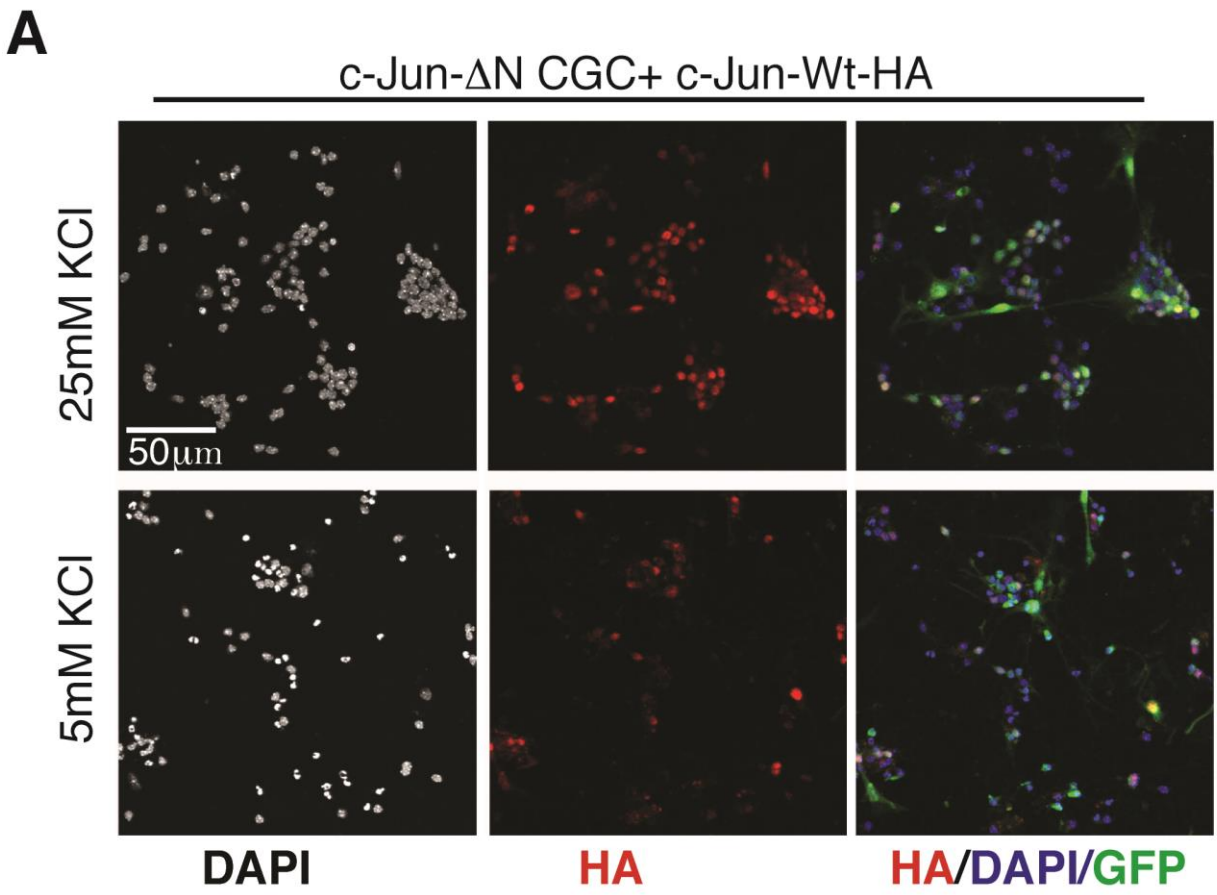
A
c-Jun-ΔN CGC+ c-Jun-Wt-HA
25mM KCl
5mM KCl
50µm
DAPI
HA
HA/DAPI/GFP

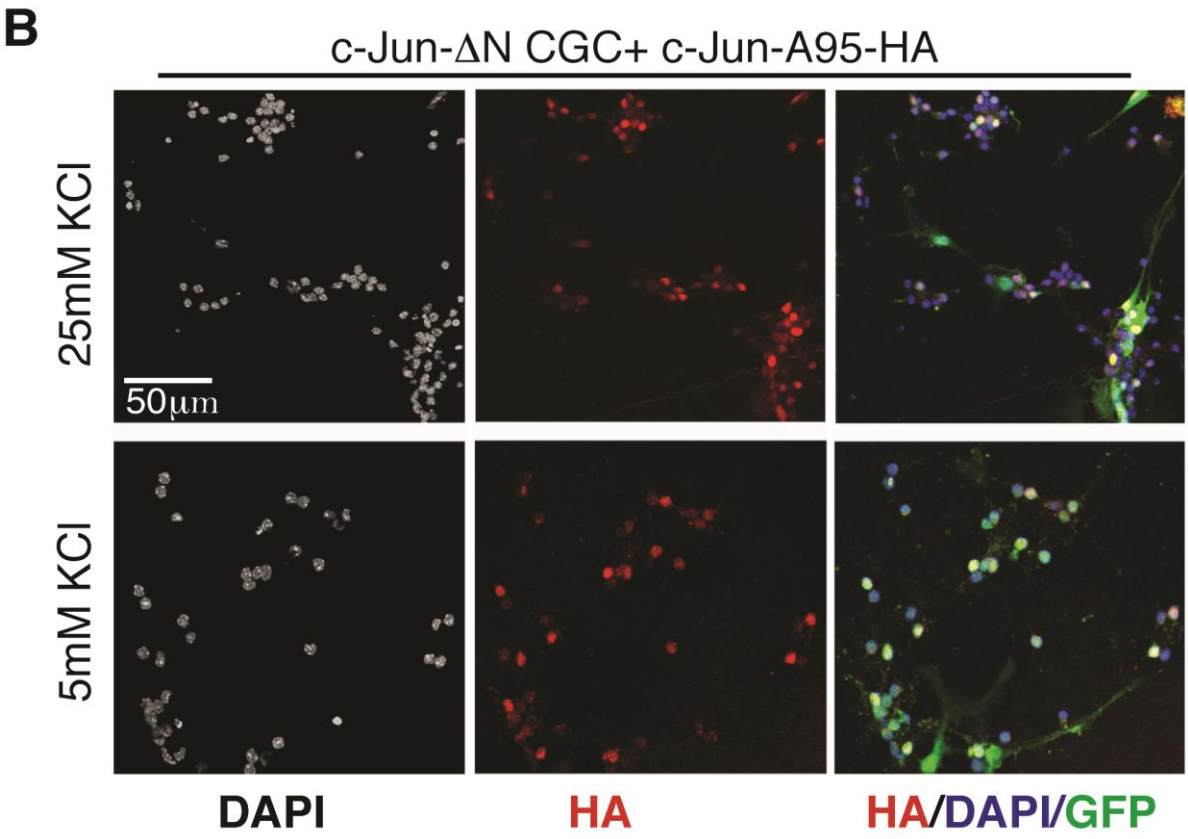
B
c-Jun-ΔN CGC+ c-Jun-A95-HA
25mM KCl
5mM KCl
50µm
DAPI
HA
HA/DAPI/GFP

C

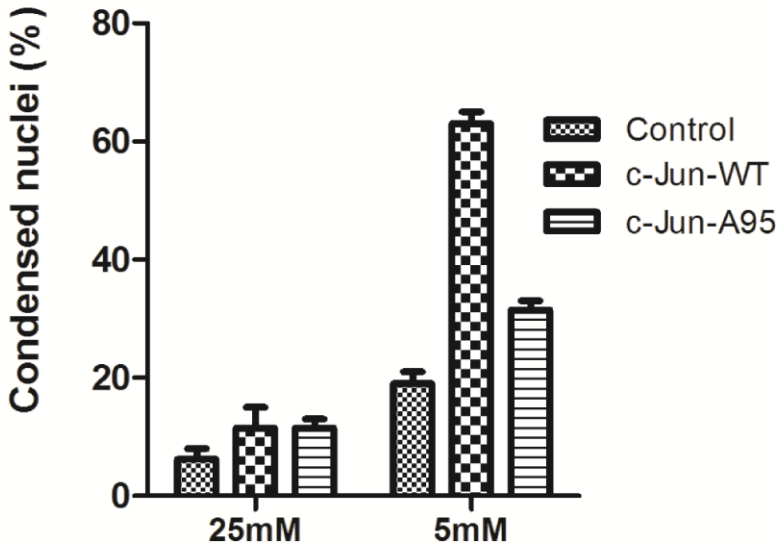
Condensed nuclei (%)
80
60
40
20
0
25mM
5mM
Control
c-Jun-WT
c-Jun-A95

D

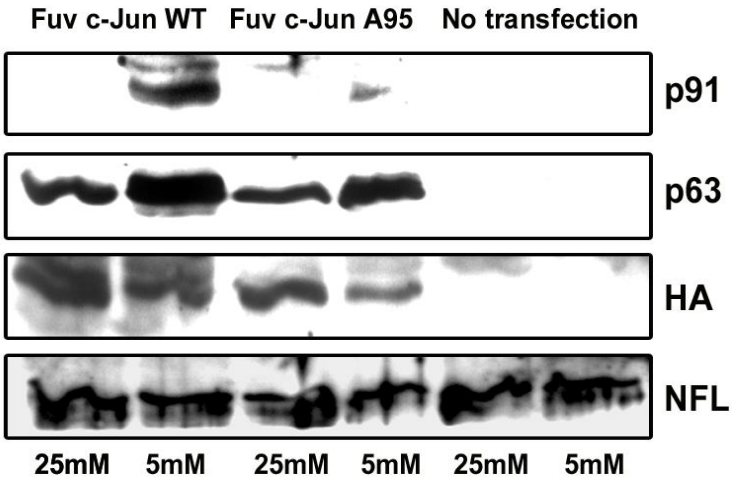
Fuv c-Jun WT
Fuv c-Jun A95
No transfection
p91
p63
HA
NFL
25mM
5mM
25mM
5mM
25mM
5mM

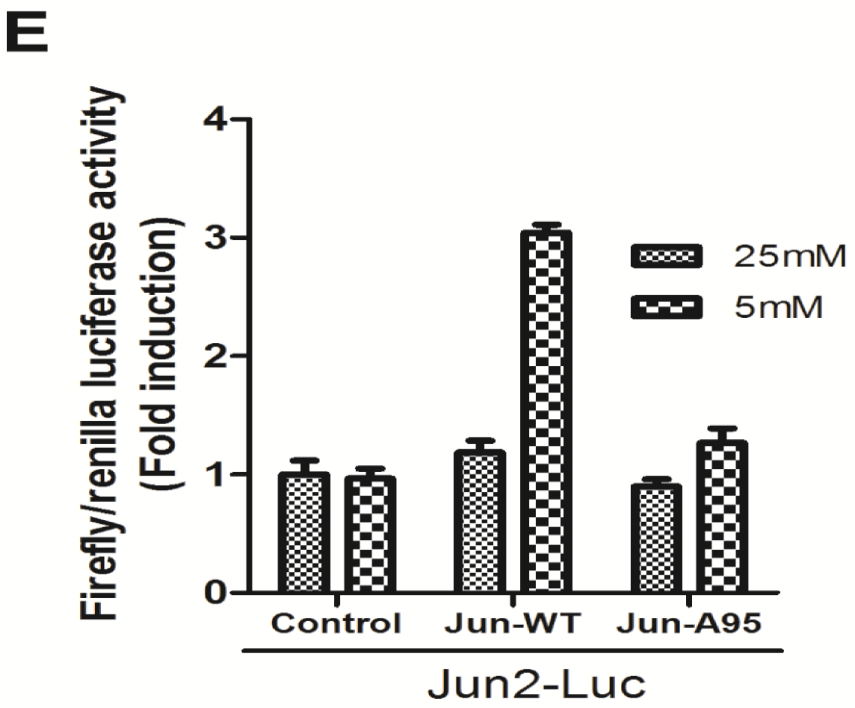

Figure 6.3: Lack of T91/93 phosphorylation protects from cell death. A-B Confocal analysis of CGCs generated from c-Jun-DN mice and infected with GFP-tagged lentivius particles expressing either hemagglutinin (HA)-tagged c-Jun proteins: c-Jun-wt-HA (A) or c-JunA95-HA (B). After infections, cells were cultured for 6 days and then treated as indicated for 18 hrs. After fixation, nuclei were stained by DAPI and immunostained with HA antibody. **C** Quantification of results shown in A-B. Columns indicate the average percentage number of condensed nuclei present in 10 different fields, with bars indicating SD. **D** Western blot analysis of CGCs from c-Jun-DN mice infected with lentiviurs as described in A-B. After infection, cells were cultured either in 25mM K or shifted to 5mM K medium for 4 hr, as indicated. Control represents not infected CGCs. c-Jun N-terminal phosphorylation was determined by using the indicated c-Jun phospho-specific antibodies. The levels of c-Jun-HA proteins was determined by using the HA antibody. Protein levels were normalized by using the NFL antibody. **E** CGCs from c-Jun-DN mice were transfected with Jun2-luc reporter plasmids in combination with plasmids expressing either c-Jun-wt-HA or c-JunA95-HA proteins or empty vector (indicated as control). After infection, cells were cultured either in 25mM K or shifted to 5mM K medium for 4 hr, as indicated. The luciferase activities were normalized to the internal transfection control. Values of CGCs transfected with empty vectors and cultured in 25mM K were set as 1-fold induction. Bar graphs represent the mean ±SD of three independent assays.

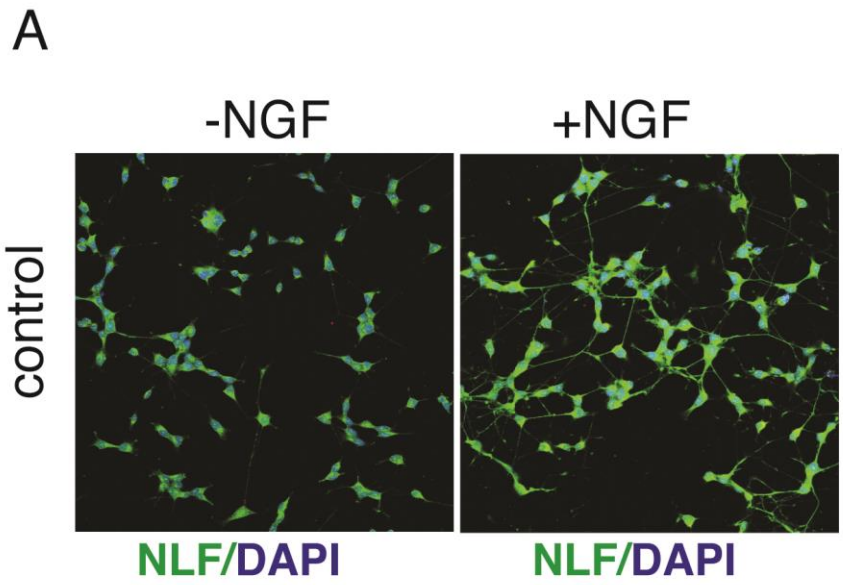
A
-NGF
+NGF
control
NLF/DAPI
NLF/DAPI

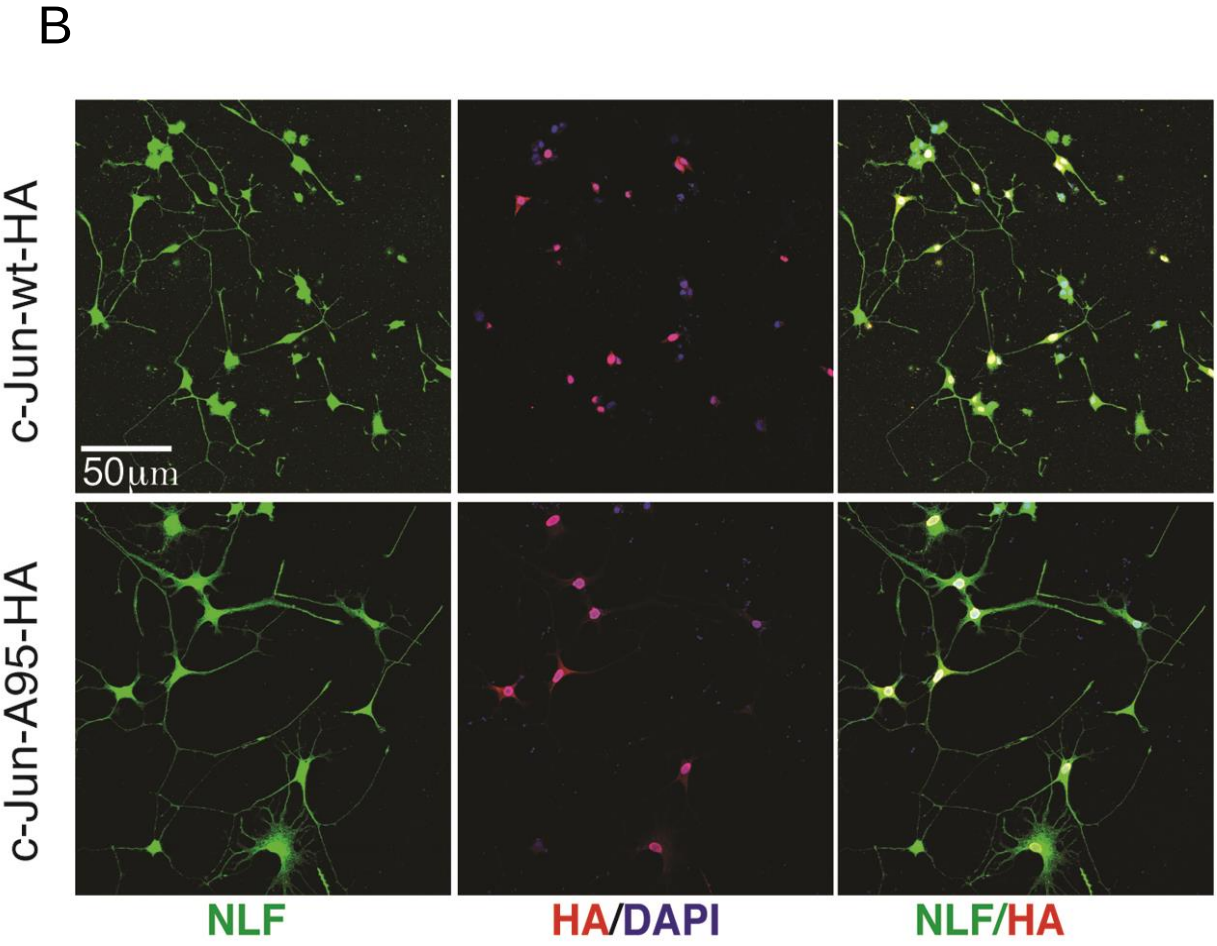
B
c-Jun-wt-HA
c-Jun-A95-HA
50µm
NLF
HA/DAPI
NLF/HA

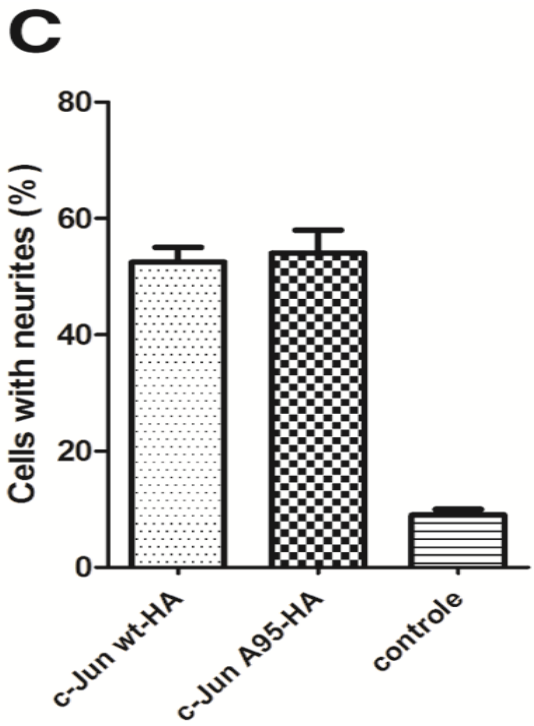

Figure 6.4: Lack of T91/93 phosphorylation does not impair neurite outgrowth. **A** Confocal analysis of PC12 cells were cultured either in absence or in presence of NFG (72 hrs) as indicated. After fixation, cells were immunostained with Neurofilament (NLF, green) antibodies. Nuclei were stained with DAPI **B** Naive PC12 cells were transfected with DNA constructs expressing either HA-tagged c-Jun-wt or Ha-tagged c-JunA95 constructs, as indicated. Transfected cells were cultured in absence of NGF for 72 hrs; after fixation cells were incubated with either HA (red) or Neurofilament (NLF, green) antibodies. **C** Quantification of PC12 cells presenting neurites.

6.1.3 Deregulation of c-Jun phosphorylation at the T91/T93 sites recovers cell death in presence of lithium

The phosphorylation pattern of site-specific c-Jun phosphorylation presented in fig.1, together with the evidence that the c-JunA95 mutant protects from cell death, suggests that lithium may inhibit the priming event preceding T91/T93 phosphorylation. To assess this hypothesis, we used a c-Jun mutant bearing aspartate substitution of T95 (c-JunD95), which was previously shown to acquire the same kinetic of S63/S73 phosphorylation in response to JNK activation (Vinciguerra *et al.*, 2008). As shown in figure 4, we found that whereas lithium strongly impaired TK deprivation-induced apoptosis in CGCs expressing c-Jun-wt proteins (Fig 6.5A), it had a poor protective effect in GCGs expressing c-JunD95 mutated proteins (Fig 6.5B). However, the JNK inhibitor SP100125 efficiently inhibited LK-induced apoptosis in both circumstances, excluding that the c-JunD95 mutant acts independently from JNK activation (Fig 6.5A-C). These results suggest that inhibition of T91/93/95 phosphorylation underlies the effect of lithium on cell death.

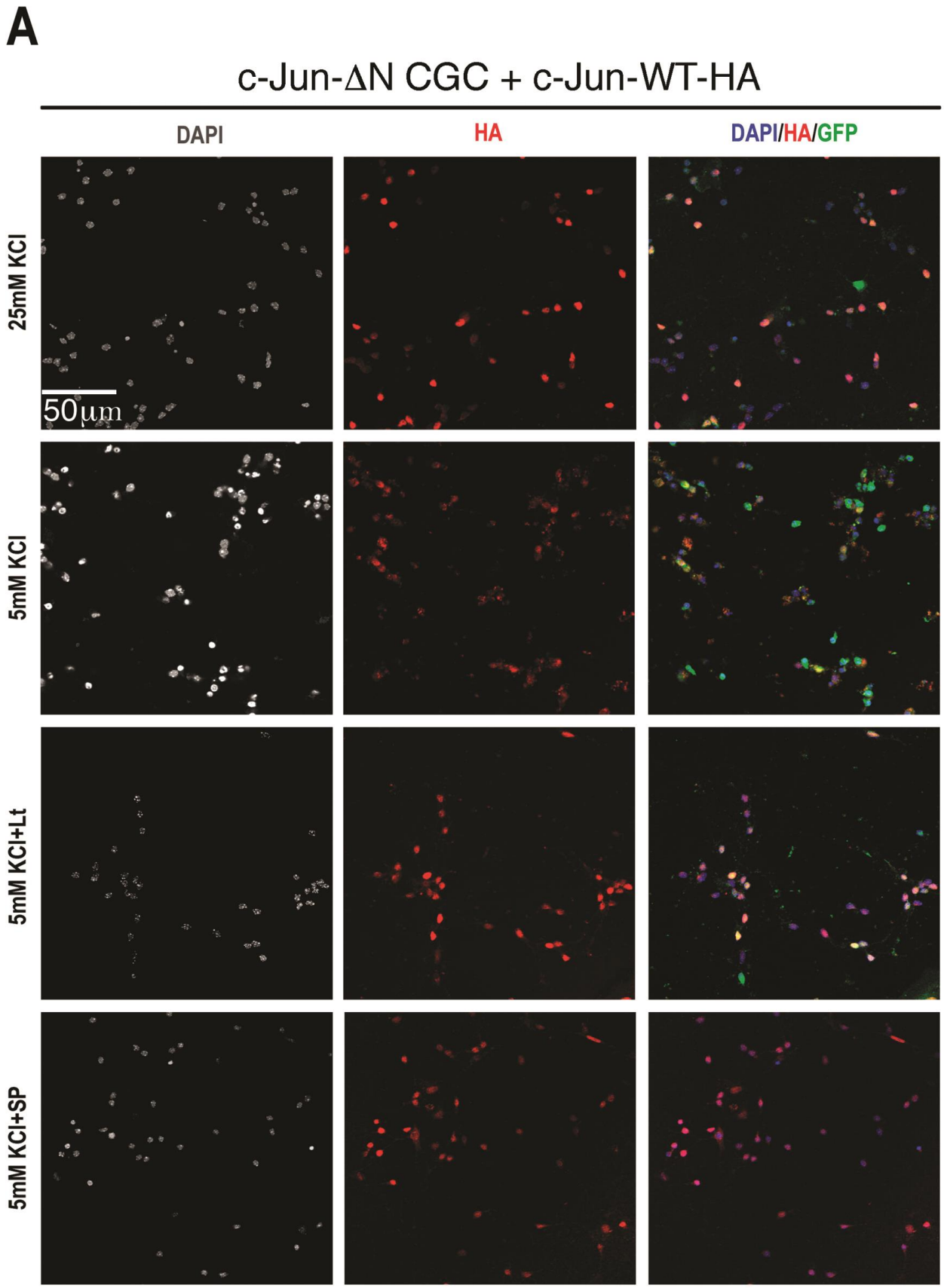
A
c-Jun-ΔN CGC + c-Jun-WT-HA
DAPI
HA
DAPI/HA/GFP
25mM KCl
5mM KCl
5mM KCl+Lt
5mM KCl+SP
50µm

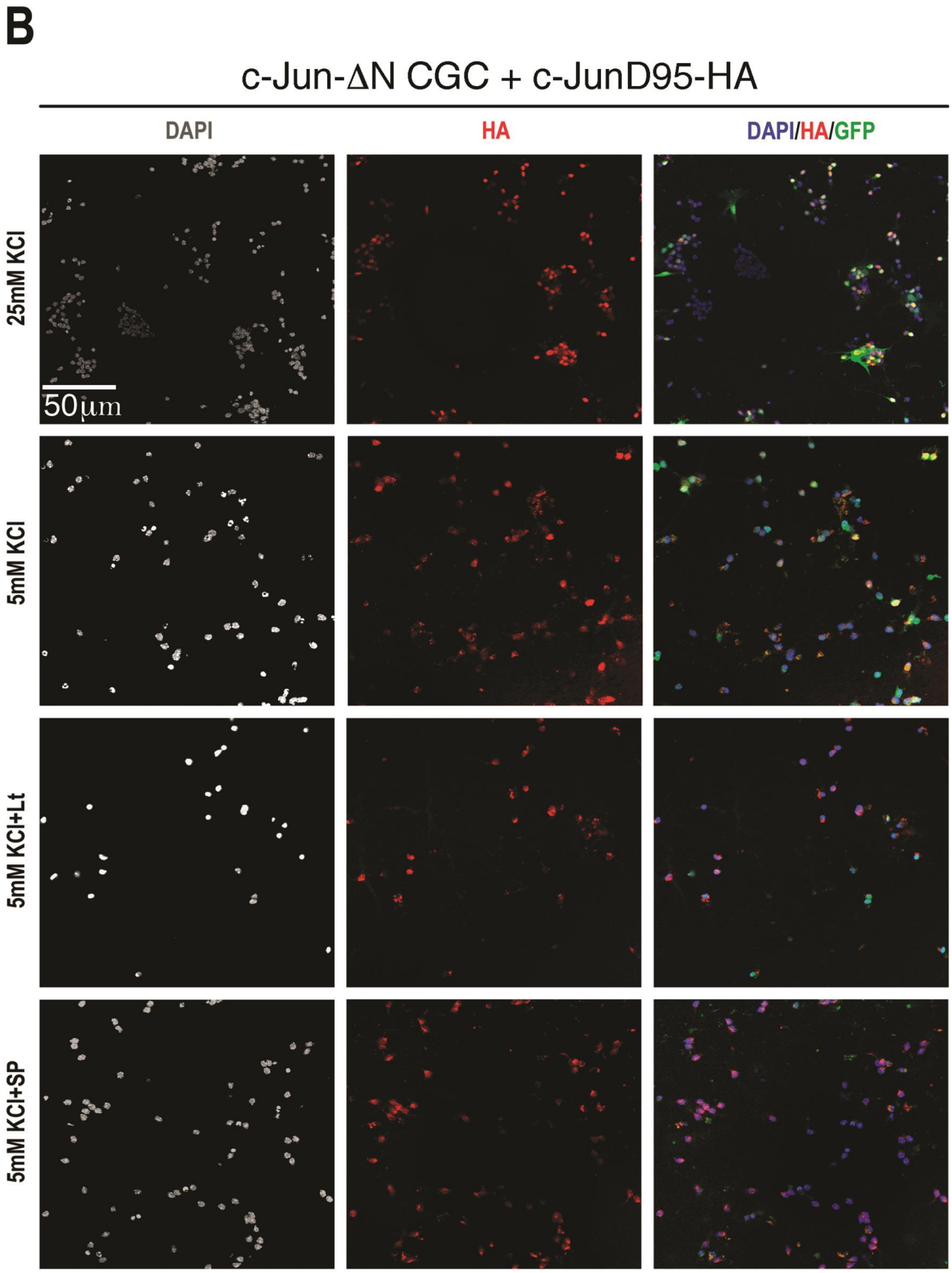
B
c-Jun-ΔN CGC + c-JunD95-HA
DAPI
HA
DAPI/HA/GFP
25mM KCl
5mM KCl
5mM KCl+Lt
5mM KCl+SP
50μm

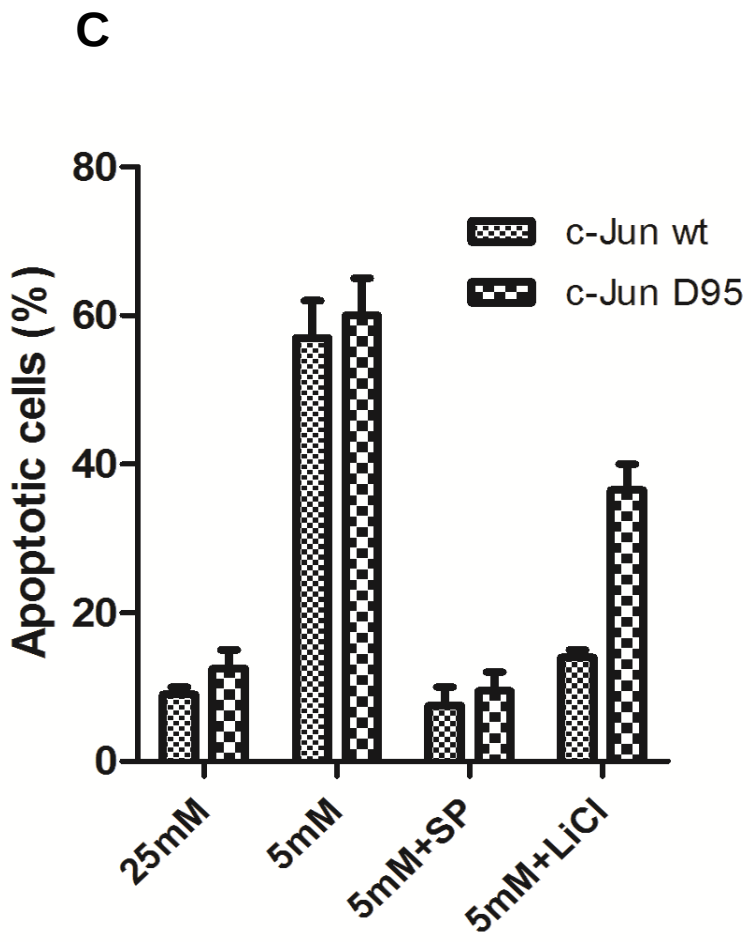

Figure 6.5: Constitutive phosphorylation at T95 impairs the neuronal protection ability of Li

Confocal analysis of CGCs generated from c-Jun Dn mice and infected with lentivirus particles expressing Ha-c-Jun-wt **(A)** or Ha-c-Jun D95 **(B)**. After transduction cells were cultured for 6 days and then treated as indicated with 25mM K or 5mM k with or without JNK and GSK3 inhibitors for 20hrs. After fixation, nuclei were stained by DAPI and immunostained with HA antibody (red). **C** Quantification of results shown in A-B Columns indicates the average percentage number of condensed nuclei present in 10 different fields, with bars indicating SD.

6.1.4 The T95 site of c-Jun is phosphorylated in vivo

Our results suggest that lithium controls c-Jun pro-apoptotic activity by regulating the priming event preceding T91/93 phosphorylation. Most probably, the priming event consists in phosphorylation of the T95 sites, as suggested by the finding that the c-JunD95 overcomes the effect of lithium on cell death. To exclude that a different post-translational modification of T95 primes T91/93 phosphorylation, we validated that T95 is phosphorylated in cells. To this aim, we firstly attempt to generate phospho-T95-specific antibodies. Unfortunately, the produced antibodies were not able to distinguish between phospho-T95 and phospho-T91/T93 residues of c-Jun proteins (data not shown). Hence, we used mass spectrometry methodologies to identify N-terminal phosphopeptides of c-Jun proteins ectopically expressed in HEK-T 293 cells. Mass spectrometric methodologies provide a rapid and sensitive tool for the identification and quantification of proteins and their post-translational modifications including phosphorylation (Hernandez *et al.*, 2006; Napoli *et al.*, 2008). Firstly, we performed analytical experiments to analyze the N-terminal phosphorylation of ectopically expressed c-Jun proteins in HEK-T 293 cells. To this aim, HEK-T 293 cells were transfected with a vector expressing human c-Jun and than treated with anisomycin, a strong activator of JNKs. As shown by western blot analysis, c-Jun resulted fully phosphorylated on both S63 and T91/T93, either before or after anisomycin treatments (Fig 6.6A). The high basal levels of c-Jun phosphorylation in HEK-293T cells has been previously described and it is due to the constitutive activation of JNKs in this cell line (Nateri *et al.*, 2005). However, c-Jun phosphorylation at T91/T93 was dependent on the priming event at T95, as the c-JunA95 mutant resulted phosphorylated only at the S63 site (6.6B). Next, c-Jun-wt proteins were immunoprecipitated from transfected cells using a pan-c-Jun antibody, immunocomplexes were then purified on PAGE, comassie stained and processed for MALDI-MS and MS/MS. In parallel, analytical aliquots of immunocomplexes were analyzed by western analysis to confirm the presence of phosphorylated T91/T93 residues in c-Jun-immunocomplexes (fig.6.6B).

Following in gel digestion of c-Jun immunocomplexes with proteinase K (PK), the fraction of phosphopeptides was enriched by hydroxyapatite affinity chromatography (HAP) and analyzed by MALDI MS and MS/MS. The mass data were processed to

assign candidate peptides in the SwissProt database using the MASCOT search program. Peptide Mass Fingerprinting (PMF) interrogation identified (P05412), TRANSCRIPTION FACTOR AP-1 (PROTO-ONCOGENE c-JUN) (P39) (G0S7) using 34 *m/z* values, sequence coverage: 62%, (score 91). All identified phosphopeptides are listed in Table 6.1. In-gel PK digestion of c-Jun immunocomplexes generated three major phosphorylated peptides. In particular, three different three-phosphopeptides were identified as residues 80-97, 82-97 and 89-98. The CID spectrum of segment 82-97 (m/z 1956.73) is given in figure 6.6C. For this segment, the MS/MS spectrum showed b (b-H_3PO_4) and y (y-H_3PO_4) ion series, allowing the assignment of either peptide sequence and phosphorylation sites at the T91, T93 and T95 residues. All the b-series fragments down to b_{10} (m/z1107.7) showed the ability to lose H_3PO_4 (-98 Da), while the b_9 (m/z 926.7) fragment was present only in a non-phosphorylated state, indicating that the ninth residue from the N-terminus (T91) is phosphorylated. In addition, the mass difference between the b_{10} (m/z 1107.7) and b_9 (m/z 926.7) ions is consistent with the mass of a phospho-threonine residue (181Da). Furthermore, the presence of the ion peak b_{14}-98 (m/z 1566.0) and of the unmodified counterpart y_2 (m/z 294.2) is consistent with a phosphorylated T95 residue. The presence of T95 phosphorylation is also reliable with the mass difference between the y_2 (m/z 294.2) and y_3 (m/z 475.1) ions (181Da). Accordingly, T93 phosphorylation was assigned by considering the mass difference between the y_5-98 (m/z 655.4) and y_4-98 (m/z 474.4) ions, as it was consistent with the mass of a phosphothreonine residue (181Da). In a similar fashion, both phosphopeptides 80-97, 89-98 resulted to be phosphorylated on T91, T93 and T95. A similar set of b (b-H_3PO_4) and y (y-H_3PO_4) ions was observed for both the doubly phosphorylated peptide (83-93) of m/z 1473.58, and the mono-phosphorylated peptide (82-97) of m/z 1796.80, allowing the assignment of T91-T93 and T91 phosphorylations, respectively (Fig. 6.7A-B,). Figure 5B shows the MS/MS spectrum for the precursor ion of m/z 1144.57 of sequence TpSDVGLLK. Interpretation of the MS/MS spectrum was straightforward because a complete b (b-H_3PO_4) and y ion series was identified, with the b_2-98 fragment indicating that phosphorylation occurred at the second residue from the N-terminus. This phosphorylation site was unambiguously assigned to S63. Similarly, phosphopeptides 56-69 and 61-68 resulted to be phosphorylated at S63.

	Sequence[a]	*M*r found[b]	*M*r calc[b]
80-97	IIQSSNGHITTpTPpTPpTQF	2182.90	2182.89
82-97	QSSNGHITTpTPpTPpTQF	1956.73	1956.72
89-98	TTpTPpTPpTQF	1233.40	1232.39
83-95	SSNGHITTpTPpTPT	1473.58	1473.57
87-98	HITTpTPTPTQFL	1436.69	1436.68
87-96	HITTpTPTPTQ	1256.50	1256.50
82-97	QSSNGHITTpTPTPTQF	1796.80	1976.79
81-96	IQSSNGHITTpTPTPTQpyr	1745.79	1745.77
54-60	RAKNSDL	803.44	803.44
61-68	LTpSPDVGL	881.41	881.40
62-70	TpSPDVGLLK*	1144.57	1144.56
56-69	KNSDLLTpSPDVGLL*	1589.73	1589.73

Table 6.1: a Amino acid sequence of phosphorylated peptides identified from peptic digests on the basis of their CID spectrum. pS denotes phosphoserine, and pT denotes phosphothreonine, * denotes [M-Na]+adduct. *b*All mass values are listed as monoisotopic mass.

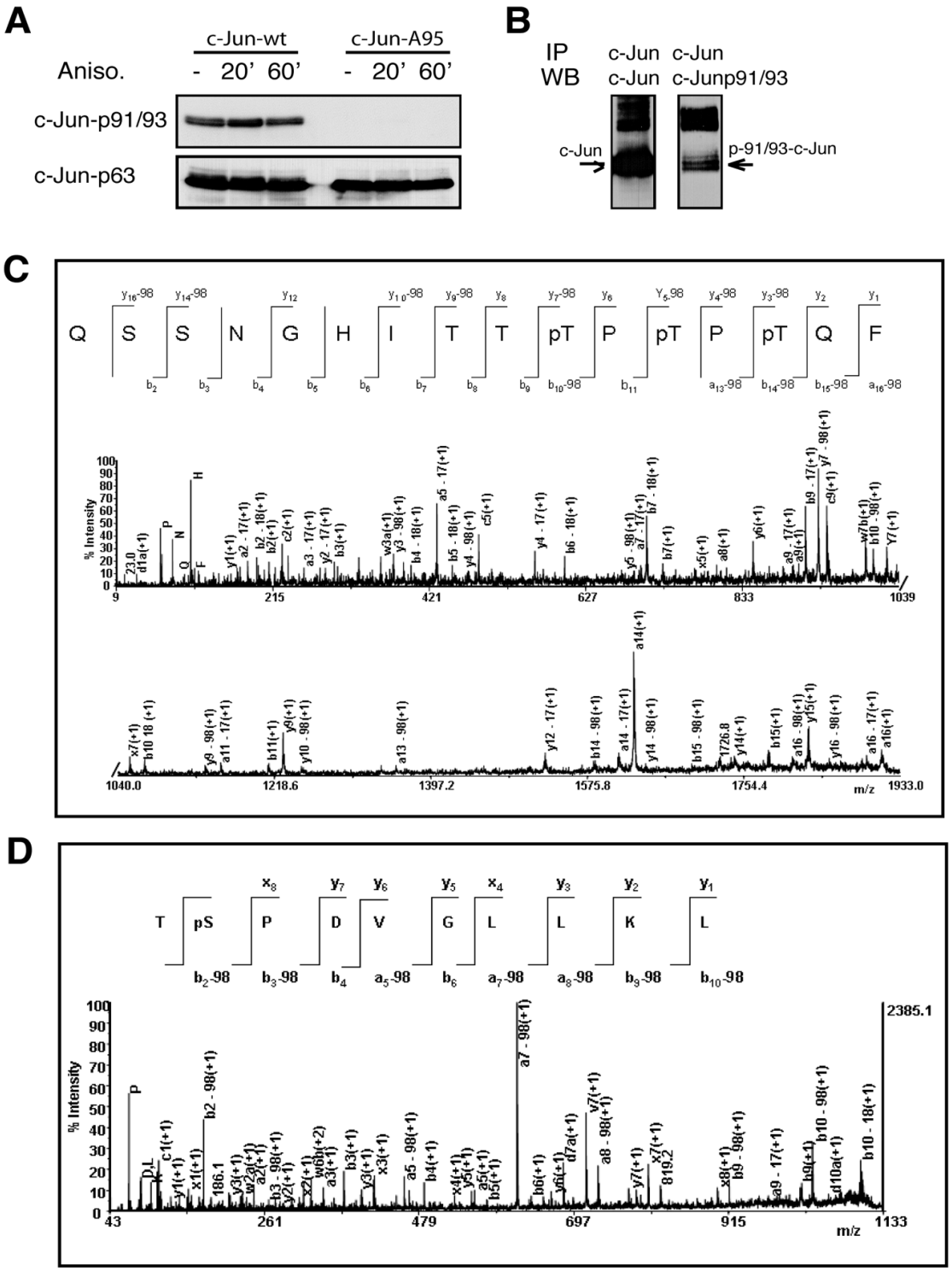

Figure 6.6: Phosphorylation of amino acid residues within c-Jun N-terminal domain. A Western blot analysis of HEK-293 cells transfected with DNA constructs expressing either HAtagged c-Jun-wt or Ha-tagged c-JunA95, as indicated. After transfection, cells were treated either without or with Anisomycin (100 ng/ml) for indicated time-periods. c-Jun N-terminal phosphorylation was determined by using the indicated antibodies. **B** Lysates from anisomycin treated c-Jun-wt-transfected

HEK-T cells were immunoprecipitated using the c-total c-Jun antibody, then aliquots from c-Jun-immunocomplexes were analysed by western blot using either c-Jun total antibodies (left panel) or c-Jun-p91/93 antibodies (right panel). **C** MALDI MS/MS spectra of the [M+H]+ of segment 82-97 carrying three phosphate groups at T91, T93 and T95. **D** MALDI MS/MS spectra of the [M+Na]+ of segment 62-70 carrying one phosphate group at S63. The a, b, and y ions are labelled in each spectrum, as well as b or y ions corresponding to the neutral loss of phosphoric acid (-98).

A

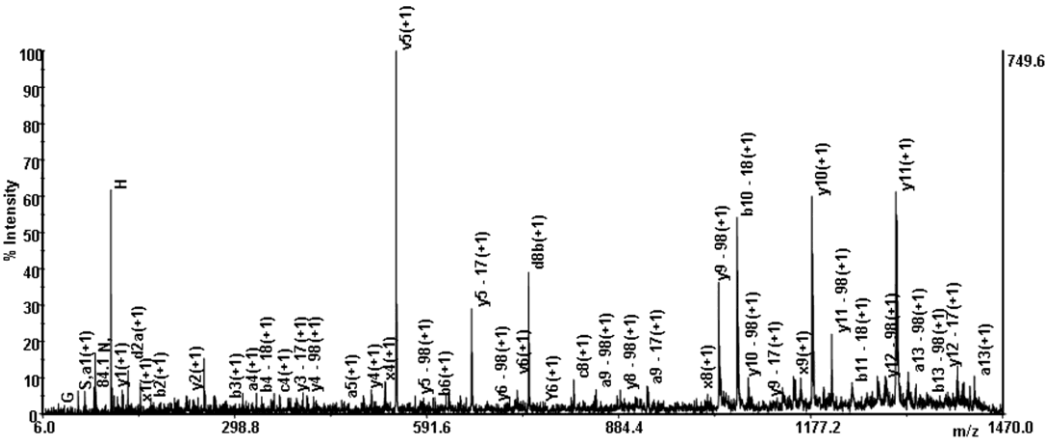

B

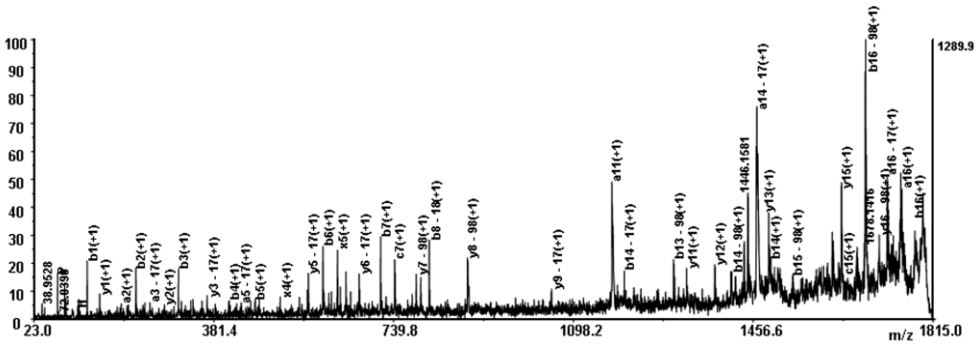

Fig 6.7: A) MALDI MS/MS spectra of the [M+H]$^+$ from segment 83-95. a, b, and y ions are labelled in the spectrum, as well as b or y ions corresponding to the neutral loss of phosphoric acid (-98).

B) MALDI MS/MS spectra of the [M+H]$^+$ from segment 82-97. a, b and y ions are labelled in the spectrum, as well as b or y ions corresponding to the neutral loss of phosphoric acid (-98).

6.1.5 JNK-1 phosphorylates T91/93 residues of recombinant c-Jun proteins in vitro

Our present results together with previous studies show that JNK activity is strictly required for c-Jun phosphorylation at T91/93 in response to various stimuli and in different cell types (Morton *et al.*, 2003; Madeo *et al.*, 2010). Yet, whether the T91/93 sites can be directly phosphorylated by JNK or by a putative JNK-induced kinase remains to be assessed. To resolve this question and to assess whether T95 phosphorylation is directly achieved by JNK or by a lithium-sensitive kinase, we set up in vitro phosphorylation assays for recombinant c-Jun proteins. To this aim, we generated recombinant GST-fused proteins containing the N-terminal portion of either c-Jun-wt, or c-JunA63/73 or c-JunA95 proteins (Fig 6.8). Purified GST/c-Jun proteins were then used in vitro phosphorylation assays using recombinant JNK-1 kinase. Site- specific phosphorylation of c-Jun was analyzed by western blot using phospho-specific antibodies for p-S63 or p-T91/93. As shown in figure 6A, JNK-1 was fully capable to phosphorylate S63 both in GST/c-Jun-wt and GST/c-Jun-A95 proteins, but not in GST/c-Jun-A63 proteins, indicating that in vitro phosphorylation of GST/c-Jun proteins by JNK-1 is highly specific for JNK sites. Notably, JNK-1 fully phosphorylated the T91/93 sites in both GST/-Jun-wt and GST/c-JunA63 proteins but not in GST/c-JunA95 proteins, confirming in vitro the dependence of T91/93 phosphorylation on the priming T95 site. In contrast, recombinant GSK3 β, used alone or in combination with JNK-1, had no effect on either sites of c-Jun phosphorylation (fig.6.9). These results suggest that JNK-1 is fully able to directly phosphorylate c-Jun at the canonical JNK T91/93 and at the T95 priming site. However, we cannot exclude that in vivo a lithium-sensitive kinase different from GSK3 β is the main kinase phosphorylating the priming T95 site.

Having shown that T95 is phosphorylated in vivo, we also asked whether the T95 site could be directly phosphorylated in vitro by JNK or by the lithium-sensitive kinase GSK3 β on immunoprecipitated c-Jun protein. To this end, we transfected NSC-34 cells with plasmids expressing either c-Jun-wt-HA or c-JunA95-HA tagged proteins and performed in vitro phosphorylation of immunoprecipitated c-Jun-HA proteins by using HA antibodies. c-Jun-HA immunocomplexes were then used as substrates for in vitro phosphorylation assays by using recombinant JNK-1, either alone or in combination with recombinant GSK3β. Given that T91/T93

phosphorylation is strictly dependent on the priming phosphorylation event at the T95 site, we assumed that the phosphorylation status of T91/T93 could indirectly monitor the capacity of either JNK or GSK3β to phosphorylate T95. Therefore, products of in vitro phosphorylation reactions were analyzed by western blot using phospho-specific antibodies for either p-T91/T93 or for p-S63. Since western analysis of NSC-34 total extracts revealed that Jun-HA proteins have quite low basal phosphorylation levels of the T239 GSK3β site, but fairly good levels of the T243 priming site for T239 phosphorylation (Fig 6.10A), we also monitored the phosphorylation status of the T239 by using a p-T239 phospho-specific antibody. As shown in the new fig 6.10B, recombinant JNK-1 was fully able to phosphorylate immunoprecipitated c-Jun-wt-HA at both S63 and T91/93 sites, whereas JNK-1 phosphorylated immunoprecipitated c-JunA95-Ha proteins only at the S63 site. In contrast, recombinant GSK3bβ had no effect of either S63 or T91/93, but t it was fully able to phosphorylate both forms of c-Jun-HA proteins at the T239 site. It's worth to note that the mobility shift of c-Jun-HA proteins detected by HA-Ab (in the samples incubated with JNK-1) is due to S63 phosphorylation and therefore is observed in both c-Jun-wt-Ha and c-Jun-A95-HA proteins.

To rule out that that T95 phosphorylation of c-Jun-HA immunocomplexes was achieved by a c-Jun-interacting kinase different from JNK, we then performed in vitro phosphorylation of FL c-Jun recombinant protein. As shown in the new fig 6.10C, we found that recombinant JNK-1 was able to phosphorylate recombinant FL-c-Jun at both the S63 and T91/93 sites. All together these experiments indicate that JNK-1 is fully able to directly phosphorylate c-Jun at the canonical JNK T91/T93 sites and at the non-canonical T95 site. However, we cannot exclude that in vivo a lithium-sensitive kinase, different from GSK3β is the main kinase phosphorylating the priming T95 site.

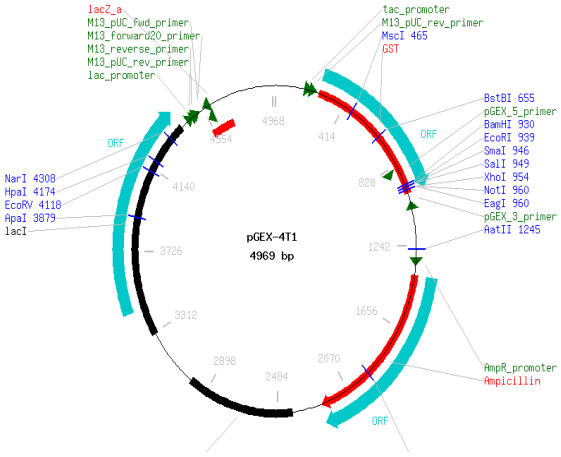

B

1 MTAKMETTFYDDALNASFLPSESGPYGYSNPKILKQSMTLNLADPVGSLKPHLRAKNSDL

61 LTSPDVGLLKLASPELERLIIQSSNGHITTTPTPTQFLCPKNVTDEQEGFAEGFVRALAE

121 LHSQNTLPSVTSAAQPVNGAGMVAPAVASVAGGSGSGGFSASLHSEPPVYANLSNFNPGA

C

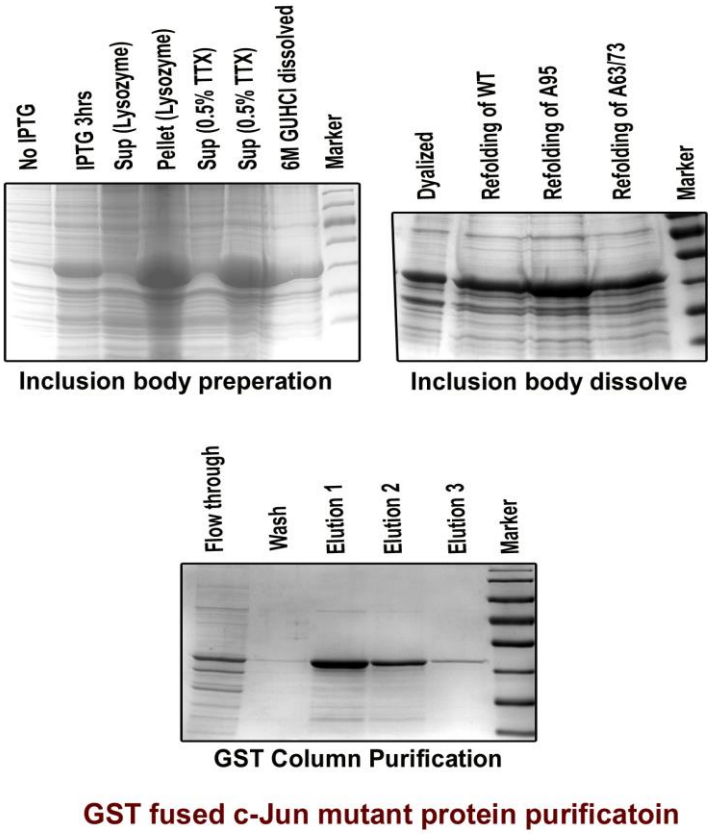

Fig 6.8: GST-fused c-Jun constructs: A the vector used for cloning of GST fused mutant c-Jun constructs. **B** Sequence showing the mutations that were cloned.

C GST fused c-Jun mutants were induced by using IPTG and purified the protein from inclusion bodies of E.Coli cultures. Inclusion bodies were dissolved in 6M GuHCl, refolded the protein by dissolving it in folding buffer and dialysed the protein to neutralized buffer containing 15mM NaCl. Finally purified the proteins by using Pierce GST tagged column kit.

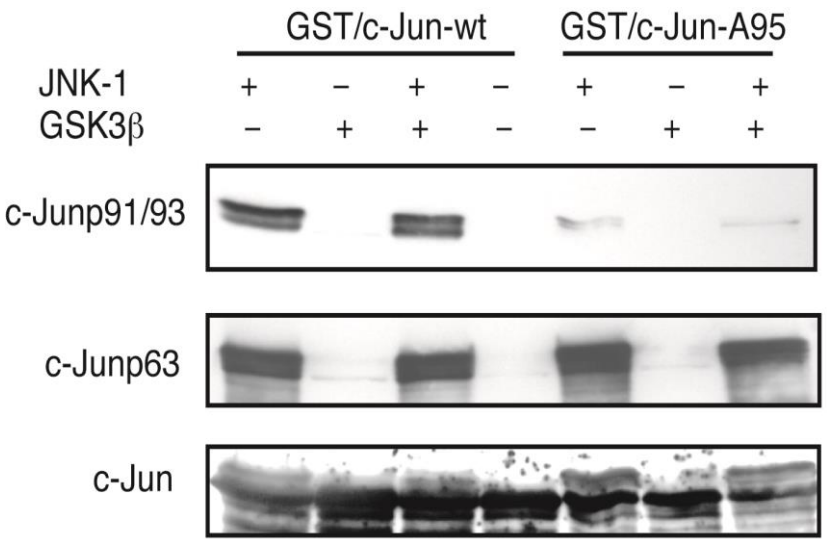

Figure 6.9: JNK1 is able to phosphorylate T91/93 but requires intact T95 in vitro

In vitro kinase assay was performed by using purified GST-c-Jun wt or GST-c-Jun-A95 protein and incubated either with JNK1, GSK3β kinases individually or with both kinases together. Kinase assay were performed for 30 minutes at 30°C and stopped the reaction by using SDS sample buffer. The phosphorylation of GST-c-Jun proteins were analysed by using western blot with either pS63, pT91/93 phospho-specific c-Jun antibodies or with total c-Jun antibody.

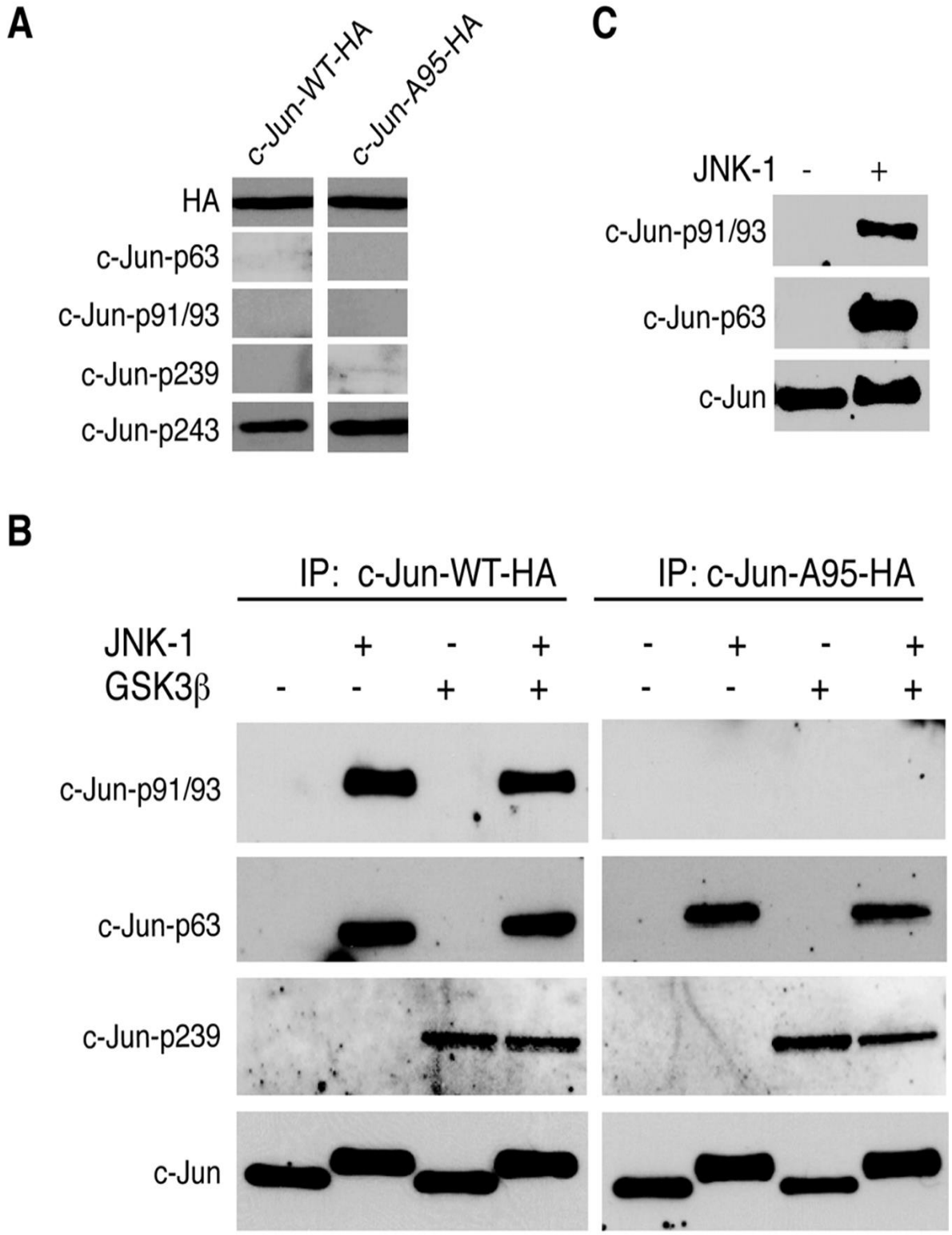

Figure 6.10: Recombinant JNK-1 phosphorylates immunoprecipitated c-Jun proteins at T91/93 in a T95-dependent manner

A NSC-34 cells were transfected with plasmids expressing either c-Jun-wt-HA or c-JunA95-HA tagged proteins (as indicated) and levels of c-Jun site-specific phosphorylation were analysed by western blot of total extracts by using the indicated antibodies. **B** Either c-Jun-wt-HA or c-JunA95-HA tagged proteins were immunoprecipitated by using HA antibodies, then c-Jun-HA immunocomplexes were used as substrates for in vitro phosphorylation assays by using recombinant JNK-1, either alone or in combination with recombinant GSK3 β as indicated. Products of in vitro phosphorylation reactions were analyzed by western blot using c-Jun-phospho-specific antibodies for p-T91/T93, p-S63 or p-239. Total amounts of c-Jun proteins were determined by using the c-Jun total antibody. **C** In vitro phosphorylation assay of recombinant FL-c-Jun protein (Ezio life sciences) incubated with recombinant JNK-1 as indicated. Reactions were analysed by western blot, using either c-Jun-p91/93 or c-Jun-pS63 phospho-specific antibodies as indicated. Total amounts of c-Jun proteins were determined by using the c-Jun total antibody.

6.2 Role of c-Jun in neuronal Inflammation

6.2.1 LPS elicits JNK-dependent phosphorylation of c-Jun in bergemann glia cells

We used DIV6 neuronal/glial cerebellar cultures established from P4 mice to examine c-Jun expression and activation in BG cells. This type of neuronal/glial culture is particularly suitable to study both physiological and inflammatory processes in BG cells, as they contain a large number of radial astrocytes derived from Bergmann glia, granule neurons and only a minor proportion of microglial cells (Xiong *et al.*, 2000; Sass *et al.*, 2001). To examine c-Jun expression in Bergmann glia-derived radial astrocytes, we performed double immunocytochemical staining of c-Jun and two Bergmann glial specific markers, the calcium binding protein S100 and the glutamate transporter GLAST (Ullensvang *et al.*, 1997; Hachem *et al.*, 2007), both expressed in the cell body and radial processes of Bergmann glia. As shown in figure 6.11A, nuclear c-Jun was highly expressed in both S100 and GLAST positive glial cells that had developed radial processes characteristic of Bergmann glia in vivo. Notably, immunocytochemical staining of the CD11b microglial marker confirmed a very low proportion of microglia in this type of cerebellar neuronal/glial cultures (Fig 6.11B, D). In contrast, standard cultures of microglial cells generated from the cortex of the same P4 mice resulted in massive staining of CD11b (Fig 6.11C, D), validating the high immunoreactivity of the Anti-Cd11b antibody.

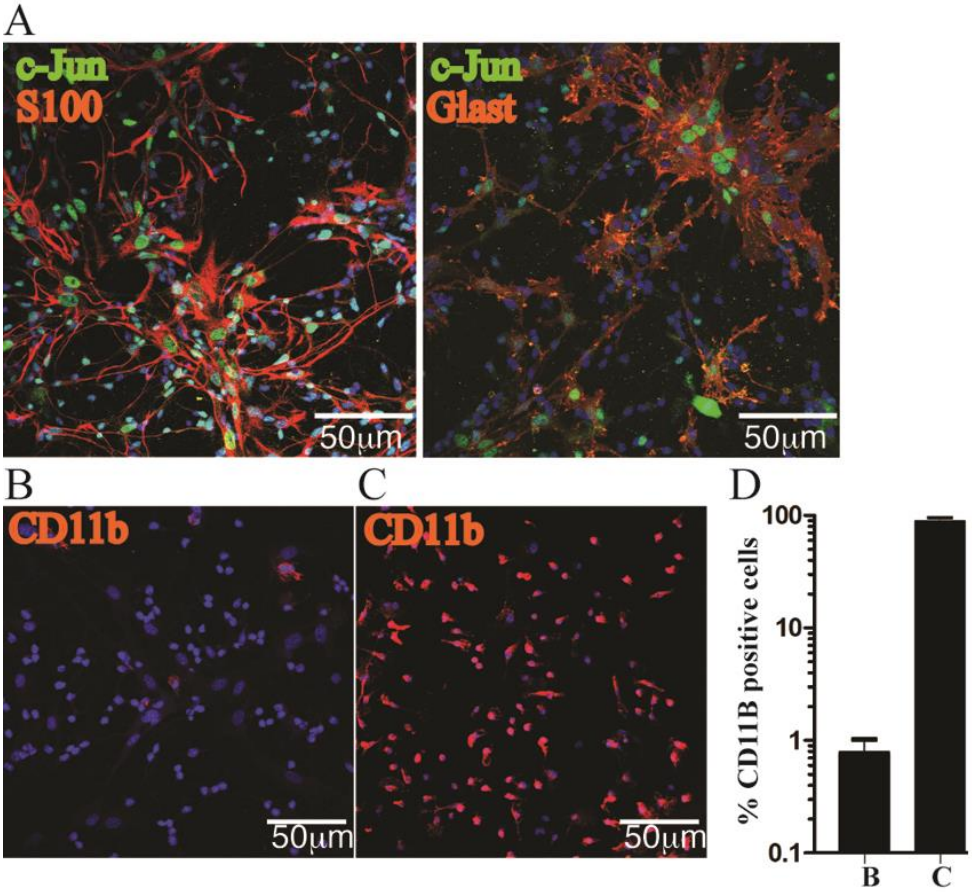

Fig 6.11: c-Jun is expressed in Bergmann glial-derived cells. **A:** Double immunostaining of DIV6 neuronal/glial cerebellar cultures generated from P4 mice with c-Jun (green) and S100 (red) or GLAST (red), as indicated. **B:** Immunostaining of neuronal/glial cerebellar cultures generated from P4 mice with CD11b (red). **C:** Immunostaining of cerebral microglia cultures generated from P4 mice with CD11b. In all described panels nuclei were stained with DAPI (blue).**D:** Quantifications of CD11b-positive cells shown in panel B and C, as indicated. Columns indicate the percentage of CD11b-positive cells per 10^3 cells. Values were plotted using a logarithmic scale with bars indicating SD from 3 different glass coverslips.

The evidence that c-Jun was highly expressed in BG cells prompted us to assess the effect of LPS, a potent activator of glial cells, on c-Jun phosphorylation at S63, a well-established hallmark of c-Jun activation (Eferl & Wagner, 2003; Karin & Gallagher, 2005; Raivich & Behrens, 2006). To this end, we performed double immunostaining of either LPS-treated or untreated neuronal/glial cultures by using the S100-specific antibody (Ab) together with either the c-Jun-specific Ab or the c-Jun-pS63 Ab, which recognizes a serine phospho epitope at amino acid position S63 of c-Jun. We found that the number of S100/c-Jun-pS63 double positive cells was quite low in control cultures, but it significantly increased upon treatment with LPS (fig 6.12A, 6.13A). Differently, the number of S100/c-Jun double positive cells detected in LPS-treated culture did not change significantly compared to control cultures (Fig. 6.12A, 6.13A), indicating that induction of c-Jun phosphorylation is the initial step of c-Jun activation by LPS. As the c-Jun N-terminal kinase (JNK) is the major kinase mediating c-Jun activation by extracellular signals, including LPS (Morton *et al.*, 2003; Ogawa *et al.*, 2004), we then examined the effect of the JNK-specific inhibitor SP600125 on c-Jun phosphorylation. We found that SP600125 clearly abolished the increase of S100/c-Jun-pS63 double positive cell number observed in LPS-treated cultures (Fig 6.12A, 6.13A). Next, the effect of LPS on c-Jun phosphorylation was validated by western-blot analysis (Fig 6.12B), demonstrating that the observed immunocytochemical variations of the c-Jun-pS63 Ab reactivity corresponded to quantitative changes of phosphorylated c-Jun levels.

Notably, LPS was unable to induce c-Jun phosphorylation in S100-negative cells, mostly corresponding to granule cells (GCs) (Fig 6.13B). Conversely, in these cells, KCl withdrawal induced c-Jun expression and phosphorylation (Fig 6.12A, 6.13A), a signaling response previously described in postmitotic GCs (Ma *et al.*, 2007; Yuan *et al.*, 2009). To confirm that LPS-unresponsive cells were granule neurons, we then performed double staining of c-Jun-pS63 and NeuroD1, a transcription factor expressed in postmitotic GCs (Miyata *et al.*, 1999). We found that KCl withdrawal, but not LPS, induced c-Jun phosphorylation in NeuroD1-positive GCs (Fig 6.13B), confirming that LPS triggers c-Jun activation specifically in BG cells.

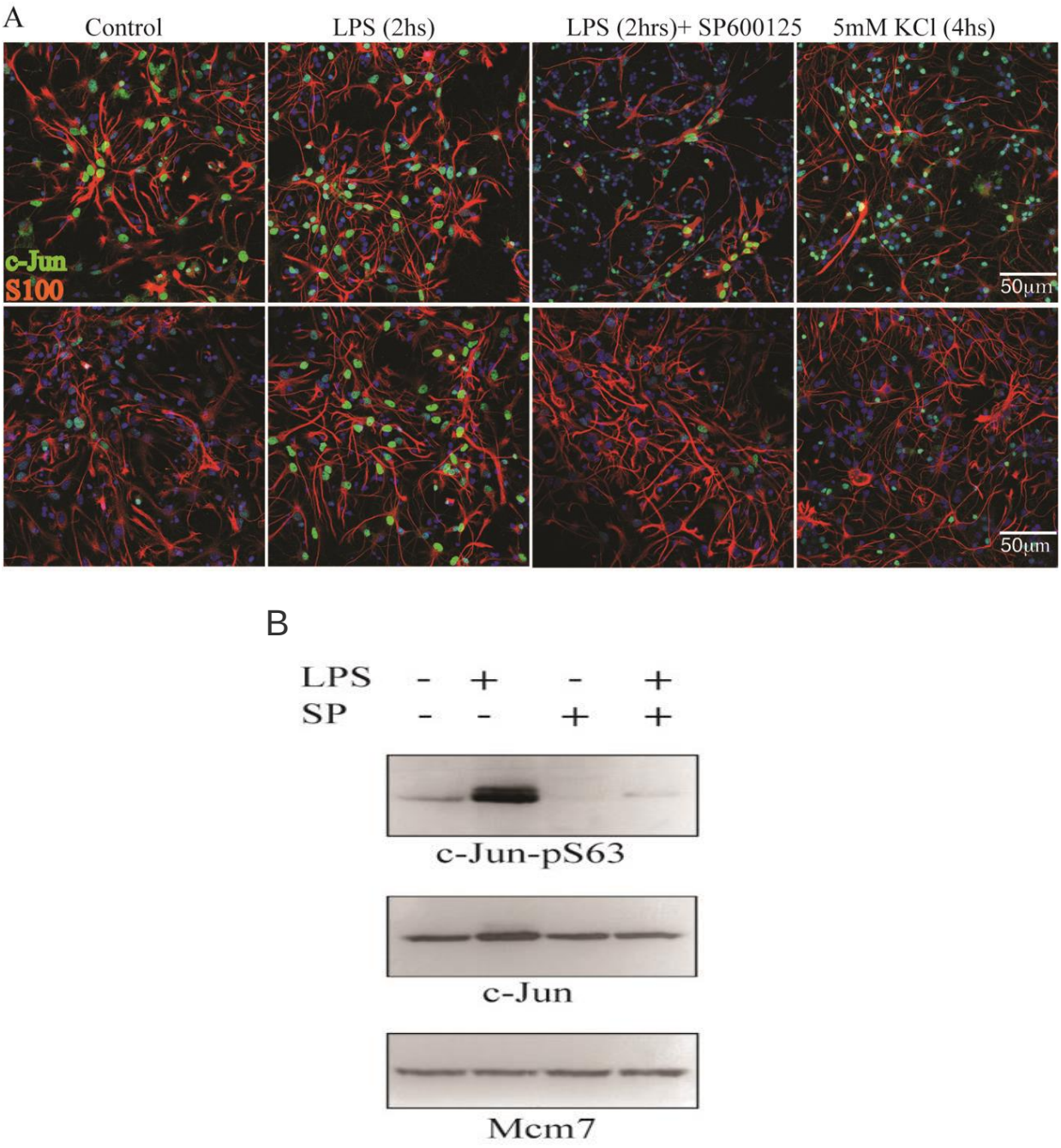

Fig 6.12: LPS induces JNK-dependent phosphorylation of c-Jun in radial glial cells. **A:** Double immunostaining of S100 (red) with either c-Jun (upper panels, green) or c-Jun-pS63 (lower panels, green) in DV6 neuronal/glial cerebellar cultures generated from P4 mice and treated either with vehicle (control) or with LPS (100ng/ml), or LPS and 5□M SP600125, or cultured in 5mM KCl, as indicated. **B:** Western-blot analysis of DV6 cerebellar cultures described in panel A and treated either with vehicle (-) or with LPS (100ng/ml for 2 hrs), or with SP600125 (SP) (5□M for 2hrs), or with LPS and SP for 2 hrs, as indicated. c-Jun expression levels were

determined by using either the c-Jun antibody or the c-Jun-pS63 antibody, as indicated. An antibody specific for the minichromosome maintenance complex component 7 protein (MCM7) was used as loading control.

A

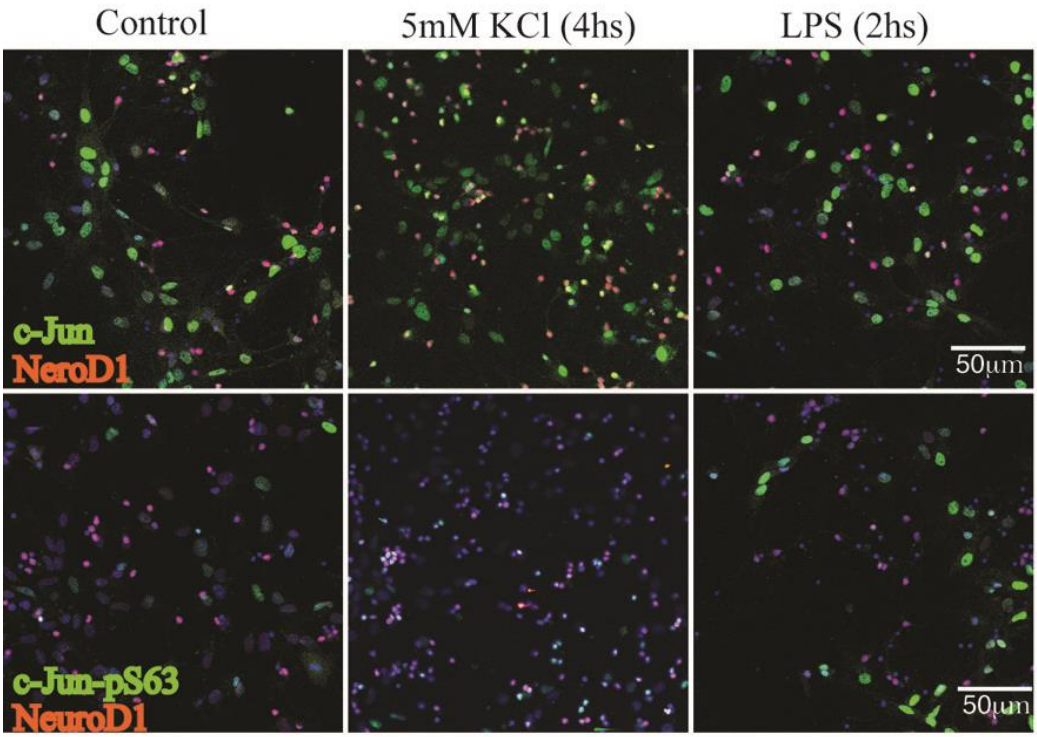

B

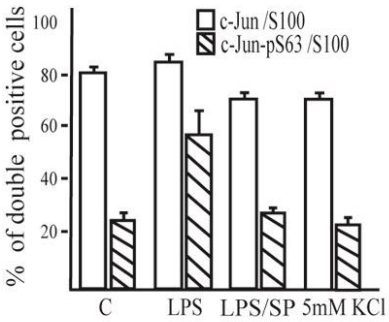

Fig 6.13: LPS does not induce c-Jun N-terminal phosphorylation in cerebellar granular neurons. Double immunostaining of NeuroD1(red) with either c-Jun (upper panels, green) or c-Jun-pS63 (lower panels, green) in DV6 cerebellar culture described in panel A and treated either with vehicle (control) or with LPS (100ng/ml),

or cultured in 5mM KCl, as indicated. **B:** Quantifications of c-Jun/S-100 and c-Jun-pS63/S100 double positive cells shown in panel A. The columns indicate the average percentage number of double positive cells present in 10 different fields, with bars indicating SD

6.2.2 Bergmann glial express TLR4 cells

As LPS acts via Toll-like receptor (TLR) 4 (Akira *et al.*, 2006), we than examined whether this receptor is expressed in Bergmann glia-derived radial astrocytes by performing double immunostaining for TLR4 and c-Jun. As shown in figure 6.14A, several c-Jun-positive Bergmann glia-derived cells showed a typical granular staining of TLR4 in the cytoplasm, suggesting that LPS can directly activate these cells. Furthermore, we show that induction of c-Jun phosphorylation by LPS was already detected after 20 minutes of treatment (Fig 6.14B), which is the minimum time required for significant induction of c-Jun phosphorylation at S63 by LPS in other inflammatory cells, including microglia (Hidding *et al.*, 2002; Morton *et al.*, 2003). Taken together, these results suggest that LPS directly activates (Hidding *et al.*, 2002) Bergmann glia-derived radial astrocytes and in turn elicits JNK-dependent activation of c-Jun.

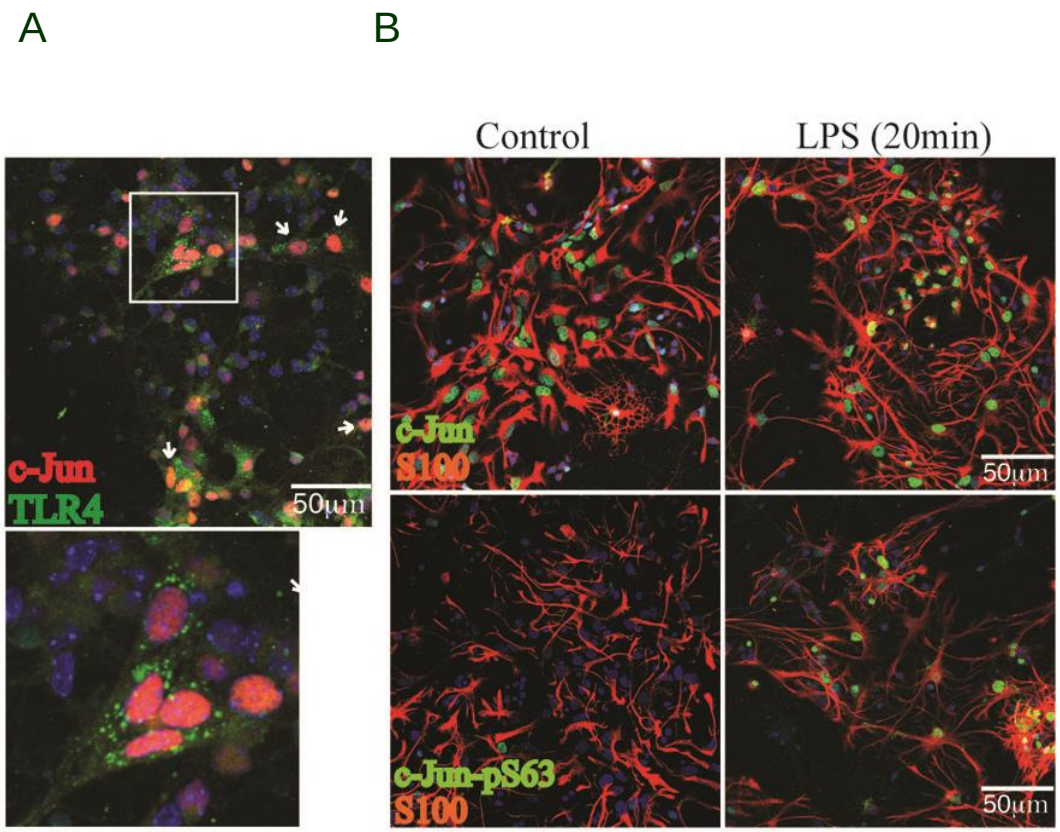

Fig 6.14 LPS induces JNK-dependent phosphorylation of c-Jun in radial glial cells via TLR4. A: Double immunostaining of c-Jun (red) and TLR4 (green) in DIV6 cerebellar cultures described in panel A. The white-boxed region delimits the correspondent higher-magnification images shown below. White arrowheads indicate examples of BG cells presenting overlapping expression for c-Jun and TLC4. **B:** Double immunostaining of S100 (red) with either c-Jun (upper panels, green) or c-Jun-pS63 (lower panels, green) in DV6 cerebellar cultures described in panel A and treated either with vehicle (control) or with LPS (100ng/ml) for 20 minutes, as indicated. In all panels nuclei were counter stained with DAPI (blue).

6.2.3 c-Jun is required for Il-1beta expression in LPS-activated Bergmann glial cells

Activated glial cells release a variety of inflammatory factors, among which cytokines and chemokines play a crucial role in both amplification and regulation of the inflammatory response. We investigated whether activation of the JNK/c-Jun pathway by LPS induced the expression of Il-1β and ccl2, two major pro-inflammatory molecules previously shown to be expressed n LPS-treated neuronal/glial cerebellar cultures (Sass *et al.*, 2001). To this aim, we performed quantitative real-time PCR experiments to monitor the expression Il-1β and ccl2 in LPS-treated neuronal/glial cultures from P4 mice. In addition, to check whether the few microglial cells present in these cultures (see Fig 6.11B, D) might contribute to the pattern of gene expression, we examined the levels of Il-18 mRNA, a cytokine that is specifically induced in microglial cells by LPS, while its expression is constitutive in primary astrocytes (Conti *et al.*, 1999). Our results show that LPS significantly induced the levels of Il-1β and ccl2 mRNAs in neuronal/glial cultures (Fig 6.15, 6.16A). In contrast, LPS had no effect on the constitutive levels of Il-18 mRNA (Fig 6.16A), confirming that, in these cultures, Bergmann glia-derived radial astrocytes are the predominant type of glial cells contributing to the pattern of gene expression. Notably, the effect of LPS on Il-1β mRNAs was abolished by co-treatment with SP600125, indicating that the JNK pathway is essential for the induction of Il-1β (Fig 6.16A). Differently, the increase of ccl2 mRNA was unaffected by SP600125 (Fig 6.16A), pointing to alternative pathways controlling ccl2 expression.

Next, we investigated whether LPS induced the release of Il-1β protein in the culture medium of neuronal/glial cerebellar cultures. As shown by ELISA analysis (Fig 6.16B), a significant amount of Il-1β accumulated in the culture medium of LPS-treated cultures, indicating that the increase of Il-1β mRNA by LPS correlates with IL-1β release. To examine the specific involvement of c-Jun in the regulation of Il-1β gene expression, we next examined the levels of IL-1β mRNA in neuronal/glial cerebellar cultures generated from conditional knockout mice lacking c-Jun expression in the CNS (c-Jun-Dn mice) (Raivich *et al.*, 2004). As shown in figure 3C, the large increase of IL-1β mRNA present in LPS-treated cultures from control mice was significantly diminished in LPS-treated cultures from c-Jun DN mice, demonstrating the requirement of c-Jun expression for the induction of Il-1 β, these

results also validate that Bergmann-derived radial astrocytes are the predominant glial cells expressing Il-1β in cerebellar neuronal/glial culture from P4 mice.

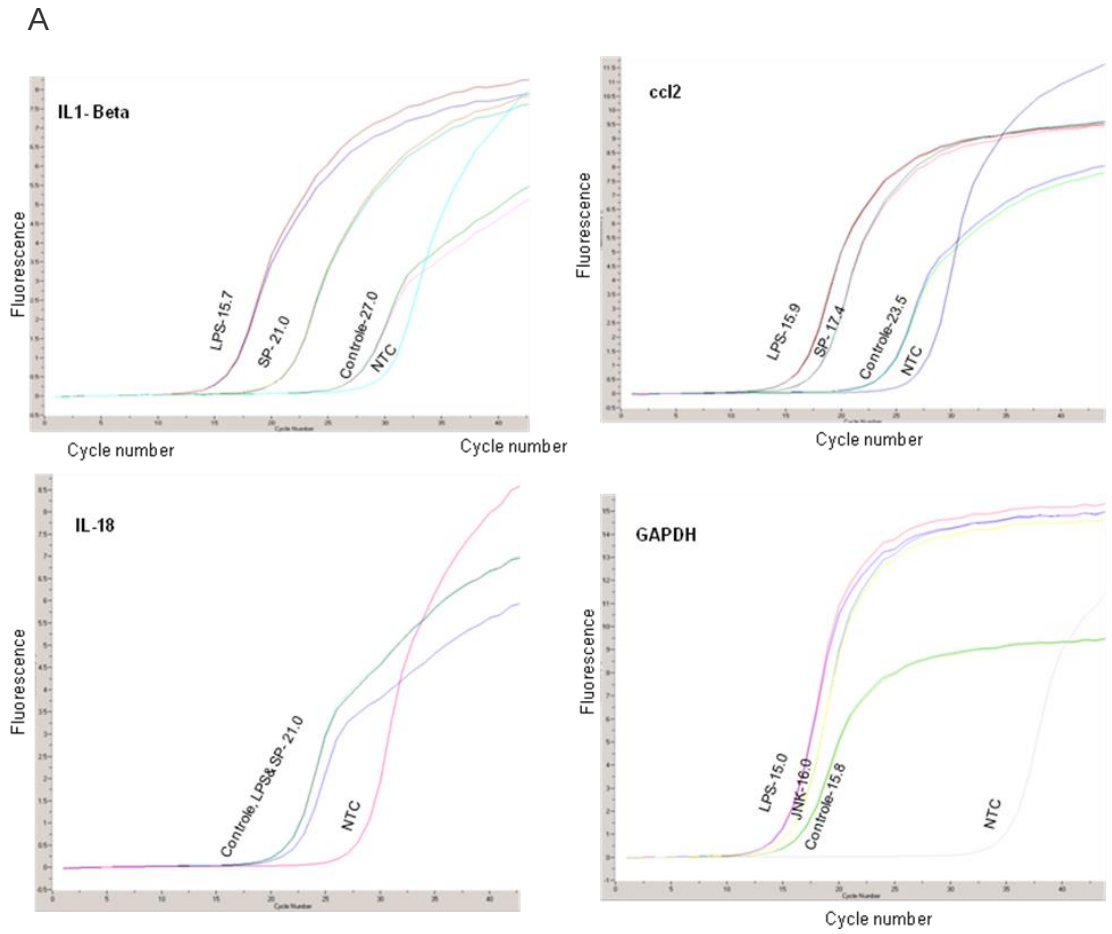

Fig 6.15: Real time PCR Amplification curves: A: Amplification curves of real-time PCR analysis of Il-1β, ccl2 and IL-18 mRNAs in DIV6 neuronal/glial cerebellar cultures generated from P4 mice and treated either with vehicle (control) or with 100ng/ml LPS for 12 hrs (Le *et al.*), or with LPS and 5mM SP600125 (SP), as indicated in the histogram legend. The data were normalized to Gapdh mRNA and represented as fold change relative to RNA levels in not treated cultures.

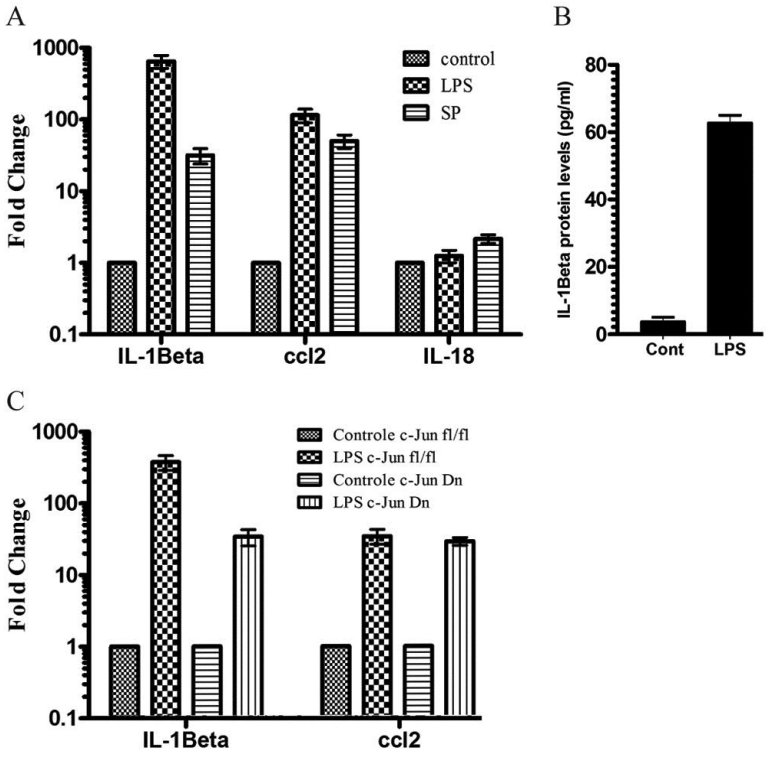

Fig 6.16: The JNK/c-Jun pathway is essential for the induction of IL-1β mRNA. A: Quantitative real-time PCR analysis of Il-1β, ccl2 and IL-18 mRNAs in DV6 neuronal/glial cerebellar cultures generated from P4 mice and treated either with vehicle (control) or with 100ng/ml LPS for 12 hrs (Le *et al.*), or with LPS and 5mM SP600125 (SP), as indicated in the histogram legend. The data were normalized to Gapdh mRNA and represented as fold change relative to RNA levels in not treated cultures, which were set to 1. Values were plotted using a logarithmic scale. Error bars represent SD of three independent experiments. **B:** IL-1β detection by ELISA in the supernatants collected from DIV6 cerebellar cultures described in panel A and treated either with vehicle (cont) or with 100ng/ml LPS for 24 hrs (Le *et al.*) as indicated. Columns represent levels of IL-1β levels in pg/ml with bars indicating SD from 3 parallel experiments. **C:** Quantitative real-time PCR analysis of Il-1β and ccl2 mRNAs from DIV6 neuronal/glial cerebellar cultures generated from either P4 c-Jun fl/fl mice or P4 c-Jun-Dn mice and treated with vehicle (control) or with 100ng/ml LPS for 12 hrs (Le *et al.*) as indicated in the histogram legend. The data were normalized as described in panel A. Scale Error bars represents SD of three independent experiments.

6.2.4 c-Jun is expressed during formation of the Bergman glial monolayer

To substantiate the relevance of astroglial expression of c-Jun in neuronal/glial cerebellar cultures, we then examined the cell-type and layer-distribution of c-Jun-expressing cells in the early postnatal cerebellum. To this end, mouse cerebellar sections from P1, P4 and P7 mice were double immunostained with c-Jun and two BG specific markers, S100 and GLAST. Confocal microscopy analyses of P1 and P4 cerebellar sections showed that the majority of c-Jun-positive cells were concentrated underneath and surrounding Purkinje cells (PCL), hence forming a cellular layer encompassing the territory of BG cells (Fig 6.17A, B, D). Furthermore, within the BG layer, several nuclei of either S100- or GLAST-positive cells were immunostained by the c-Jun Ab (Fig 6.17A, B, C), indicating c-Jun expression during formation of the BG monolayer. In contrast, at P7, c-Jun positive cells were mainly distributed in the IGL and only few cells were double positive for c-Jun and S100 (Fig 6.17C), revealing a developmental stage-specific expression of Jun in BG cells.

To validate c-Jun expression in BG cells, we examined the mitotic activity of c-Jun-positive in P1 mice, as BG cells have been described to be highly proliferative at this developmental stage (Yuasa, 1996). To this end, we performed BrdU pulse-labelling in P1 mice and analysed cerebellar sections by double-immunostaining with c-Jun and BrdU. As shown in figure 6.17E, several cells were c-Jun/BrdU double positive and primarily located in the BG layer, confirming c-Jun expression in proliferating cells of the BG layer.

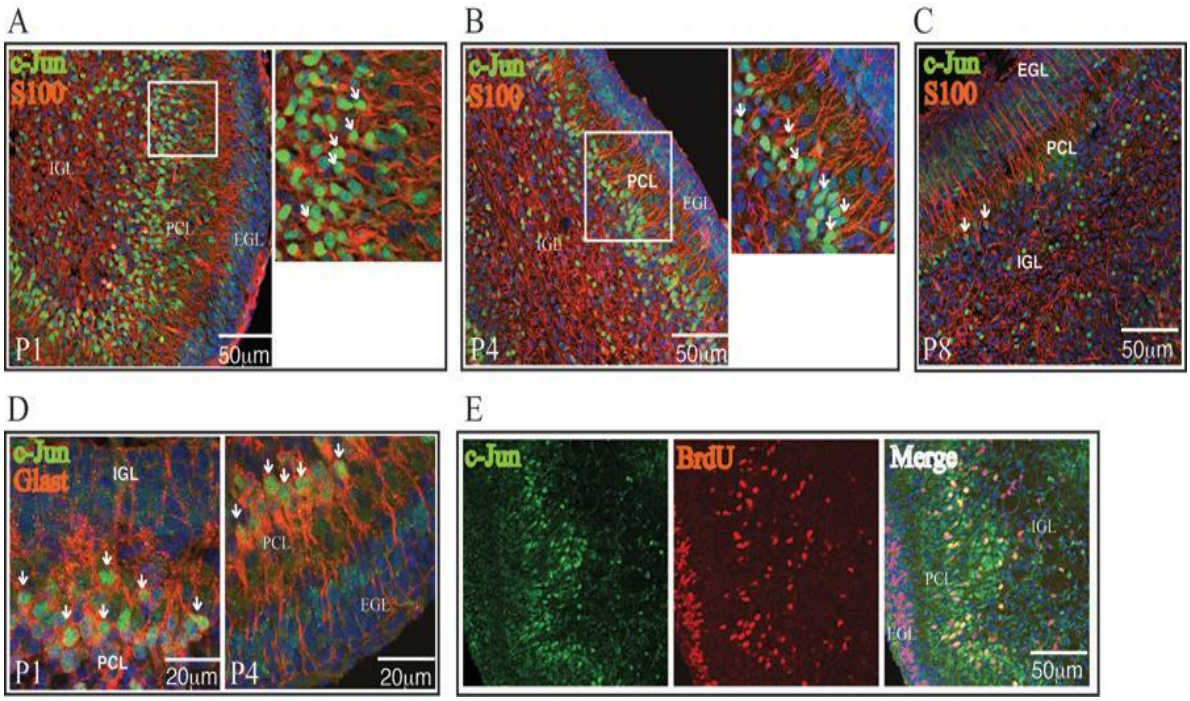

Fig 6.17: c-Jun is expressed in Bergmann glial cells. A-C: Double immunostaining of c-Jun (green) and S-100 (red) on sections of P1 (A), P4 (B) and P7 (C) mouse cerebella, as indicated. Nuclei were counter stained with DAPI (blue). White-boxed regions in P1 and P4 delimit the correspondent higher-magnification images shown alongside**.** Double immunostaining of c-Jun (green) and GLAST (red) on sections of in P1 mad P4 mouse cerebella, as indicated. **E:** Double immunostaining of coronal sections of P1 cerebella showing either c-Jun (green) or BrdU (red) positive cells, as indicated. Overlapping staining (orange) for c-Jun and BrdU are merged in the left panel, as indicated. White arrowheads indicate examples of BG cells presenting overlapping expression for c-Jun and each of the indicated markers.

6.2.5 c-Jun expression in Purkinje cells and granule neurons

To investigate the cellular identity of c-Jun-positive cells not expressing BG markers, we performed double immunostaining of c-Jun and a set of cell-type specific markers in cerebellar sections from P1, P4 and P7 mice. Firstly, we carried out double staining for c-Jun and calbindin, a specific marker for Purkinje cells (PCs) (Celio, 1990). Sections from P1 and P7 cerebella showed lack of c-Jun expression in PCs (Fig 6.18A). However, at P4, few cells were reproducibly double positive for c-Jun and calbindin, revealing that c-Jun can be expressed in Purkinje neurons during a narrow developmental window.

Next, we examined the co-expression pattern of c-Jun and markers of NeuN, a transcription factor widely used to mark post-mitotic neurons and expressed in differentiated GCs (Weyer & Schilling, 2003). As shown in Fig 6.18B, c-Jun/NeuN double-positive cells were detected in the IGL of all three developmental stages. In contrast, NeuN was not expressed in c-Jun-positive cells located in the BG layer, confirming that these cells are mostly BG cells. Same results were obtained by double staining of c-Jun and NeuroD1 (Fig 6.18C), validating c-Jun expression in postmitotic GC of the IGL. We also examined the co-expression pattern of c-Jun and Pax6, a transcription factor that is expressed in postmitotic GC precursors and throughout the course of their migration and differentiation (Yamasaki *et al.*, 2001). As shown in Fig 6.18D, at all examined stages, c-Jun was expressed in Pax6-positive located in the IGL. Furthermore, at the P4 stage, several Pax6/c-Jun double-positive cells encompassed the BG layer (Fig 6.18D), presumably representing post-migratory GC precursors at the onset of differentiation.

c-Jun expression was then examined in GABAergic interneurons by performing double immunostaining of c-Jun and Pax2, a transcription factor expressed in GABAergic interneurons of the developing cerebellum (Maricich & Herrup, 1999). As shown in figure 6.19, most of Pax-2 positive neurons were negative for c-Jun expression, with only few cells presenting overlapping expression of c-Jun and Pax2. Finally, we investigate the pattern of c-Jun N-terminal phosphorylation on S63. To this end, we performed immunostaining of cerebellar sections with the c-Jun-pS63 Ab. Several c-Jun-pS63 positive cells were detected in the IGL throughout the

P1-P7 stages (Fig 6.18E) and resulted mostly positive to NeuN and NeuroD1 (Fig 6.20). In contrast, c-Jun-pS63 positive cells were very rarely detected in the BG layer (Fig 6.18E, Fig 6.20), suggesting that developmentally regulated signaling modulate c-Jun activation in a cell-type specific fashion. Taken together these observations indicate that, in the early postnatal cerebellum, neuronal expression of c-Jun is mainly restricted to the IGL, where it is present in post-migratory GC precursors at the onset of their differentiation and continues during their terminal differentiation.

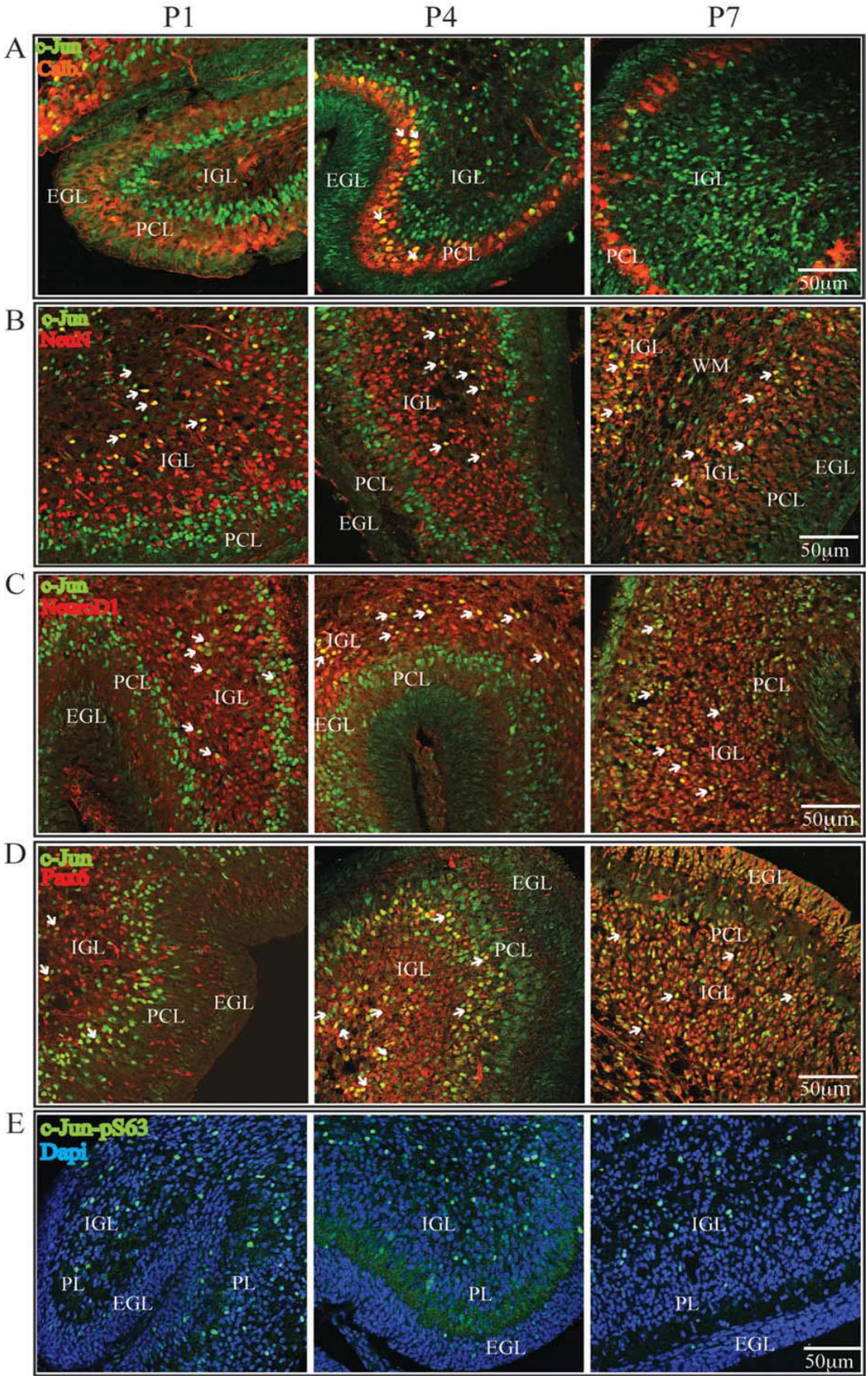
P1
P4
P7
A
c-Jun
Calb.
EGL
IGL
PCL
50µm
B
c-Jun
NeuN
IGL
PCL
EGL
WM
C
c-Jun
NeuroD1
D
c-Jun
Pax6
E
c-Jun-pS63
Dapi
PL

Fig 6.18: Dynamic distribution of c-Jun positive cells in the early postnatal cerebellum. A: Double immunostaining of c-Jun (green) and calbindin (red) on sections of P1, P4 and P7 mouse cerebella, as indicated. Purkinje cell immunostaining by anti-calbindin clearly distinguishes the forming PCL. At P1 and P4 , c-Jun immunostaining shapes a cellular layer underneath the PCL. White arrowheads indicate Purkinje cells presenting overlapping expression for calbindin and c-Jun at P4. **B-D:** Double immunostaining of c-Jun (green) and NeuN (B), or NeuroD1 (C) or Pax6 (D) on of sections of P1, P4 and P7 mouse cerebella, as indicated. White arrowheads indicate examples of neuronal cells presenting overlapping expression for c-Jun and each of the indicated markers. **E:** Immunostaining of c-Jun-pS63 (green) on tissue sections of P1, P4 and P7 mouse cerebella, as indicated. In all panels nuclei were stained with DAPI (blue). EGL, external granular layer; PLC, Purkinje cell layer; IGL internal granular layer.

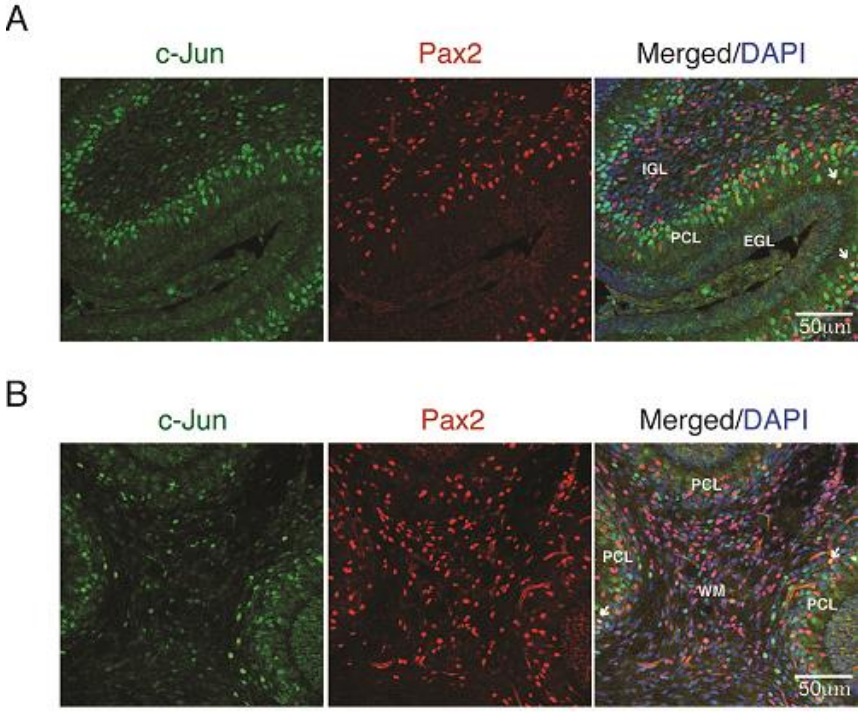

Fig 6.19: c-Jun expression in inhibitory interneurons. A-B: Double immuno staining of sections from P1 (A) or P4 (B) cerebella showing either c-Jun (green) or Pax2 (red) positive cells, as indicated. Overlapping staining (orange) for c-Jun and Pax2 are merged in the left panel, as indicated. Nuclei were counter stained with DAPI (blue). White arrowheads indicate examples of neuronal cells presenting overlapping expression for c-Jun and Pax2. EGL, external granular layer; PLC, Purkinje cell layer; IGL internal granular layer; WM, white matter.

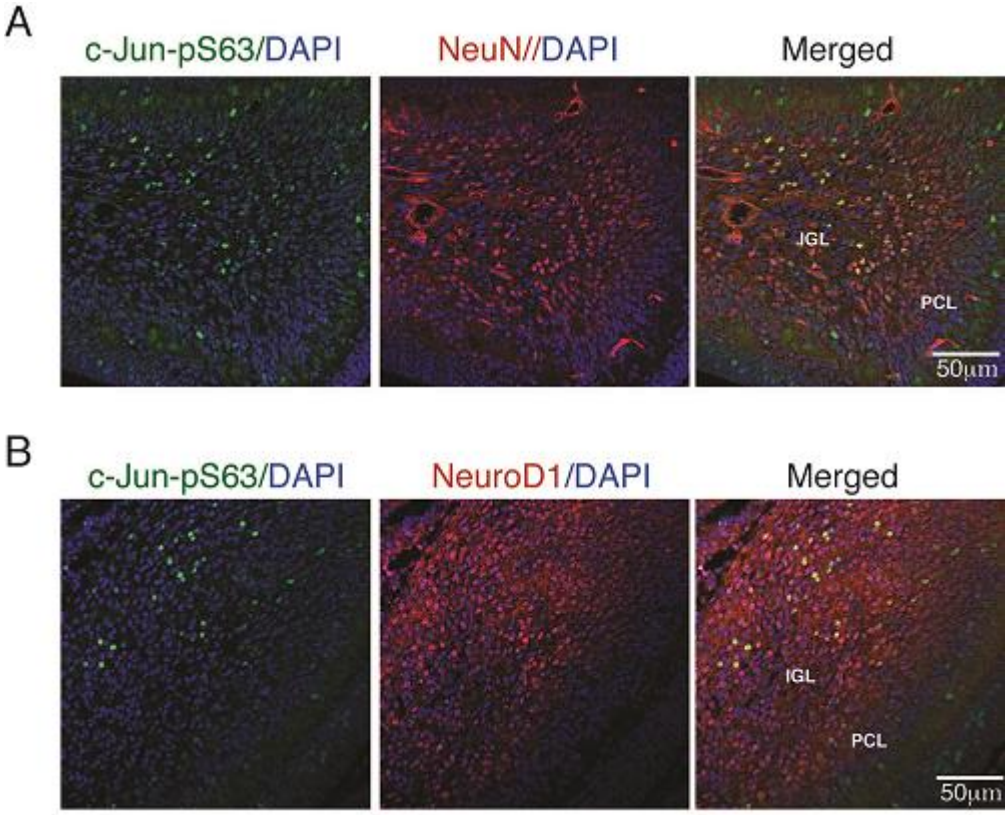

Fig 6.20: c-Jun N-terminal phosphorylation in granule cells. A-B: Double immunostaining on sections of P4 cerebella with the c-Jun-pS63 antibody (green) in combination with either (A) NeuN antibody (red) or (B) NeuroD1 antibody (red), as indicated. Overlapping staining (orange) are merged in the left panel, as indicated.

7 Discussion

Gene expression by the JNK/c-Jun pathway is involved in very different cellular programs, including cell cycle progression, differentiation and apoptosis. In turn, deregulation of the JNKs/c-Jun pathway may give rise to pathological conditions, including tumor progression, neuroinflammation and degenerative loss of neurons (Waetzig & Herdegen, 2004; Vinciguerra *et al.*, 2008). The challenging question is how the same signaling pathway can regulate the expression of genes involved in quite different cellular programs. One possible mechanism underlying the functional dicothomy of c-Jun/Ap-1 may be based on the type of c-Jun partner forming the dimeric Ap-1 transcription factor, which in turn might determine the class of activated target genes (Hess *et al.*, 2004; Yuan *et al.*, 2009). On the other side, the kinetic of the JNK/c-Jun signaling pathway is ceartainly involved in determining the diverse outputs of c-Jun biological activity. Several studies have shown that depending on the kinetic of JNK activation, variations in c-Jun levels and activation periods are coupled to different patterns of gene expression (Raman *et al.*, 0000; Ventura *et al.*, 2006; Comalada *et al.*, 2012). Our results suggest that depending on the complexity of external signals and their interplay with intrinsic cues, c-Jun phosphorylation by JNK may result differential at a site-specific level and in turn elicit different physiological responses.

7.1 Differential phosphorylation of N-terminal c-Jun in neuronal cells

Based on our results, we propose that depending on the complexity of external signals and their interplay with intrinsic cues, c-Jun phosphorylation by JNK may result differential at a site-specific level and in turn elicit different physiological responses. In particular, we provide evidence that in cerebellar granule cells, apoptotic cues lead to extensive phosphorylation of c-Jun N-terminal domain, with T91/T93 phosphorylation setting the threshold for c-Jun pro-apoptotic activity. In contrast, a concomitant activation of survival pathways initiated by lithium inhibits T91T93 phosphorylation with no effects on S63 phosphorylation, hence preventing the onset of c-Jun pro-apoptotic activity without interfering with possible non-destructive functions of c-Jun requiring S63 phosphorylation.

Two lines of evidence indicate that T91/T93 phosphorylation results in a threshold for c-Jun pro-apoptotic activity. The first evidence addresses the type of response of T91/T93 phosphorylation to apoptotic clues and comes from immunofluorescence analysis of c-Jun site-specific phosphorylation. This analysis shows that the response of T91/T93 phosphorylation to TK-deprivation is not graded but rather sensitive and mirrors the switch-like apoptotic response of TK-deprived neurons. The second evidence addresses the functional role of T91/T93 phosphorylation in triggering c-Jun pro-apoptotic activity and comes from the functional analysis of the c-JunA95 mutant in CGC apoptosis. This analysis shows c-JunA95-mutated proteins are not phosphorylated at T91/T93 in response to TK-deprivation and failed to promote CGC apoptosis. These findings confirm that in absence of T91/T93 phosphorylation, S63-phopshorylated c-Jun is not able to promote cell death. Also, they corroborate the regulatory role of the T95 site in priming T91/T93 phosphorylation by JNK. Furthermore, the finding that c-JunA95 is fully capable to induce neurite outgrowth in naïve PC12 cells validates that lack of T91/T93/T95 phosphorylation does not interferes with regenerative functions of c-Jun. However, whether such a functional role of c-Jun phosphorylation is a general principle, or applies to specific neuron populations, needs to be explored in future studies.

A further important question addressed by our study is the mechanism through which lithium blocks c-Jun pro-apoptotic function without inhibiting JNK activity. The specific effect of lithium on T91/T93 phosphorylation, together with the evidence that the c-JunD95 mutant resumes GCG apoptosis in presence of lithium is consistent with a model whereby lithium blocks c-Jun pro-apoptotic activity by targeting the priming T95 phosphorylation event for T91/T93 phosphorylation. In such a scenario, the priming event for T91/T93 phosphorylation acquires a crucial role in determining the output of c-Jun biological activity in response to JNK activation.

Lithium is a widely used drug for treatment of mood disorders, and yet the mechanism of action of lithium in neuronal disorders is unclear (Lenox RH, 2000). Interestingly, in a number of neurodegenerative disease models, both GSK-3β and JNK have been linked to pathogenic mechanisms. For example, both JNK and GSK-3β are implicated in Alzheimer's disease (MIGHELI *et al.*, 1997; Thakur *et al.*, 2007). In the study by Marcus and collaborators, it was shown that cortical neurons lacking

JNK3 expression, or cells expressing dominant-negative c-Jun mutant proteins, are protected from Beta amyloid aggregates (a key player in Alzheimer's pathogenesis). Furthermore, elevated JNK activity and c-Jun protein levels were detected in post-mortem brains of Alzheimer's patients (Marcus *et al.*, 1998; Shoji *et al.*, 2000; Zhu *et al.*, 2001). Similarly, GSK-3 activity was also shown to be elevated in post-mortem brains of Alzheimer's patients and induced by B-amyloid peptides in cultured hippocampal neurons (Takashima *et al.*, 1998; PEI *et al.*, 1999). Therefore, it would be of interest to examine the frequency of such tandem regulation of JNK and GSK-3β in diverse models of neurodegenerative diseases.

7.2 In vivo and In vitro phosphorylation of c-Jun at T95-T93-T91

Previous studies by Vinciguerra and colleagues have clearly shown that alanine substitution of T95 strongly impairs the induction of T91/93 phosphorylation of c-Jun by genotoxic stress (Vinciguerra *et al.*, 2008), suggesting that T95 acts as a phosphoacceptor site priming T91/T93 phosphorylation. However, till now T95 phosphorylation in cells was not addressed. In the present study, we performed mass-spectrometry analysis demonstrating that c-Jun is phosphorylated in cells at tall three T91/T93/T95 sites. As regard the mechanism through which lithium control the levels of T93/T93, our results could not establish whether lithium inhibits a kinase phosphorylating the T95 priming site, or by inducing a phosphatase removing T95 phosphorylation. However, our experiments show that recombinant JNK-1 fully phosphorylates c-Jun in vitro at the T91/T93 sites in a T95-dependent manner. These results suggest that in CGCs JNK sequentially phosphorylates c-Jun at T95-T93-T91 in response to TK-deprivation, whereas lithium may induce a T95-specific phosphatase. Although the T95 site does not contain the minimal S/TP sequence for MAP kinases, it has been previously shown that both JNK-2 and JNK-1 can phosphorylate a similar site in histone H2AX (Lu *et al.*, 2006; Sluss & Davis, 2006). Future experiments will elucidate whether in vivo T95 is phosphorylated by JNKs or by a lithium-sensitive kinase. Alternatively, lithium might inhibit T95 phosphorylation by regulating nuclear translocation of JNKs, hence limiting the local concentration of active JNKs necessary to phosphorylate the non-canonical T95 site. Accordingly, inhibition of JNK2-3 nuclear translocation has been described to protect from

neuronal apoptosis in sympathetic neurons and CGCs (Sengupta Ghosh *et al.*, 2011; Benny *et al.*, 2012).

In conclusion, Our results provide the first evidence that in the CGCs apoptotic and survival cues give rises to different site-specific configurations of c-Jun N-terminal phosphorylation, each of which having different functional outputs. Furthermore, our study suggests that inhibition of T91/T93/T95 phosphorylation may represent a pharmacological tool to selectively target c-Jun-dependent degenerative pathways in the nervous system.

7.3 Role of c-Jun in LPS-mediated activation of Bergmann Glial cells

We have used neuronal/glial mouse cerebellar cultures generated from P4 mice neonatal mice to assess putative functions of c-Jun in activated Bergmann glial cells. By using BG glial specific markers and granule neurons expressing postmitotic neuronal markers we show that these neuronal/glial cerebellar cultures contain mainly two types of cells: radial glial cells and granule neurons. To check the microglia population in these cultures we have used CD11 as a marker and confirmed that on an average of 1% population stained with the microglia marker, indicating that these cultures are adequate to dissect inflammatory pathways specific of BG-derived cells.

Firstly, from immunohistochemical staining we confirmed that c-Jun is highly expressed in the nucleus of radial astrocytes derived from Bergmann glia, also we show that Jun-positive cells coexpressed with BG specific markers in their soma and uni/bipolar processes, a characteristic of BG cells in vivo. Secondly, we show that upon addition of bacterial LPS triggers activation of the JNK/c-Jun pathway in BG cells, as indicated by a robust JNK-dependent phosphorylation of c-Jun on S63. Notably, induction of c-Jun phosphorylation by LPS was specifically detected in BG-derived astrocytes and abrogated by pharmacological inhibition of JNK, suggesting a functional role of the JNK/c-Jun pathway in the activation of Bergmann glial cells. LPS has been widely shown to activate inflammatory cells via TLR4 (Akira *et al.*, 2006). Within the CNS, TLR4 is predominantly expressed by microglia, however its expression has been also reported in astrocytes (Forshammar *et al.*; Gorina *et al.*; Bowman *et al.*, 2003; Sun *et al.*, 2008), suggesting that LPS can directly activate Bergman glia-derived cells and in turn induce c-Jun activation. Accordingly, we

observed a significant expression of TLR4 in c-Jun-positive Bergman glia-derived astrocytes. Moreover, we show that the induction of Jun phosphorylation by LPS is as rapid as in microglia or macrophages (Hidding *et al.*, 2002; Morton *et al.*, 2003), making unlikely an indirect effect of LPS (mediated by microglia) on Bergman glia-derived cells.

7.4 c-Jun is required for LPS-induced expression of Il-1β

We confirmed the involvement of the JNK/c-Jun pathway in the activation of BG-derived cells by showing that LPS induced IL-1β gene expression and pharmacological inhibition of JNK activity abolished both c-Jun phosphorylation and the increase of IL-1β mRNA. Most importantly, our results demonstrate an essential role of c-Jun in mediating activation of Bergmann glial cells, as the increase of IL-1β mRNA by LPS was abolished in neuronal/glial cultures from the c.Jun-Dn mutant mice, lacking c-Jun expression specifically in the CNS. In addition, this observation corroborates that Bergmann glia-derived cells are the predominant cell type contributing to the induction of Il-1β in the neuronal/glial cultures used in the present study, given that c-Jun is normally expressed in microglial cells from c-Jun-Dn mice(Raivich *et al.*, 2004).

Whether c-Jun is directly involved in the activation of the IL-1β gene in cerebellar astroglial cells remains to be elucidated. However, previous observations have shown the requirement of AP-1 activity for activation of the IL-1β promoter in macrophages (Kang *et al.*, 2004), suggesting a direct contribution of c-Jun to the regulation of IL-1β gene expression.

7.5 In vivo expression of c-Jun in the postnatal cerebellum

The finding that c-Jun is expressed in Bergmann glia-derived radial glial cells was confirmed and extended in vivo by immunohistochemical analyses of the early postnatal cerebellum. We found high levels of c-Jun expression in the nuclei of S100- and GLAST-positive cells, both in P1 and P4 mice. Besides, c-Jun positive cells defined a cellular layer underneath the PCL and were mitotically active, two characteristics of BG cells at this developmental stages (Yuasa, 1996). In addition, the significant loss of c-Jun staining in the BG monolayer of P7 mice suggests a developmental stage-specific expression of c-Jun, corresponding to the formation of

the BG monolayer. As previously described (Carulli *et al.*, 2002), we found c-Jun expression in postmitotic differentiated GC of the IGL, as proved by the large number of c-Jun/NeuN and c-Jun/NeuroD1 double positive cells. In addition, our results reveal c-Jun expression in post-migratory GC precursors, as proved by the presence of c-Jun/Pax6 double positive cells both across the PCL and in the IGL.
We currently have no hints on the possible function of c-Jun expression during the formation of the BG monolayer. c-Jun has been shown to be crucial for cell cycle progression of several type of cells, suggesting that it may be important for BG cell proliferation. However, this hypothesis is not supported by our results showing that c-Jun phosphorylation on S63, a critical requirement for c-Jun proliferative function (Shaulian E, 2001 Apr 30; Wada *et al.*, 2004; Wada & Penninger, 2004), was exclusively detected in postmitotic GCs of the IGL. Moreover, our preliminary analyses of either P4 or P14 c-Jun Dn mice indicate no significant anomaly in the number or localization of BG cells (LA and AMM, unpublished observations).

On the other hand, the evidence that c-Jun is essential for the induction of IL-1β expression in vitro activated BG cells, together with the evidence that it is highly expressed during formation of the BG monolayer, points to a putative role of c-Jun in neuroinflammatory responses of the neonatal cerebellum. IL-1β, besides being the major cytokine induced by acute brain injury (Patel *et al.*, 2003), plays an important role in kainite-induced cerebellar ataxia (Andoh *et al.*, 2008), suggesting that signaling pathways controlling its expression may participate to the pathogenesis of sporadic cerebellar ataxia. Future experiments in mouse models of neuroinflammatory diseases or sporadic cerebellar ataxia will then establish the role of c-Jun in astroglia-mediated dysfunction of the cerebellum.

8 References

Aguilera, C., Nakagawa, K., Sancho, R., Chakraborty, A., Hendrich, B. & Behrens, A. (2011) c-Jun N-terminal phosphorylation antagonises recruitment of the Mbd3/NuRD repressor complex. *Nature*, **469**, 231-235.

Akira, S., Uematsu, S. & Takeuchi, O. (2006) Pathogen recognition and innate immunity. *Cell*, **124**, 783-801.

Albanese, C., Johnson, J., Watanabe, G., Eklund, N., Vu, D., Arnold (1), A. & Pestell, R.G. (1995) Transforming p21 Mutants and c-Ets-2 Activate the Cyclin D1 Promoter through Distinguishable Regions. *Journal of Biological Chemistry*, **270**, 23589-23597.

Albanito, L., Reddy, C.E. & Musti, A.M. (2011) c-Jun is essential for the induction of Il-1β gene expression in in vitro activated Bergmann glial cells. *Glia*, **59**, 1879-1890.

Ambacher, K.K., Pitzul, K.B., Karajgikar, M., Hamilton, A., Ferguson, S.S. & Cregan, S.P. (2012) The JNK- and AKT/GSK3β- Signaling Pathways Converge to Regulate Puma Induction and Neuronal Apoptosis Induced by Trophic Factor Deprivation. *PLoS ONE*, **7**, e46885.

Andoh, T., Kishi, H., Motoki, K., Nakanishi, K., Kuraishi, Y. & Muraguchi, A. (2008) Protective effect of IL-18 on kainate- and IL-1 beta-induced cerebellar ataxia in mice. *J Immunol*, **180**, 2322-2328.

Angel, P., Hattori, K., Smeal, T. & Karin, M. (1988) The jun proto-oncogene is positively autoregulated by its product, Jun/AP-1. *Cell*, **55**, 875-885.

Angel, P. & Karin, M. (1991) The role of Jun, Fos and the AP-1 complex in cell-proliferation and transformation. *Biochimica et Biophysica Acta (BBA) - Reviews on Cancer*, **1072**, 129-157.

Anouar, Y., Lee, H.-W. & Eiden, L.E. (1999) Both Inducible and Constitutive Activator Protein-1-Like Transcription Factors Are Used for Transcriptional Activation of the Galanin Gene by Different First and Second Messenger Pathways. *Molecular Pharmacology*, **56**, 162-169.

Arany, Z., Newsome, D., Oldread, E., Livingston, D.M. & Eckner, R. (1995) A family of transcriptional adaptor proteins targeted by the E1A oncoprotein. *Nature*, **374**, 81-84.

Arias, J., Alberts, A.S., Brindle, P., Claret, F.X., Smeal, T., Karin, M., Feramisco, J. & Montminy, M. (1994) Activation of cAMP and mitogen responsive genes relies on a common nuclear factor. *Nature*, **370**, 226-229.

Bagowski, C.P., Besser, J., Frey, C.R. & Ferrell, J.E. (2003) The JNK Cascade as a Biochemical Switch in Mammalian Cells: Ultrasensitive and All-or-None Responses. *Current biology : CB*, **13**, 315-320.

Bakiri, L., Lallemand, D., Bossy-Wetzel, E. & Yaniv, M. (2000) Cell cycle-dependent variations in c-Jun and JunB phosphorylation: a role in the control of cyclin D1 expression. *EMBO J*, **19**, 2056-2068.

Bannister AJ, O.T., Wilhelm D,Angel P,Kouzarides T. (1995) Stimulation of c-Jun activity by CBP: c-Jun residues Ser63/73 are required for CBP induced stimulation in vivo and CBP binding in vitro. Oncogene.

Barnat, M., Enslen, H., Propst, F., Davis, R.J., Soares, S. & Nothias, F. (2010) Distinct Roles of c-Jun N-Terminal Kinase Isoforms in Neurite Initiation and Elongation during Axonal Regeneration. *The Journal of Neuroscience*, **30**, 7804-7816.

Behrens, A., Sibilia, M., David, J.P., Mohle-Steinlein, U., Tronche, F., Schutz, G. & Wagner, E.F. (2002) Impaired postnatal hepatocyte proliferation and liver regeneration in mice lacking c-jun in the liver. *Embo J*, **21**, 1782-1790.

Behrens, A., Sibilia, M. & Wagner, E.F. (1999) Amino-terminal phosphorylation of c-Jun regulates stress-induced apoptosis and cellular proliferation. *Nat Genet*, **21**, 326-329.

Bennett, G.D., Lau, F., Calvin, J.A. & Finnell, R.H. (1997) Phenytoin-Induced Teratogenesis: A Molecular Basis for the Observed Developmental Delay During Neurulation. *Epilepsia*, **38**, 415-423.

Benny, B., C., V.J., Vesa, H. & al, e. (2012) All JNKs can kill, but nuclear localization is critical for neuronal death. JOURNAL OF BIOLOGICAL CHEMISTRY.

Besirli, C.G., Wagner, E.F. & Johnson, E.M. (2005) The limited role of NH2-terminal c-Jun phosphorylation in neuronal apoptosis: Identification of the nuclear pore complex as a potential target of the JNK pathway. *The Journal of Cell Biology*, **170**, 401-411.

Bianchi, E., Denti, S., Catena, R., Rossetti, G., Polo, S., Gasparian, S., Putignano, S., Rogge, L. & Pardi, R. (2003) Characterization of Human Constitutive Photomorphogenesis Protein 1, a RING Finger Ubiquitin Ligase That Interacts with Jun Transcription Factors and Modulates Their Transcriptional Activity. *Journal of Biological Chemistry*, **278**, 19682-19690.

Blau, L., Knirsh, R., Ben-Dror, I., Oren, S., Kuphal, S., Hau, P., Proescholdt, M., Bosserhoff, A.K. & Vardimon, L. (2012) Aberrant expression of c-Jun in glioblastoma by internal ribosome entry site (IRES)-mediated translational activation. *Proceedings of the National Academy of Sciences*, **109**, E2875-E2884.

Borsello, T. & Forloni, G. (2007) JNK signalling: a possible target to prevent neurodegeneration. *Current pharmaceutical design*, **13**, 1875-1886.

Bossis, G., Malnou, C.E., Farras, R., Andermarcher, E., Hipskind, R., Rodriguez, M., Schmidt, D., Muller, S., Jariel-Encontre, I. & Piechaczyk, M. (2005) Down-Regulation of c-Fos/c-Jun AP-1 Dimer Activity by Sumoylation. *Molecular and Cellular Biology*, **25**, 6964-6979.

Bowman, C.C., Rasley, A., Tranguch, S.L. & Marriott, I. (2003) Cultured astrocytes express toll-like receptors for bacterial products. *Glia*, **43**, 281-291.

Boyle, W.J., Smeal, T., Defize, L.H.K., Angel, P., Woodgett, J.R., Karin, M. & Hunter, T. (1991) Activation of protein kinase C decreases phosphorylation of c-Jun at sites that negatively regulate its DNA-binding activity. *Cell*, **64**, 573-584.

Brecht, S., Kirchhof, R., Chromik, A., Willesen, M., Nicolaus, T., Raivich, G., Wessig, J., Waetzig, V., Goetz, M., Claussen, M., Pearse, D., Kuan, C.Y., Vaudano, E., Behrens, A., Wagner, E., Flavell, R.A., Davis, R.J. & Herdegen, T. (2005) Specific pathophysiological functions of JNK isoforms in the brain. *Eur.J.Neurosci.*, **21**, 363-377.

Brown, J.R., Nigh, E., Lee, R.J., Ye, H., Thompson, M.A., Saudou, F., Pestell, R.G. & Greenberg, M.E. (1998) Fos Family Members Induce Cell Cycle Entry by Activating Cyclin D1. *Molecular and Cellular Biology*, **18**, 5609-5619.

Brüsselbach S, M.-S.U., Wang ZQ,Schreiber M,Lucibello FC,Müller R,Wagner EF (1995) Cell proliferation and cell cycle progression are not impaired in fibroblasts and ES cells lacking c-Fos. Oncogene.

Carulli, D., Buffo, A., Botta, C., Altruda, F. & Strata, P. (2002) Regenerative and survival capabilities of Purkinje cells overexpressing c-Jun. *The European journal of neuroscience*, **16**, 105-118.

Celio, M.R. (1990) Calbindin D-28k and parvalbumin in the rat nervous system. *Neuroscience*, **35**, 375-475.

Charlotta Lindwall, M.K. (2012) The Janus role of c-Jun: Cell death versus survival and regeneration of neonatal sympathetic and sensory neurons.

Chen, B.-K., Huang, C.-C., Chang, W.-C., Chen, Y.-J., Kikkawa, U., Nakahama, K.-i., Morita, I. & Chang, W.-C. (2007) PP2B-mediated Dephosphorylation of c-Jun C Terminus Regulates Phorbol Ester-induced c-Jun/Sp1 Interaction in A431 Cells. *Molecular Biology of the Cell*, **18**, 1118-1127.

Chen, C.Y., Weng, Y.H., Chien, K.Y., Lin, K.J., Yeh, T.H., Cheng, Y.P., Lu, C.S. & Wang, H.L. (2012) (G2019S) LRRK2 activates MKK4-JNK pathway and causes degeneration of SN dopaminergic neurons in a transgenic mouse model of PD. *Cell Death Differ*, **19**, 1623-1633.

Cheng, J., Perkins, N.D. & Yeh, E.T.H. (2005) Differential Regulation of c-Jun-dependent Transcription by SUMO-specific Proteases. *Journal of Biological Chemistry*, **280**, 14492-14498.

Chinenov Y, K.T. (2001) Fos-Jun interactions that mediate transcription regulatory specificity. *Oncogene*, **20**, 2378–2389.

Ciechanover, A. (1998) The ubiquitin-proteasome pathway: on protein death and cell life. *EMBO J*, **17**, 7151-7160.

Coffey, E.T., Smiciene, G., Hongisto, V., Cao, J., Brecht, S., Herdegen, T. & Courtney, M.J. (2002) c-Jun N-Terminal Protein Kinase (JNK) 2/3 Is Specifically Activated by Stress, Mediating c-Jun Activation, in the Presence of Constitutive JNK1 Activity in Cerebellar Neurons. *The Journal of Neuroscience*, **22**, 4335-4345.

Comalada, M., Lloberas, J. & Celada, A. (2012) MKP-1: A critical phosphatase in the biology of macrophages controlling the switch between proliferation and activation. *European Journal of Immunology*, **42**, 1938-1948.

Conti, B., Park, L.C., Calingasan, N.Y., Kim, Y., Kim, H., Bae, Y., Gibson, G.E. & Joh, T.H. (1999) Cultures of astrocytes and microglia express interleukin 18. *Brain research*, **67**, 46-52.

Crocker, S.J., Lamba, W.R., Smith, P.D., Callaghan, S.M., Slack, R.S., Anisman, H. & Park, D.S. (2001) c-Jun mediates axotomy-induced dopamine neuron death in vivo. *Proc Natl Acad Sci U S A*, **98**, 13385-13390.

Davies, C.C., Chakraborty, A., Cipriani, F., Haigh, K., Haigh, J.J. & Behrens, A. (2010) Identification of a co-activator that links growth factor signalling to c-Jun/AP-1 activation. *Nat.Cell Biol.*, **12**, 963-972.

Davies, C.C., Chakraborty, A., Diefenbacher, M.E., Skehel, M. & Behrens, A. (2013) Arginine methylation of the c-Jun coactivator RACO-1 is required for c-Jun/AP-1 activation. *EMBO J*, **32**, 1556-1567.

Davis, R.J. (2000) Signal Transduction by the JNK Group of MAP Kinases. *Cell*, **103**, 239-252.

Donahue, C.P., Jensen, R.V., Ochiishi, T., Eisenstein, I., Zhao, M., Shors, T. & Kosik, K.S. (2002) Transcriptional profiling reveals regulated genes in the hippocampus during memory formation. *Hippocampus*, **12**, 821-833.

Dornan, D., Shimizu, H., Mah, A., Dudhela, T., Eby, M., O'Rourke, K., Seshagiri, S. & Dixit, V.M. (2006) ATM Engages Autodegradation of the E3 Ubiquitin Ligase COP1 After DNA Damage. *Science*, **313**, 1122-1126.

Dorsman, J.C., Hagmeyer, B.M., Veenstra, J., Elfferich, P., Nabben, N., Zantema, A. & van der Eb, A.J. (1995) The N-terminal region of the adenovirus type 5 E1A proteins can repress expression of cellular genes via two distinct but overlapping domains. *Journal of Virology*, **69**, 2962-2967.

Dragunow, M., Xu, R., Walton, M., Woodgate, A., Lawlor, P., MacGibbon, G.A., Young, D., Gibbons, H., Lipski, J., Muravlev, A., Pearson, A. & During, M. (2000) c-Jun promotes neurite outgrowth and survival in PC12 cells. *Brain research. Molecular brain research*, **83**, 20-33.

Duchala, C.S., Shick, H.E., Garcia, J., Deweese, D.M., Sun, X., Stewart, V.J. & Macklin, W.B. (2004) The toppler mouse: a novel mutant exhibiting loss of Purkinje cells. *The Journal of comparative neurology*, **476**, 113-129.

Eferl, R., Ricci, R., Kenner, L., Zenz, R., David, J.P., Rath, M. & Wagner, E.F. (2003) Liver Tumor Development: c-Jun Antagonizes the Proapoptotic Activity of p53. *Cell*, **112**, 181-192.

Eferl, R. & Wagner, E.F. (2003) AP-1: a double-edged sword in tumorigenesis. *Nat Rev Cancer*, **3**, 859-868.

Eilers, A., Whitfield, J., Babij, C., Rubin, L.L. & Ham, J. (1998) Role of the Jun Kinase Pathway in the Regulation of c-Jun Expression and Apoptosis in Sympathetic Neurons. *The Journal of Neuroscience*, **18**, 1713-1724.

Eilers, A., Whitfield, J., Shah, B., Spadoni, C., Desmond, H. & Ham, J. (2001) Direct inhibition of c-Jun N-terminal kinase in sympathetic neurones prevents c-jun promoter activation and NGF withdrawal-induced death. *Journal of neurochemistry*, **76**, 1439-1454.

Ejarque-Ortiz, A., Medina, M.G., Tusell, J.M., Perez-Gonzalez, A.P., Serratosa, J. & Saura, J. (2007) Upregulation of CCAAT/enhancer binding protein beta in activated astrocytes and microglia. *Glia*, **55**, 178-188.

El-Deiry, W.S., Tokino, T., Velculescu, V.E., Levy, D.B., Parsons, R., Trent, J.M., Lin, D., Mercer, W.E., Kinzler, K.W. & Vogelstein, B. (1993) WAF1, a potential mediator of p53 tumor suppression. *Cell*, **75**, 817-825.

Ertürk, A., Hellal, F., Enes, J. & Bradke, F. (2007) Disorganized Microtubules Underlie the Formation of Retraction Bulbs and the Failure of Axonal Regeneration. *The Journal of Neuroscience*, **27**, 9169-9180.

Fonseca, M.B., Nunes, A.F. & Rodrigues, C.M.P. (2012) c-Jun Regulates the Stability of Anti-Apoptotic ΔNp63 in Amyloid-β-Induced Apoptosis. *Journal of Alzheimer's Disease*, **28**, 685-694.

Fontana, X., Hristova, M., Da Costa, C., Patodia, S., Thei, L., Makwana, M., Spencer-Dene, B., Latouche, M., Mirsky, R., Jessen, K.R., Klein, R., Raivich, G. & Behrens, A. (2012) c-Jun in Schwann cells promotes axonal regeneration and motoneuron survival via paracrine signaling. *The Journal of Cell Biology*, **198**, 127-141.

Forshammar, J., Block, L., Lundborg, C., Biber, B. & Hansson, E. Naloxone and ouabain in ultra-low concentrations restore Na+/K+-ATPase and cytoskeleton in lipopolysaccharide-treated astrocytes. *The Journal of biological chemistry*.

Fuchs, S.Y., Xie, B., Adler, V., Fried, V.A., Davis, R.J. & Ronai, Z. (1997) c-Jun NH2-terminal Kinases Target the Ubiquitination of Their Associated Transcription Factors. *Journal of Biological Chemistry*, **272**, 32163-32168.

Furuoka, H., Horiuchi, M., Yamakawa, Y. & Sata, T. Predominant Involvement of the Cerebellum in Guinea Pigs Infected with Bovine Spongiform Encephalopathy (BSE). *Journal of comparative pathology*, **144**, 269-276.

Gall, C., Lauterborn, J., Isackson, P. & White, J. (1990) Chapter 27 Chapter Seizures, neuropeptide regulation, and mRNA expression in the hippocampus. In J. Storm-Mathisen, J.Z., Ottersen, O.P. (eds) *Progress in Brain Research*. Elsevier, pp. 371-390.

Gao, M., Labuda, T., Xia, Y., Gallagher, E., Fang, D., Liu, Y.C. & Karin, M. (2004) Jun Turnover Is Controlled Through JNK-Dependent Phosphorylation of the E3 Ligase Itch. *Science*, **306**, 271-275.

Gass, P., Herdegen, T., Bravo, R. & Kiessling, M. (1993) Spatiotemporal Induction of Immediate Early Genes in the Rat Brain after Limbic Seizures: Effects of NMDA Receptor Antagonist MK-801. *European Journal of Neuroscience*, **5**, 933-973.

Gaudilli+¿re, B., Konishi, Y., de la Iglesia, N., Yao, G.l. & Bonni, A. (2004) A CaMKII-NeuroD Signaling Pathway Specifies Dendritic Morphogenesis. *Neuron*, **41**, 229-241.

Giles, R.H., van Es, J.H. & Clevers, H. (2003) Caught up in a Wnt storm: Wnt signaling in cancer. *Biochimica et Biophysica Acta (BBA) - Reviews on Cancer*, **1653**, 1-24.

Goldberg, J.L. (2003) How does an axon grow? *Genes & Development*, **17**, 941-958.

Goldstein, L.S.B. (2001) When Worlds Collide--Trafficking in JNK. *Science*, **291**, 2102-2103.

Goodman, R.H. & Smolik, S. (2000) CBP/p300 in cell growth, transformation, and development. *Genes & Development*, **14**, 1553-1577.

Gorina, R., Font-Nieves, M., Marquez-Kisinousky, L., Santalucia, T. & Planas, A.M. Astrocyte TLR4 activation induces a proinflammatory environment through

the interplay between MyD88-dependent NFkappaB signaling, MAPK, and Jak1/Stat1 pathways. *Glia*, **59**, 242-255.

Gruda MC, K.K., Metz R, Bravo R. (1994) Regulation of Fra-1 and Fra-2 phosphorylation differs during the cell cycle of fibroblasts and phosphorylation in vitro by MAP kinase affects DNA binding activity. *Oncogene*, **9**, 2537-2547.

Guma, M., Kashiwakura, J.-i., Crain, B., Kawakami, Y., Beutler, B., Firestein, G.S., Kawakami, T., Karin, M. & Corr, M. (2010) JNK1 controls mast cell degranulation and IL-1β production in inflammatory arthritis. *Proceedings of the National Academy of Sciences*, **107**, 22122-22127.

Hachem, S., Laurenson, A.S., Hugnot, J.P. & Legraverend, C. (2007) Expression of S100B during embryonic development of the mouse cerebellum. *BMC developmental biology*, **7**, 17.

Haeusgen, W., Boehm, R., Zhao, Y., Herdegen, T. & Waetzig, V. (2009) Specific activities of individual c-Jun N-terminal kinases in the brain. *Neuroscience*, **161**, 951-959.

Hao, B., Oehlmann, S., Sowa, M.E., Harper, J.W. & Pavletich, N.P. (2007) Structure of a Fbw7-Skp1-Cyclin E Complex: Multisite-Phosphorylated Substrate Recognition by SCF Ubiquitin Ligases. *Molecular cell*, **26**, 131-143.

Hatten, M.E. & Mason, C.A. (1990) Mechanisms of glial-guided neuronal migration in vitro and in vivo. *Experientia*, **46**, 907-916.

Hauwel, M., Furon, E., Canova, C., Griffiths, M., Neal, J. & Gasque, P. (2005) Innate (inherent) control of brain infection, brain inflammation and brain repair: the role of microglia, astrocytes, "protective" glial stem cells and stromal ependymal cells. *Brain Res Brain Res Rev*, **48**, 220-233.

Hayakawa, J., Mittal, S., Wang, Y., Korkmaz, K.S., Adamson, E., English, C., Ohmichi, M., Omichi, M., McClelland, M. & Mercola, D. (2004) Identification of promoters bound by c-Jun/ATF2 during rapid large-scale gene activation following genotoxic stress. *Molecular cell*, **16**, 521-535.

Herdegen, T., Kummer, W., Fiallos, C.E., Leah, J. & Bravo, R. (1991) Expression of c-JUN, JUN B and JUN D proteins in rat nervous system following transection of vagus nerve and cervical sympathetic trunk. *Neuroscience*, **45**, 413-422.

Herdegen, T. & Leah, J.D. (1998) Inducible and constitutive transcription factors in the mammalian nervous system: control of gene expression by Jun, Fos and Krox, and CREB/ATF proteins. *Brain Research Reviews*, **28**, 370-490.

Herdegen, T. & Waetzig, V. (2001) The JNK and p38 signal transduction following axotomy. *Restorative Neurology and Neuroscience*, **19**, 29-39.

Hernandez, P., Müller, M. & Appel, R.D. (2006) Automated protein identification by tandem mass spectrometry: Issues and strategies. *Mass Spectrometry Reviews*, **25**, 235-254.

Hess, J., Angel, P. & Schorpp-Kistner, M. (2004) AP-1 subunits: quarrel and harmony among siblings. *Journal of Cell Science*, **117**, 5965-5973.

Hidding, U., Mielke, K., Waetzig, V., Brecht, S., Hanisch, U., Behrens, A., Wagner, E. & Herdegen, T. (2002) The c-Jun N-terminal kinases in cerebral microglia: immunological functions in the brain. *Biochemical Pharmacology*, **64**, 781-788.

Holt, J.T., Gopal, T.V., Moulton, A.D. & Nienhuis, A.W. (1986) Inducible production of c-fos antisense RNA inhibits 3T3 cell proliferation. *Proceedings of the National Academy of Sciences*, **83**, 4794-4798.

Hongisto, V., Smeds, N., Brecht, S., Herdegen, T., Courtney, M.J. & Coffey, E.T. (2003) Lithium Blocks the c-Jun Stress Response and Protects Neurons via Its Action on Glycogen Synthase Kinase 3. *Molecular and Cellular Biology*, **23**, 6027-6036.

Huang, C.C., Wang, J.M., Kikkawa, U., Mukai, H., Shen, M.R., Morita, I., Chen, B.K. & Chang, W.C. (2007) Calcineurin-mediated dephosphorylation of c-Jun Ser-243 is required for c-Jun protein stability and cell transformation. *Oncogene*, **27**, 2422-2429.

Ishida, K., Mitoma, H., Wada, Y., Oka, T., Shibahara, J., Saito, Y., Murayama, S. & Mizusawa, H. (2007) Selective loss of Purkinje cells in a patient with anti-glutamic acid decarboxylase antibody-associated cerebellar ataxia. *Journal of neurology, neurosurgery, and psychiatry*, **78**, 190-192.

Jenkins R, H.S. (1991) Long-term increase in the levels of c-jun mRNA and jun protein-like immunoreactivity in motor and sensory neurons following axon damage. *Neurosci Lett.*, **Aug 5;129**, 107-110.

Jenkins, R. & Hunt, S.P. (1991) Long-term increase in the levels of c-jun mRNA and jun protein-like immunoreactivity in motor and sensory neurons following axon damage. *Neuroscience Letters*, **129**, 107-110.

Jessen, K.í.R. & Mirsky, R. (2008) Negative regulation of myelination: Relevance for development, injury, and demyelinating disease. *Glia*, **56**, 1552-1565.

Jessen, K.R. & Mirsky, R. (2005) The origin and development of glial cells in peripheral nerves. *Nat Rev Neurosci*, **6**, 671-682.

Jochum, W., Passegué, E. & Wagner, E.F. (2001) AP-1 in mouse development and tumorigenesis. *Oncogene*, **20**, 2401-2412.

Johnson, R., Spiegelman, B., Hanahan, D. & Wisdom, R. (1996) Cellular transformation and malignancy induced by ras require c-jun. *Molecular and Cellular Biology*, **16**, 4504-4511.

Johnson, R.S., van Lingen, B., Papaioannou, V.E. & Spiegelman, B.M. (1993) A null mutation at the c-jun locus causes embryonic lethality and retarded cell growth in culture. *Genes & Development*, **7**, 1309-1317.

Jopling, C., Boue, S. & Belmonte, J.C.I. (2011) Dedifferentiation, transdifferentiation and reprogramming: three routes to regeneration. *Nat Rev Mol Cell Biol*, **12**, 79-89.

Kang, J.S., Yoon, Y.D., Lee, K.H., Park, S.K. & Kim, H.M. (2004) Costunolide inhibits interleukin-1beta expression by down-regulation of AP-1 and MAPK activity in LPS-stimulated RAW 264.7 cells. *Biochemical and biophysical research communications*, **313**, 171-177.

Karin, M. & Gallagher, E. (2005) From JNK to Pay Dirt: Jun Kinases, their Biochemistry, Physiology and Clinical Importance. *IUBMB Life*, **57**, 283-295.

Konstantin, V.A. & Steven, P.R.R. (2006) Learning-induced Increase of Immediate Early Gene Messenger RNA in the Chick Forebrain. *Eur J Neurosci*, **3**, 162-167.

Kovary, K. & Bravo, R. (1991a) Expression of different Jun and Fos proteins during the G0-to-G1 transition in mouse fibroblasts: in vitro and in vivo associations. *Molecular and Cellular Biology*, **11**, 2451-2459.

Kovary, K. & Bravo, R. (1991b) The jun and fos protein families are both required for cell cycle progression in fibroblasts. *Molecular and Cellular Biology*, **11**, 4466-4472.

Kristiansen, M., Hughes, R., Patel, P., Jacques, T.S., Clark, A.R. & Ham, J. (2010) Mkp1 Is a c-Jun Target Gene That Antagonizes JNK-Dependent Apoptosis in Sympathetic Neurons. *The Journal of Neuroscience*, **30**, 10820-10832.

Kuan, C.-Y., Whitmarsh, A.J., Yang, D.D., Liao, G., Schloemer, A.J., Dong, C., Bao, J., Banasiak, K.J., Haddad, G.G., Flavell, R.A., Davis, R.J. & Rakic, P. (2003) A critical role of neural-specific JNK3 for ischemic apoptosis. *Proceedings of the National Academy of Sciences*, **100**, 15184-15189.

Laderoute, K.R., Mendonca, H.L., Calaoagan, J.M., Knapp, A.M., Giaccia, A.J. & Stork, P.J.S. (1999) Mitogen-activated Protein Kinase Phosphatase-1 (MKP-1) Expression Is Induced by Low Oxygen Conditions Found in Solid Tumor Microenvironments: A CANDIDATE MKP FOR THE INACTIVATION OF HYPOXIA-INDUCIBLE STRESS-ACTIVATED PROTEIN KINASE/c-Jun N-TERMINAL PROTEIN KINASE ACTIVITY. *Journal of Biological Chemistry*, **274**, 12890-12897.

Lafarga, M., Andres, M.A., Calle, E. & Berciano, M.T. (1998) Reactive gliosis of immature Bergmann glia and microglial cell activation in response to cell death of granule cell precursors induced by methylazoxymethanol treatment in developing rat cerebellum. *Anatomy and embryology*, **198**, 111-122.

Lafarga, M., Berciano, M.T., Suarez, I., Viadero, C.F., Andres, M.A. & Berciano, J. (1991) Cytology and organization of reactive astroglia in human cerebellar cortex with severe loss of granule cells: a study on the ataxic form of Creutzfeldt-Jakob disease. *Neuroscience*, **40**, 337-352.

Lamph, W.W., Wamsley, P., Sassone-Corsi, P. & Verma, I.M. (1988) Induction of proto-oncogene JUN/AP-1 by serum and TPA. *Nature*, **334**, 629-631.

Le-Niculescu, H., Bonfoco, E., Kasuya, Y., Claret, F.-X., Green, D.R. & Karin, M. (1999) Withdrawal of Survival Factors Results in Activation of the JNK Pathway in Neuronal Cells Leading to Fas Ligand Induction and Cell Death. *Molecular and Cellular Biology*, **19**, 751-763.

Le, S.S., Loucks, F.A., Udo, H., Richardson-Burns, S., Phelps, R.A., Bouchard, R.J., Barth, H., Aktories, K., Tyler, K.L., Kandel, E.R., Heidenreich, K.A. & Linseman, D.A. (2005) Inhibition of Rac GTPase triggers a c-Jun- and Bim-

dependent mitochondrial apoptotic cascade in cerebellar granule neurons. *Journal of Neurochemistry*, **94**, 1025-1039.

Lee, J.S., See, R.H., Deng, T. & Shi, Y. (1996) Adenovirus E1A downregulates cJun- and JunB-mediated transcription by targeting their coactivator p300. *Molecular and Cellular Biology*, **16**, 4312-4326.

Lee, T.H., Klampfer, L., Shows, T.B. & Vilcek, J. (1993) Transcriptional regulation of TSG6, a tumor necrosis factor- and interleukin-1-inducible primary response gene coding for a secreted hyaluronan-binding protein. *Journal of Biological Chemistry*, **268**, 6154-6160.

Lenox RH, H.C. (2000) Overview of the mechanism of action of lithium in the brain: fifty-year update. *J Clin Psychiatry*, **61**, Suppl 9:5-15.

Leppa, S., Saffrich, R., Ansorge, W. & Bohmann, D. (1998) Differential regulation of c-Jun by ERK and JNK during PC12 cell differentiation. *EMBO J*, **17**, 4404-4413.

Lin, A., Frost, J., Deng, T., Smeal, T., Al-Alawi, N., Kikkawa, U., Hunter, T., Brenner, D. & Karin, M. (1992) Casein kinase II is a negative regulator of c-Jun DNA binding and AP-1 activity. *Cell*, **70**, 777-789.

Lindwall, C. & Kanje, M. (2005) Retrograde axonal transport of JNK signaling molecules influence injury induced nuclear changes in p-c-Jun and ATF3 in adult rat sensory neurons. *Molecular and Cellular Neuroscience*, **29**, 269-282.

Lingor, P., Koeberle, P., Kugler, S. & Bahr, M. (2005) Down-regulation of apoptosis mediators by RNAi inhibits axotomy-induced retinal ganglion cell death in vivo. *Brain*, **128**, 550-558.

Liu, N., Stoica, G., Yan, M., Scofield, V.L., Qiang, W., Lynn, W.S. & Wong, P.K. (2005) ATM deficiency induces oxidative stress and endoplasmic reticulum stress in astrocytes. *Laboratory investigation; a journal of technical methods and pathology*, **85**, 1471-1480.

Lois, C., Hong, E.J., Pease, S., Brown, E.J. & Baltimore, D. (2002) Germline Transmission and Tissue-Specific Expression of Transgenes Delivered by Lentiviral Vectors. *Science*, **295**, 868-872.

Lu, C., Zhu, F., Cho, Y.Y., Tang, F., Zykova, T., Ma, W.y., Bode, A.M. & Dong, Z. (2006) Cell Apoptosis: Requirement of H2AX in DNA Ladder Formation, but Not for the Activation of Caspase-3. *Molecular Cell*, **23**, 121-132.

Lu, Z., Xu, S., Joazeiro, C., Cobb, M.H. & Hunter, T. (2002) The PHD Domain of MEKK1 Acts as an E3 Ubiquitin Ligase and Mediates Ubiquitination and Degradation of ERK1/2. *Molecular cell*, **9**, 945-956.

Ma, C. & D'Mello, S.R. (2011) Neuroprotection by histone deacetylase-7 (HDAC7) occurs by inhibition of c-jun expression through a deacetylase-independent mechanism. *J.Biol.Chem.*, **286**, 4819-4828.

Ma, C., Ying, C., Yuan, Z., Song, B., Li, D., Liu, Y., Lai, B., Li, W., Chen, R., Ching, Y.-P. & Li, M. (2007) dp5/HRK Is a c-Jun Target Gene and Required for Apoptosis Induced by Potassium Deprivation in Cerebellar Granule Neurons. *Journal of Biological Chemistry*, **282**, 30901-30909.

Madeo, A., Vinciguerra, M., Lappano, R., Galgani, M., Gasperi-Campani, A., Maggiolini, M. & Musti, A.M. (2010) c-Jun activation is required for 4-hydroxytamoxifen-induced cell death in breast cancer cells. *Oncogene*, **29**, 978-991.

Marcus, D.L., Strafaci, J.A., Miller, D.C., Masia, S., Thomas, C.G., Rosman, J., Hussain, S. & Freedman, M.L. (1998) Quantitative neuronal c-Fos and c-Jun expression in Alzheimer's disease1 1 To whom correspondence should be addressed. *Neurobiology of aging*, **19**, 393-400.

Marek, K.W., Kurtz, L.M. & Spitzer, N.C. (2010) cJun integrates calcium activity and tlx3 expression to regulate neurotransmitter specification. *Nat Neurosci*, **13**, 944-950.

Maria B.Fonseca1, A.F.N., Cecília M.P.Rodrigues1,2 (2012) c-Jun Regulates the Stability of Anti-Apoptotic ?Np63 in Amyloid-?-Induced Apoptosis.

Maricich, S.M. & Herrup, K. (1999) Pax-2 expression defines a subset of GABAergic interneurons and their precursors in the developing murine cerebellum. *Journal of neurobiology*, **41**, 281-294.

Mattson, M.P. (2000) Apoptosis in neurodegenerative disorders. *Nat Rev Mol Cell Biol*, **1**, 120-130.

Mechta-Grigoriou, F., Gerald, D. & Yaniv, M. (2001) The mammalian Jun proteins: redundancy and specificity. *Oncogene*, **20**, 2378-2389.

Mellström, B., Achaval, M., Montero, D., Naranjo, J.R. & Sassone-Corsi, P. (1991) Differential expression of the jun family members in rat brain. *Oncogene*, **6**, 1959-1964.

MIGHELI, A., PIVA, R., ATZORI, C., TROOST, D. & SCHIFFER, D. (1997) c-Jun, JNK/SAPK Kinase and Transcription Factor NF-[kappa]B Are Selectively Activated in Astrocytes, but not Motor Neurons, in Amyotrophic Lateral Sclerosis. *Journal of Neuropathology & Experimental Neurology*, **56**, 1314-1322.

Migliorini, D., Bogaerts, S., Defever, D., Vyas, R., Denecker, G., Radaelli, E., Zwolinska, A., Depaepe, V., Hochepied, T., Skarnes, W.C. & Marine, J.-C. (2011) Cop1 constitutively regulates c-Jun protein stability and functions as a tumor suppressor in mice. *The Journal of Clinical Investigation*, **121**, 1329-1343.

Miyata, T., Maeda, T. & Lee, J.E. (1999) NeuroD is required for differentiation of the granule cells in the cerebellum and hippocampus. *Genes & development*, **13**, 1647-1652.

Monique CA Duyndam, H.v.D., Paul HM Smits,Matty Verlaan,Alex J van der Eb and Alt Zantemaa (1999) The N-terminal transactivation domain of ATF2 is a target for the co-operative activation of the c-jun promoter by p300 and 12S E1A. Oncogene.

Morgan, J.I. & Curran, T.O.M. (1989) Calcium and Proto-Oncogene Involvement in the Immediate-Early Response in the Nervous System. *Annals of the New York Academy of Sciences*, **568**, 283-290.

Morrison, B.E., Majdzadeh, N., Zhang, X., Lyles, A., Bassel-Duby, R., Olson, E.N. & D'Mello, S.R. (2006) Neuroprotection by Histone Deacetylase-Related Protein. *Molecular and Cellular Biology*, **26**, 3550-3564.

Morton, S., Davis, R.J., McLaren, A. & Cohen, P. (2003) A reinvestigation of the multisite phosphorylation of the transcription factor c-Jun. *EMBO J*, **22**, 3876-3886.

Müller, S., Berger, M., Lehembre, F., Seeler, J.-S., Haupt, Y. & Dejean, A. (2000) c-Jun and p53 Activity Is Modulated by SUMO-1 Modification. *Journal of Biological Chemistry*, **275**, 13321-13329.

Musti, A.M., Treier, M. & Bohmann, D. (1997) Reduced ubiquitin-dependent degradation of c-Jun after phosphorylation by MAP kinases. *Science*, **275**, 400-402.

Napoli, A., Aiello, D., Di Donna, L., Moschidis, P. & Sindona, G. (2008) Vegetable Proteomics: The Detection of Ole e 1 Isoallergens by Peptide Matching of MALDI MS/MS Spectra of Underivatized and Dansylated Glycopeptides. *Journal of Proteome Research*, **7**, 2723-2732.

Napoli, A., Athanassopoulos, C.M., Moschidis, P., Aiello, D., Di Donna, L., Mazzotti, F. & Sindona, G. (2010) Solid Phase Isobaric Mass Tag Reagent for Simultaneous Protein Identification and Assay. *Analytical Chemistry*, **82**, 5552-5560.

Nateri, A.S., Riera-Sans, L., Da, C.C. & Behrens, A. (2004) The ubiquitin ligase SCFFbw7 antagonizes apoptotic JNK signaling. *Science*, **303**, 1374-1378.

Nateri, A.S., Spencer-Dene, B. & Behrens, A. (2005) Interaction of phosphorylated c-Jun with TCF4 regulates intestinal cancer development. *Nature*, **437**, 281-285.

Nishikura, K. & Murray, J.M. (1987) Antisense RNA of proto-oncogene c-fos blocks renewed growth of quiescent 3T3 cells. *Molecular and Cellular Biology*, **7**, 639-649.

Ogawa, S., Lozach, J., Jepsen, K., Sawka-Verhelle, D., Perissi, V., Sasik, R., Rose, D.W., Johnson, R.S., Rosenfeld, M.G. & Glass, C.K. (2004) A nuclear receptor corepressor transcriptional checkpoint controlling activator protein 1-dependent gene networks required for macrophage activation. *Proceedings of the National Academy of Sciences of the United States of America*, **101**, 14461-14466.

Oo, T., Henchcliffe, C., James, D. & Burke, R.E. (1999) Expression of c-fos, c-jun, and N-terminal kinase (JNK) in a Development Model of Induced Apoptotic Death in Neurons of the Substantia Nigra. *Journal of Neurochemistry*, **72**, 557-564.

Palmada, M., Kanwal, S., Rutkoski, N.J., Gustafson-Brown, C., Johnson, R.S., Wisdom, R. & Carter, B.D. (2002) c-jun is essential for sympathetic neuronal death induced by NGF withdrawal but not by p75 activation. *J Cell Biol*, **158**, 453-461.

Papavassiliou, A.G., Treier, M. & Bohmann, D. (1995) Intramolecular signal transduction in c-Jun. *The EMBO journal*, **14**, 2014-2019.

Parkinson, D.B., Bhaskaran, A., Droggiti, A., Dickinson, S., D'Antonio, M., Mirsky, R. & Jessen, K.R. (2004) Krox-20 inhibits Jun-NH2-terminal kinase/c-Jun to control Schwann cell proliferation and death. *The Journal of Cell Biology*, **164**, 385-394.

Passegue, E. & Wagner, E.F. (2000) JunB suppresses cell proliferation by transcriptional activation of p16INK4a expression. *EMBO J*, **19**, 2969-2979.

Patel, H.C., Boutin, H. & Allan, S.M. (2003) Interleukin-1 in the brain: mechanisms of action in acute neurodegeneration. *Annals of the New York Academy of Sciences*, **992**, 39-47.

Pearson, A.G., Byrne, U.T.E., MacGibbon, G.A., Faull, R.L.M. & Dragunow, M. (2006) Activated c-Jun is present in neurofibrillary tangles in Alzheimer's disease brains. *Neuroscience Letters*, **398**, 246-250.

PEI, J.-J., BRAAK, E., BRAAK, H., GRUNDKE-IQBAL, I., IQBAL, K., WINBLAD, B. & COWBURN, R.F. (1999) Distribution of Active Glycogen Synthase Kinase 3[beta] (GSK-3[beta]) in Brains Staged for Alzheimer Disease Neurofibrillary Changes. *Journal of Neuropathology & Experimental Neurology*, **58**, 1010-1019.

Polazzi, E. & Contestabile, A. (2006) Overactivation of LPS-stimulated microglial cells by co-cultured neurons or neuron-conditioned medium. *Journal of neuroimmunology*, **172**, 104-111.

Pulverer, B.J., Kyriakis, J.M., Avruch, J., Nikolakaki, E. & Woodgett, J.R. (1991) Phosphorylation of c-jun mediated by MAP kinases. *Nature*, **353**, 670-674.

Quantin, B. & Breathnach, R. (1988) Epidermal growth factor stimulates transcription of the c-jun proto-oncogene in rat fibroblasts. *Nature*, **334**, 538-539.

Raivich, G. (2008) c-Jun Expression, activation and function in neural cell death, inflammation and repair. *Journal of Neurochemistry*, **107**, 898-906.

Raivich, G. & Behrens, A. (2006) Role of the AP-1 transcription factor c-Jun in developing, adult and injured brain. *Prog.Neurobiol.*, **78**, 347-363.

Raivich, G., Bohatschek, M., Da, C.C., Iwata, O., Galiano, M., Hristova, M., Nateri, A.S., Makwana, M., Riera-Sans, L., Wolfer, D.P., Lipp, H.P., Aguzzi, A., Wagner, E.F. & Behrens, A. (2004) The AP-1 transcription factor c-Jun is required for efficient axonal regeneration. *Neuron*, **43**, 57-67.

Rakic, P. (1971) Neuron-glia relationship during granule cell migration in developing cerebellar cortex. A Golgi and electronmicroscopic study in Macacus Rhesus. *The Journal of comparative neurology*, **141**, 283-312.

Raman, M., Chen, W. & Cobb, M.H. (0000) Differential regulation and properties of MAPKs. *Oncogene*, **26**, 3100-3112.

Rangatia, J., Vangala, R.K., Treiber, N., Zhang, P., Radomska, H., Tenen, D.G., Hiddemann, W. & Behre, G. (2002) Downregulation of c-Jun Expression by Transcription Factor C/EBP+¦ Is Critical for Granulocytic Lineage Commitment. *Molecular and Cellular Biology*, **22**, 8681-8694.

Rieger, M.A., Duellman, T., Hooper, C., Ameka, M., Bakowska, J.C. & Cuevas, B.D. (2012) The MEKK1 SWIM domain is a novel substrate receptor for c-Jun ubiquitylation. *Biochemical Journal*, **445**, 431-439.

rthur-Farraj, P., Latouche, M., Wilton, D., Quintes, S., Chabrol, E., Banerjee, A., Woodhoo, A., Jenkins, B., Rahman, M., Turmaine, M., Wicher, G., Mitter, R., Greensmith, L., Behrens, A., Raivich, G., Mirsky, R. & Jessen, K. (2012) c-Jun Reprograms Schwann Cells of Injured Nerves to Generate a Repair Cell Essential for Regeneration. *Neuron*, **75**, 633-647.

Ryder, K. & Nathans, D. (1988) Induction of protooncogene c-jun by serum growth factors. *Proceedings of the National Academy of Sciences of the United States of America*, **85**, 8464-8467.

Saporito, M.S., Brown, E.M., Miller, M.S. & Carswell, S. (1999) CEP-1347/KT-7515, an Inhibitor of c-jun N-Terminal Kinase Activation, Attenuates the 1-Methyl-4-Phenyl Tetrahydropyridine-Mediated Loss of Nigrostriatal Dopaminergic Neurons In Vivo. *Journal of Pharmacology and Experimental Therapeutics*, **288**, 421-427.

Sass, J.B., Haselow, D.T. & Silbergeld, E.K. (2001) Methylmercury-induced decrement in neuronal migration may involve cytokine-dependent mechanisms: a novel method to assess neuronal movement in vitro. *Toxicol Sci*, **63**, 74-81.

Savio, M.G., Rotondo, G., Maglie, S., Rossetti, G., Bender, J.R. & Pardi, R. (2007) COP1D, an alternatively spliced constitutive photomorphogenic-1 (COP1) product, stabilizes UV stress-induced c-Jun through inhibition of full-length COP1. *Oncogene*, **27**, 2401-2411.

Schreiber, M., Kolbus, A., Piu, F., Szabowski, A., M+Âhle-Steinlein, U., Tian, J., Karin, M., Angel, P. & Wagner, E.F. (1999) Control of cell cycle progression by c-Jun is p53 dependent. *Genes & Development*, **13**, 607-619.

Schwaiger, F.W., Hager, G., Raivich, G. & Kreutzberg, G.W. (1998) Chapter 16 Cellular activation in neuroregeneration. In Callow, J.A. (ed) *Progress in Brain Research*. Elsevier, pp. 197-210.

Sendtner, M., Gotz, R., Holtmann, B., Escary, J.L., Masu, Y., Carroll, P., Wolf, E., Brem, G., Brulet, P. & Thoenen, H. (1996) Cryptic physiological trophic support of motoneurons by LIF revealed by double gene targeting of CNTF and LIF. *Curr Biol*, **6**, 686-694.

Sengupta Ghosh, A., Wang, B., Pozniak, C.D., Chen, M., Watts, R.J. & Lewcock, J.W. (2011) DLK induces developmental neuronal degeneration via selective regulation of proapoptotic JNK activity. *The Journal of Cell Biology*, **194**, 751-764.

Shaulian, E. & Karin, M. (2002) AP-1 as a regulator of cell life and death. *Nat Cell Biol*, **4**, E131-E136.

Shaulian E, K.M. (2001 Apr 30) AP-1 in cell proliferation and survival. *Oncogene*, **20**, 2390-2400.

Shaulian, E., Schreiber, M., Piu, F., Beeche, M., Wagner, E.F. & Karin, M. (2000) The Mammalian UV Response: c-Jun Induction Is Required for Exit from p53-Imposed Growth Arrest. *Cell*, **103**, 897-908.

Sheu, J.Y., Kulhanek, D.J. & Eckenstein, F.P. (2000) Differential Patterns of ERK and STAT3 Phosphorylation after Sciatic Nerve Transection in the Rat. *Experimental Neurology*, **166**, 392-402.

Shin, Jung E., Cho, Y., Beirowski, B., Milbrandt, J., Cavalli, V. & DiAntonio, A. (2012) Dual Leucine Zipper Kinase Is Required for Retrograde Injury Signaling and Axonal Regeneration. *Neuron*, **74**, 1015-1022.

Shoji, M., Iwakami, N., Takeuchi, S., Waragai, M., Suzuki, M., Kanazawa, I., Lippa, C.F., Ono, S. & Okazawa, H. (2000) JNK activation is associated with intracellular β-amyloid accumulation. *Molecular Brain Research*, **85**, 221-233.

Silva, R.M., Kuan, C.-Y., Rakic, P. & Burke, R.E. (2005) Mixed lineage kinase–c-jun N-terminal kinase signaling pathway: A new therapeutic target in Parkinson's disease. *Movement Disorders*, **20**, 653-664.

Sluss, H.K. & Davis, R.J. (2006) H2AX Is a Target of the JNK Signaling Pathway that Is Required For Apoptotic DNA Fragmentation. *Molecular Cell*, **23**, 152-153.

Smeal, T., Binetruy, B., Mercola, D.A., Birrer, M. & Karin, M. (1991) Oncogenic and transcriptional cooperation with Ha-Ras requires phosphorylation of c-Jun on serines 63 and 73. *Nature*, **354**, 494-496.

Smits PH, d.W.L., van der Eb AJ,Zantema A (1996) The adenovirus E1A-associated 300 kDa adaptor protein counteracts the inhibition of the collagenase promoter by E1A and represses transformation. Oncogene.

Stoll, G. & Müller, H.W. (1999) Nerve Injury, Axonal Degeneration and Neural Regeneration: Basic Insights. *Brain Pathology*, **9**, 313-325.

Sun, J., Zheng, J.H., Zhao, M., Lee, S. & Goldstein, H. (2008) Increased in vivo activation of microglia and astrocytes in the brains of mice transgenic for an infectious R5 human immunodeficiency virus type 1 provirus and for CD4-specific expression of human cyclin T1 in response to stimulation by lipopolysaccharides. *Journal of virology*, **82**, 5562-5572.

Sun, W., Gould, T.W., Newbern, J., Milligan, C., Choi, S.Y., Kim, H. & Oppenheim, R.W. (2005) Phosphorylation of c-Jun in Avian and Mammalian Motoneurons In Vivo during Programmed Cell Death: An Early Reversible Event in the Apoptotic Cascade. *The Journal of Neuroscience*, **25**, 5595-5603.

Taira, N., Mimoto, R., Kurata, M., Yamaguchi, T., Kitagawa, M., Miki, Y. & Yoshida, K. (2012a) DYRK2 priming phosphorylation of c-Jun and c-Myc modulates cell cycle progression in human cancer cells. *The Journal of Clinical Investigation*, **0**, 0-0.

Taira, N., Mimoto, R., Kurata, M., Yamaguchi, T., Kitagawa, M., Miki, Y. & Yoshida, K. (2012b) DYRK2 priming phosphorylation of c-Jun and c-Myc modulates cell cycle progression in human cancer cells. *The Journal of Clinical Investigation*, **122**, 859-872.

Takashima, A., Honda, T., Yasutake, K., Michel, G., Murayama, O., Murayama, M., Ishiguro, K. & Yamaguchi, H. (1998) Activation of tau protein kinase I/glycogen synthase kinase-3β by amyloid β peptide (25–35) enhances phosphorylation of tau in hippocampal neurons. *Neuroscience Research*, **31**, 317-323.

Thakur, A., Wang, X., Siedlak, S.L., Perry, G., Smith, M.A. & Zhu, X. (2007) c-Jun phosphorylation in Alzheimer disease. *Journal of Neuroscience Research*, **85**, 1668-1673.

Tom, V.J., Steinmetz, M.P., Miller, J.H., Doller, C.M. & Silver, J. (2004) Studies on the Development and Behavior of the Dystrophic Growth Cone, the Hallmark of Regeneration Failure, in an In Vitro Model of the Glial Scar and after Spinal Cord Injury. *The Journal of Neuroscience*, **24**, 6531-6539.

Towers, E., Gilley, J., Randall, R., Hughes, R., Kristiansen, M. & Ham, J. (2009) The proapoptotic dp5 gene is a direct target of the MLK-JNK-c-Jun pathway in sympathetic neurons. *Nucleic Acids Research*, **37**, 3044-3060.

Tronche, F., Kellendonk, C., Kretz, O., Gass, P., Anlag, K., Orban, P.C., Bock, R., Klein, R. & Schutz, G. (1999) Disruption of the glucocorticoid receptor gene in the nervous system results in reduced anxiety. *Nat Genet*, **23**, 99-103.

Ullensvang, K., Lehre, K.P., Storm-Mathisen, J. & Danbolt, N.C. (1997) Differential developmental expression of the two rat brain glutamate transporter proteins GLAST and GLT. *The European journal of neuroscience*, **9**, 1646-1655.

Veeman, M.T., Axelrod, J.D. & Moon, R.T. (2003) A Second Canon: Functions and Mechanisms of ²-Catenin-Independent Wnt Signaling. *Developmental cell*, **5**, 367-377.

Ventura, J.-J., Hübner, A., Zhang, C., Flavell, R.A., Shokat, K.M. & Davis, R.J. (2006) Chemical Genetic Analysis of the Time Course of Signal Transduction by JNK. *Molecular cell*, **21**, 701-710.

Verhey, K.J. & Rapoport, T.A. (2001) Kinesin carries the signal. *Trends in Biochemical Sciences*, **26**, 545-549.

Vinciguerra, M., Esposito, I., Salzano, S., Madeo, A., Nagel, G., Maggiolini, M., Gallo, A. & Musti, A.M. (2008) Negative charged threonine 95 of c-Jun is essential for c-Jun N-terminal kinase-dependent phosphorylation of threonine 91/93 and stress-induced c-Jun biological activity. *Int.J.Biochem.Cell Biol.*, **40**, 307-316.

Vinciguerra, M., Vivacqua, A., Fasanella, G., Gallo, A., Cuozzo, C., Morano, A., Maggiolini, M. & Musti, A.M. (2004) Differential phosphorylation of c-Jun and JunD in response to the epidermal growth factor is determined by the structure of MAPK targeting sequences. *J.Biol.Chem.*, **279**, 9634-9641.

Vries, R.G.J., Prudenziati, M., Zwartjes, C., Verlaan, M., Kalkhoven, E. & Zantema, A. (2001) A specific lysine in c-Jun is required for transcriptional repression by E1A and is acetylated by p300. *EMBO J*, **20**, 6095-6103.

Wada, T., Joza, N., Cheng, H.Y., Sasaki, T., Kozieradzki, I., Bachmaier, K., Katada, T., Schreiber, M., Wagner, E.F., Nishina, H. & Penninger, J.M. (2004) MKK7 couples stress signalling to G2/M cell-cycle progression and cellular senescence. *Nature cell biology*, **6**, 215-226.

Wada, T. & Penninger, J.M. (2004) Stress kinase MKK7: savior of cell cycle arrest and cellular senescence. *Cell cycle (Georgetown, Tex*, **3**, 577-579.

Waetzig, V., Czeloth, K., Hidding, U., Mielke, K., Kanzow, M., Brecht, S., Goetz, M., Lucius, R., Herdegen, T. & Hanisch, U.K. (2005) c-Jun N-terminal kinases (JNKs) mediate pro-inflammatory actions of microglia. *Glia*, **50**, 235-246.

Waetzig, V. & Herdegen, T. (2004) Neurodegenerative and physiological actions of c-Jun N-terminal kinases in the mammalian brain. *Neuroscience Letters*, **361**, 64-67.

Wang, W., Shi, L., Xie, Y., Ma, C., Li, W., Su, X., Huang, S., Chen, R., Zhu, Z., Mao, Z., Han, Y. & Li, M. (2004) SP600125, a new JNK inhibitor, protects dopaminergic neurons in the MPTP model of Parkinson's disease. *Neuroscience Research*, **48**, 195-202.

Wang, Z., Cao, N., Nantajit, D., Fan, M., Liu, Y. & Li, J.J. (2008) Mitogen-activated Protein Kinase Phosphatase-1 Represses c-Jun NH2-terminal Kinase-mediated Apoptosis via NF-κB Regulation. *Journal of Biological Chemistry*, **283**, 21011-21023.

Watkins, T.A., Wang, B., Huntwork-Rodriguez, S., Yang, J., Jiang, Z., Eastham-Anderson, J., Modrusan, Z., Kaminker, J.S., Tessier-Lavigne, M. & Lewcock, J.W. (2013) DLK initiates a transcriptional program that couples apoptotic and regenerative responses to axonal injury. *Proceedings of the National Academy of Sciences*, **110**, 4039-4044.

Watson, A., Eilers, A., Lallemand, D., Kyriakis, J., Rubin, L.L. & Ham, J. (1998) Phosphorylation of c-Jun Is Necessary for Apoptosis Induced by Survival Signal Withdrawal in Cerebellar Granule Neurons. *The Journal of Neuroscience*, **18**, 751-762.

Wei, W., Jin, J., Schlisio, S., Harper, J.W. & Kaelin, J. (2005) The v-Jun point mutation allows c-Jun to escape GSK3-dependent recognition and destruction by the Fbw7 ubiquitin ligase. *Cancer Cell*, **8**, 25-33.

Weimer, J.M., Benedict, J.W., Getty, A.L., Pontikis, C.C., Lim, M.J., Cooper, J.D. & Pearce, D.A. (2009) Cerebellar defects in a mouse model of juvenile neuronal ceroid lipofuscinosis. *Brain Res*, **1266**, 93-107.

Weiss, C., Schneider, S., Wagner, E.F., Zhang, X., Seto, E. & Bohmann, D. (2003) JNK phosphorylation relieves HDAC3-dependent suppression of the transcriptional activity of c-Jun. *EMBO J*, **22**, 3686-3695.

Welcker, M. & Clurman, B.E. (2008) FBW7 ubiquitin ligase: a tumour suppressor at the crossroads of cell division, growth and differentiation. *Nat Rev Cancer*, **8**, 83-93.

Wertz, I.E., O'Rourke, K.M., Zhang, Z., Dornan, D., Arnott, D., Deshaies, R.J. & Dixit, V.M. (2004) Human De-Etiolated-1 Regulates c-Jun by Assembling a CUL4A Ubiquitin Ligase. *Science*, **303**, 1371-1374.

Wessel, T.C., Joh, T.H. & Volpe, B.T. (1991) In situ hybridization analysis of c-fos and c-jun expression in the rat brain following transient forebrain ischemia. *Brain Research*, **567**, 231-240.

Weyer, A. & Schilling, K. (2003) Developmental and cell type-specific expression of the neuronal marker NeuN in the murine cerebellum. *Journal of neuroscience research*, **73**, 400-409.

Whitfield, J., Neame, S.J., Paquet, L., Bernard, O. & Ham, J. (2001) Dominant-Negative c-Jun Promotes Neuronal Survival by Reducing BIM Expression and Inhibiting Mitochondrial Cytochrome c Release. *Neuron*, **29**, 629-643.

Whitmarsh, A.J. & Davis*, R.J. (2000) Regulation of transcription factor function by phosphorylation. *CMLS, Cell.Mol.Life Sci.*, **57**, 1172-1183.

Wilkinson, D.G., Bhatt, S., Ryseck, R.P. & Bravo, R. (1989) Tissue-specific expression of c-jun and junB during organogenesis in the mouse. *Development*, **106**, 465-471.

Willis, D., Li, K.W., Zheng, J.-Q., Chang, J.H., Smit, A., Kelly, T., Merianda, T.T., Sylvester, J., van Minnen, J. & Twiss, J.L. (2005) Differential Transport and Local Translation of Cytoskeletal, Injury-Response, and Neurodegeneration Protein mRNAs in Axons. *The Journal of Neuroscience*, **25**, 778-791.

Witowsky, J.A. & Johnson, G.L. (2003) Ubiquitylation of MEKK1 Inhibits Its Phosphorylation of MKK1 and MKK4 and Activation of the ERK1/2 and JNK Pathways. *Journal of Biological Chemistry*, **278**, 1403-1406.

Wu, B.Y., Fodor, E.J., Edwards, R.H. & Rutter, W.J. (1989) Nerve growth factor induces the proto-oncogene c-jun in PC12 cells. *The Journal of biological chemistry*, **264**, 9000-9003.

Xia, X.G., Harding, T., Weller, M., Bieneman, A., Uney, J.B. & Schulz, J.B. (2001) Gene transfer of the JNK interacting protein-1 protects dopaminergic neurons in the MPTP model of Parkinson's disease. *Proceedings of the National Academy of Sciences*, **98**, 10433-10438.

Xia, Y., Wang, J., Liu, T.-J., Yung, W.K.A., Hunter, T. & Lu, Z. (2007a) c-Jun Downregulation by HDAC3-Dependent Transcriptional Repression Promotes Osmotic Stress-Induced Cell Apoptosis. *Molecular cell*, **25**, 219-232.

Xia, Y., Wang, J., Xu, S., Johnson, G.L., Hunter, T. & Lu, Z. (2007b) MEKK1 Mediates the Ubiquitination and Degradation of c-Jun in Response to Osmotic Stress. *Molecular and Cellular Biology*, **27**, 510-517.

Xiong, Y., Hannon, G.J., Zhang, H., Casso, D., Kobayashi, R. & Beach, D. (1993) p21 is a universal inhibitor of cyclin kinases. *Nature*, **366**, 701-704.

Xiong, Z., O'Hanlon, D., Becker, L.E., Roder, J., MacDonald, J.F. & Marks, A. (2000) Enhanced calcium transients in glial cells in neonatal cerebellar cultures derived from S100B null mice. *Experimental cell research*, **257**, 281-289.

Xu, Z., Maroney, A.C., Dobrzanski, P., Kukekov, N.V. & Greene, L.A. (2001) The MLK family mediates c-Jun N-terminal kinase activation in neuronal apoptosis. *Mol Cell Biol*, **21**, 4713-4724.

Yamada, K., Fukaya, M., Shibata, T., Kurihara, H., Tanaka, K., Inoue, Y. & Watanabe, M. (2000) Dynamic transformation of Bergmann glial fibers proceeds in correlation with dendritic outgrowth and synapse formation of cerebellar Purkinje cells. *The Journal of comparative neurology*, **418**, 106-120.

Yamada, K. & Watanabe, M. (2002) Cytodifferentiation of Bergmann glia and its relationship with Purkinje cells. *Anatomical science international*, **77**, 94-108.

Yamasaki, T., Kawaji, K., Ono, K., Bito, H., Hirano, T., Osumi, N. & Kengaku, M. (2001) Pax6 regulates granule cell polarization during parallel fiber formation in the developing cerebellum. *Development (Cambridge, England)*, **128**, 3133-3144.

Yang, D.D., Kuan, C.Y., Whitmarsh, A.J., Rincón, M., Zheng, T.S., Davis, R.J., Rakic, P. & Flavell, R.A. (1997) Absence of excitotoxicity-induced apoptosis in the hippocampus of mice lacking the Jnk3 gene. *Nature*, **389**, 865-870.

Young, M.R., Li, J.J., Rinc+¦n, M., Flavell, R.A., Sathyanarayana, B.K., Hunziker, R. & Colburn, N. (1999) Transgenic mice demonstrate AP-1 (activator protein-1) transactivation is required for tumor promotion. *Proceedings of the National Academy of Sciences*, **96**, 9827-9832.

Yuan, Z., Gong, S., Luo, J., Zheng, Z., Song, B., Ma, S., Guo, J., Hu, C., Thiel, G., Vinson, C., Hu, C.-D., Wang, Y. & Li, M. (2009) Opposing Roles for ATF2 and c-Fos in c-Jun-Mediated Neuronal Apoptosis. *Molecular and Cellular Biology*, **29**, 2431-2442.

Yuasa, S. (1996) Bergmann glial development in the mouse cerebellum as revealed by tenascin expression. *Anatomy and embryology*, **194**, 223-234.

Zhang, J., Zhu, F., Li, X., Dong, Z., Xu, Y., Peng, C., Li, S., Cho, Y.Y., Yao, K., Zykova, T.A., Bode, A.M. & Dong, Z. (2012) Rack1 protects N-terminal phosphorylated c-Jun from Fbw7-mediated degradation. *Oncogene*, **31**, 1835-1844.

Zhu, X., Castellani, R.J., Takeda, A., Nunomura, A., Atwood, C.S., Perry, G. & Smith, M.A. (2001) Differential activation of neuronal ERK, JNK/SAPK and p38 in Alzheimer disease: the 'two hit' hypothesis. *Mechanisms of Ageing and Development*, **123**, 39-46.

9 List of figures and tables

	Page No:
Fig 3.1: The AP-1 transcription factor	8
Fig 3.2: Overview of diverging c-Jun activation pathways	11
Fig 3.3: Schematic of an E 3 SCF ubiquitin ligase	17
Fig 3.4: Schematic representation of a JNK-dependent interaction between c-Jun and TCF4/b-catenin on the c-Jun promoter	22
Fig 3.5: Hypothetical model showing the role of the MLK-JNK-c-Jun pathway	29
Fig 3.6: A model of the transcriptional regulation of myelination	33
Fig 6.1: c-Jun N-terminal phosphorylation in cerebellar granule Neurons	68-71
Fig 6.2: Generation of lentivirus	74-75
Fig 6.3: Lack of T91/93 phosphorylation protects from cell death	76-78
Fig 6.4: Lack of T91/93 phosphorylation does not impair neurite outgrowth	79-80
Fig 6.5: Constitutive phosphorylation at T95 impairs the neuronal protection ability of Li	82-84
Fig 6.6: Phosphorylation of amino acid residues within c-Jun N-terminal domain	88-89
Fig 6.7: MALDI MS/MS spectra of the $[M+H]^+$ from segment	90
Fig 6.8: GST-fused c-Jun constructs	93-94
Fig 6.9: JNK1 able to phosphorylate T91/93 but requires intact T95 in vitro	94
Fig 6.10: JNK-1 phosphorylates in vitro c-Jun at T91/93 in a T95-dependent manner	95-96
Fig 6.11: c-Jun is expressed in Bergmann glial-derived cells	98
Fig 6.12: LPS induces JNK-dependent phosphorylation of c-Jun in radial glial cells	100
Fig 6.13: LPS don’t induce the JNK-phosphorylation in cerebellar granular neurons	101-102

Fig 6.14 LPS induces JNK-dependent phosphorylation of c-Jun in radial glial cells via TLR receptors 103
Fig 6.15: Real time PCR Amplification curves 105
Fig 6.16: The JNK/c-Jun pathway is essential for the induction of IL-1β mRNA 106
Fig 6.17: c-Jun is expressed in Bergmann glial cells 108
Fig 6.18: Dynamic distribution of c-Jun positive cells in the early postnatal cerebellum 111-112
Fig 6.19: c-Jun expression in inhibitory interneurons 112
Fig 6.20: c-Jun N-terminal phosphorylation in granule cells 113

List of tables

Table 3.1: Positive modulators of c-Jun 18
Table 3.2: Negative modulators of c-Jun 22
Table 4.1: List of Plasmids Used 40
Table 4.2: List of Primary Antibodies Used 41
Table 4.3: List of secondary antibodies Used 42
Table 4.4: List of primers used 42
Table 6.1: Amino acid sequence of phosphorylated peptides 87

10 Abbreviations

JNK	c-Jun N-terminal kinase
CGCs	cerebellar granular cells
GLAST	Glutamate – aspartate transporter
BG	Bergmann Glia Cells
TLR 4	Toll-like receptor
IL-1□	Interleukin 1 beta
LPS	Lipopolysaccaride
TPA	12-*O*-tetradecanoylphorbol-13-acetate
TRE	12-*O*-tetradecanoylphorbol-13-acetate (TPA) responsive element
CRE	Cyclic AMP responsive element
JBD	JNK binding domain
IRES	Internal ribosomal entry site
FBW7	F-box&WD domain repeated 7
ATF	activating transcription factor
MAF	musculoaponeurotic fibrosarcoma
GSK3a	glycogen synthase kinase 3 a
DYRKs	Dual-specificity tyrosine phosphorylation-regulated kinases
HDACs	Histone deacetylases
Mkp-1	MAPK phosphotases
MEFs	Mouse embryonic fibroblasts
NGF	Neurotrophic growth factor
NuRD	Nucleosome remodelling and deacetylation complex
CBP	CREB-binding protein
MAPK	Mitogen activated protein kinase (MAP) Kinase
COP1	constitutive photomorphogenesis protein 1

Rack1	Receptor for activated C-kinase 1
PMA	Phorbol 12-myristate 13-acetate
CaN	Calcineurin
CDI	CDK inhibitor
CNS	Central nervous system
PNS	Pheripheral nervous system
NG	Nodose ganglia
DRG	Dorsal root ganglia
PCL	Purkinje cells layer
PORN	Poly-DL-ornithine hydrobromide
DAPI	(4′,6′-diamidino-2-phenylindole hydrochloride)
TK	trophic/potassium

11Affidavit

I hereby declare that my thesis entitled **'Role of differential phosphorylation of c-Jun N-terminal domain in degenerative and inflammatory pathways of the CNS'** is the result of my own work. I did not receive any help or support from commercial consultants. All sources and / or materials applied are listed and specified in the thesis.

Furthermore, I verify that this thesis has not yet been submitted as part of another examination process neither in identical nor in similar form.

Würzburg……

Date Signature

Eidesstattliche Erklärung

Hiermit erkläre ich an Eides statt, die Dissertation **Die Rolle der unterschiedlichen Phosphorylierung von c-Jun N-terminale Domäne bei degenerativen und entzündlichen Wirkungen im Nervengewebe** eigenständig, d.h. insbesondere selbstständig und ohne Hilfe eines kommerziellen Promotionsberaters, angefertigt und keine anderen als die von mir angegebenen Quellen und Hilfsmittel verwendet zu haben.

Ich erkläre außerdem, dass die Dissertation weder in gleicher noch in ähnlicher Form bereitsin einem anderen Prüfungsverfahren vorgelegen hat.

Würzburg……

Date Signature

12 Curriculum vitae

Research Experience:

Doctoral Experience:

Dec 2008-Till date : Graduate Student (Ph.D.) Institute for Clinical neurobiology, Bayerischen Julius-Maximilians- Universität, Würzburg, Germany
Thesis Title: Role of differential phosphorylation of c-Jun transactivation domain in degenerative and inflammatory pathways of the central nervous system (CNS) and in cerebellar stem cells
Supervisor – Anna Maria Musti, Micheal Sendtner & Sybille Jablonka

Predoctoral Experience:

Aug 2005-Nov 2008 : Project Assistant at Laboratory of Molecular Oncology, Centre for DNA Fingerprinting and Diagnostics (CDFD), Hyderabad, India
Project 1: Identification and characterization of pancreatic cancer genes located within novel localized copy number alterations
Project 2: Molecular genetics analyses of inborn genetic disorders
Supervisor: Dr. MD Bashyam

Publications

1) **Reddy EC**, *Albanito L, De Marco P,* D. Aiello, *Napoli A, Musti AM*
   Multi site phosphorylation of c-Jun at threonine 91/93/95 triggers the onset of c-Jun pro-apoptotic activity in cerebellar granule cells; 2013, **Cell Death & Disease (2013) 4, e852**

2) *Albanito L,* **Reddy EC**, *Musti AM*
   c-Jun is essential for the induction of Il-1beta expression in invitro activated Bergmann glial cells**; GLIA** 59:1879–1890 (2011)

3) **Reddy EC,** *Albanito L, Musti AM*
   c-Jun is required for maintenance and differentiation of postnatal cerebellar stem cells *in vitro* **(In Progress)**

4) *Bashyam MD*, Chaudhary AK**, **Reddy EC***, *Devi AR, Savithri GR, Ratheesh R, Bashyam L, Mahesh E, Sen D, Puri R, Verma IC, Nampoothiri S, Vaidyanathan S, Chandrashekar MD, Kantheti P*
   ***Equal contribution**
   Phenylalanine Hydroxylase gene mutations in Phenylketonuria patients from India: Identification of novel mutations that effect PAH RNA; **Molecular Genetics and Metabolism**; 100 (2010) 96–99

5) *A R Devi*,* **Reddy EC*,** *Sarita Ranjan, Murali D Bashyam*
   ***Equal contribution**
   Molecular genetic analysis of Hypohidrotic Ectodermal Dysplasia patients from India reveals novel mutations in the EDA and EDAR genes; **British Journal of Dermatology**; 158, pp163–167(2008)

6) *Kevin A. Kwei*,M D Bashyam*, Jessica Kao, Raman Ratheesh,* **Reddy EC,** *Young H. Kim, Kelli Montgomery,Craig P.Giacomini,Yoon-La Choi,Sreejata Chatterjee,Collins A. Karikari, Keyan Salari, Pei Wang, Tina Hernandez-Boussard, Gowrishankar Swarnalata, Matt van de Rijn, Anirban Maitra, Murali D. Bashyam, Jonathan R. Pollack*
   Genomic profiling identifies GATA6 as a candidate oncogene amplified in pancreatobiliary cancer; **PLoS Genetics,** 2008 May 23; 4(5):e1000081

7) *MDBashyam, AK.Chaudhary*, **ReddyEC**, *VenkatReddy, VishalAcharya, Hampapathalu A Nagarajaram, A Radha Rama Devi, Leena Bashyam, Ashwin B Dalal, Neerja Gupta, Madhulika Kabra, Meenal Mittal, Shubha R. Phadke, Ram Tainwala, Rajesh Kumar, Sankar V Hariharan*

An Ectodysplasin A receptor (EDAR) founder mutation results in a high frequency of the autosomal recessive form of Hypohidrotic Ectodermal Dysplasia in India; **British Journal of Dermatology;** 2012 166, pp819–829

8) *M D Bashyam, A K Chaudhary, Manjari, H A Nagarajaram, A R Devi,* **Reddy EC**, *Ashwin Dalal*

Molecular genetic analysis of MSUD from India reveals mutations causing altered protein truncation affecting the C-termini of E1A and E1b; **Journal of Cellular Biochemistry:** 2012 Oct; 113(10):3122-32)

Würzburg,

……..……..

Place, date Signature: Chandrakanth Reddy Edamakanti

13 Acknowledgements

My experience at Institute for Clinical Neurobiology, Wuerzburg has been nothing short of amazing. Since my first day November 16th, 2008 I have felt at home at UKW with summer parties and get-togethers. I have been given unique opportunities and taken advantage of state of art laboratory equipment like genomic, proteomics, microscopic and ultra-structural analysis.

First and foremost, I would like to convey my gratitude and sincere thanks to my supervisor Dr. Anna Maria Musti for her supervision, advice, and guidance from the very early stage of this research. In addition, she provided me unflinching encouragement and support in various ways. Her commitment and passion inspired and enriched my growth as a researcher. She has been understanding and was willing to share my problems with her and sometimes she has gone out of the way to help me.

I would like to express my deep gratitude and respect to Prof. Michael Sendtner whose advices and insight was invaluable to me. I am very thankful to him for all I learned from him and for giving wonderful advice during weekly seminars. His attitude to research inspired me to continue to a PhD program, passion towards research and want to be a member of the academic family.

In addition, I would like to thank Dr. Sibylle Jablonka for accepting to be my supervisor in this project and for her interesting suggestion during my seminars, which helped me to improve my seminar skills and my research skills. I also wanted to thank my mentor Dr. Muralidaran Bashyam from my previous institute, CDFD for his unconditional support throughout my research tenure.

I thank Regine Sendtner, Helga Brunner, J.Horschig and V.Buterus for their assistance in maintaining and availing the laboratory animals to carry out my experiments. I also would like to thank the technical staff, Kohels Manuela, Zuzana, Michi, Simone, Mehling Christian, Nicole, Elke and Hilde for their valuable support and co-operation. I would also like to thank Judita Grimm, Urveen Oberoi- Lehrieder and Christ Birgit for their administrative assistance.

I am very happy to be part of Prof. M. Sendtner group and I thank all colleagues for the extensive co-operative, interactive and for helpful environment. This includes Andrea Wetzel, Andreska Thomas, Benjamin Dombert, Bhuvaneish Selvaraj, Briese Michael, Prof. Dr. Bruchner Erich, Carsten Drepper, Christian Simon, Christina Mais, Dirk Pühringer, Elena Nekhorhoshkova, Florian Bender, FrankKrieger, Juliane Jäpel, Lena Saal, Lidia Albanito, Dr. Luningschror Patrick. Michael Glinka, Moradi Mehri, Nicholas Frank, PD. Dr. Rudolf Götz,Preeti Yadav, Prof. Micheal sendtner, Rajeeve Sivadasan, Reena Rathod, Dr. Rauskolb Stefenie, Sameehan Mahajani, Stephan Weise, Steven Havlicek, Saal Leena, Samtleben Samira and Prof. Dt. Villmann Carmen.

My family is an important part of my life and I am extremely grateful for their love and encouragement throughout my PhD tenure. I thank my parents and brothers for their unconditional support in all the decisions of my life and I owe them my sincere gratitude for being my pillars of strength and a virtual backbone throughout this work. The unconditional love, care, support showered by my wife, Sampurna, is priceless. She has given me a wonderful gift in form of Nihal, which brought me luck and joy in my life.

Life in Würzburg would have been meaningless without the presence of my friends.
A special thanks to all of them for made my life with full of joy and fun.